

**R-11-21**

**Effects of earthquake induced  
rock shear on containment  
system integrity**

**Laboratory testing plan development**

Rodney S. Read, RSRead Consulting Inc.

July 2011

**Svensk Kärnbränslehantering AB**

Swedish Nuclear Fuel  
and Waste Management Co

Box 250, SE-101 24 Stockholm  
Phone +46 8 459 84 00



# **Effects of earthquake induced rock shear on containment system integrity**

## **Laboratory testing plan development**

Rodney S. Read, RSRead Consulting Inc.

July 2011

*Keywords:* Bentonite, Canister, Constant volume test, Deposition borehole, Earthquake, Laboratory testing, Rock shear, Scaled analogue test, Shear rate, Swelling pressure, Unconfined compression test, Undrained shear strength.

This report concerns a study which was conducted for SKB. The conclusions and viewpoints presented in the report are those of the author. SKB may draw modified conclusions, based on additional literature sources and/or expert opinions.

A pdf version of this document can be downloaded from [www.skb.se](http://www.skb.se).

## **Abstract**

This report describes a laboratory-scale testing program plan to address the issue of earthquake induced rock shear effects on containment system integrity. The document contains a review of relevant literature from SKB covering laboratory testing of bentonite clay buffer material, scaled analogue tests, and the development of related material models to simulate rock shear effects. The proposed testing program includes standard single component tests, new two-component constant volume tests, and new scaled analogue tests. Conceptual drawings of equipment required to undertake these tests are presented along with a schedule of tests. The information in this document is considered sufficient to engage qualified testing facilities, and to guide implementation of laboratory testing of rock shear effects. This document was completed as part of a collaborative agreement between SKB and Nuclear Waste Management Organization (NWMO) in Canada.

## Sammanfattning

Denna rapport beskriver planering för ett provningsprogram i lab-skala för att undersöka effekterna av bergskjuvning, inducerad av jordbävning, på integriteten hos systemets inneslutning. Dokumentet innehåller en genomgång av relevant litteratur från SKB som täcker laboratorietester av buffertmaterial av bentonitlera, nedskalade provningar och utveckling av korresponderande materialmodeller använda för att simulera skjuveffekter. Det föreslagna testprogrammet inkluderar standard enkel-komponenttester, nya två-komponenttester med konstant volym och nya nedskalade tester. Översiktliga ritningar av utrustning som krävs för att genomföra dessa tester presenteras tillsammans med ett schema för provningen. Informationen i detta dokument anses tillräcklig för att kontakta kvalificerade provningsanläggningar, och att styra genomförandet av laboratorieprov på bergskjuveffekter. Detta dokument slutfördes som en del av ett samarbetsprojekt mellan SKB och avfallsorganisationen Nuclear Waste Management Organisation (NWMO) i Kanada.

# Contents

<b>1</b>	<b>Introduction</b>	7
<b>2</b>	<b>Synopsis of activities</b>	9
<b>3</b>	<b>Laboratory testing and numerical modeling review</b>	11
3.1	Functional requirements of the buffer	11
3.2	Bentonite buffer properties and stress-strain behaviour	11
	3.2.1 Laboratory testing on buffer material to support SR-Can	11
	3.2.2 Laboratory testing on buffer material to support SR-Site	19
3.3	Scaled buffer/canister shear tests	25
	3.3.1 Description of scaled laboratory tests	25
	3.3.2 Numerical simulation of scaled laboratory tests	29
3.4	Numerical modeling of rock shear at field scale	32
	3.4.1 Modeling to support SR-Can	32
	3.4.2 Modeling to support SR-Site	36
3.5	Summary of literature review	41
<b>4</b>	<b>Rock shear laboratory testing program</b>	43
4.1	General	43
4.2	Standard single component tests	43
4.3	Two-component constant volume tests	44
4.4	Scaled analogue tests	47
4.5	Technical considerations	51
4.6	Work scope	55
4.7	Schedule	59
<b>5</b>	<b>Conclusions and recommendations</b>	61
5.1	Conclusions	61
5.2	Recommendations	62
	<b>References</b>	63
<b>Appendix A</b>	<b>Background on the Rock Shear Experiment (ROSE)</b>	65
<b>Appendix B</b>	<b>Background on JAEA BORE-SHEAR tests</b>	69
<b>Appendix C</b>	<b>Translated JAEA abstracts</b>	75

# 1 Introduction

Concepts for isolation of spent nuclear fuel have been studied by organizations in countries that employ nuclear power. These concepts typically involve a deep geological repository in bedrock, with processed radioactive waste encased in deposition canisters (or containers) emplaced in underground excavations (either tunnels or deposition holes) and surrounded by clay-based buffer and backfill materials. This multi-barrier approach is intended to provide long-term isolation of the waste package from the biosphere.

In the Swedish KBS-3V concept for nuclear waste disposal (Figure 1-1), earthquake-induced shearing of the rock mass along existing fractures intersecting deposition holes is considered one of the few processes with the potential to affect canister integrity. Considerable effort has been spent to estimate the magnitude and rate of shear displacement on secondary fractures and the relation of these parameters to earthquake moment magnitude and epicentral distance /LaPointe et al. 1997, Munier and Hökmark 2004, Hedin 2005/. The possible effects associated with this key technical issue on boreholes are illustrated in Figure 1-2 and Figure 1-3. Estimating the probability of canister failure by this mechanism requires a thorough understanding of the behaviour of bentonite clay buffer, rock, and canister materials, and their interaction under sudden shear displacement conditions. Numerical models developed to simulate these behaviours and interactions are central to safety assessment of candidate sites in Sweden (e.g. /SKB 2006/). Validation of these models has relied upon standard laboratory-scale tests to determine material properties, and a series of three 1:10 scale analogue tests of the rock shear scenario /Börgesson 1986/.

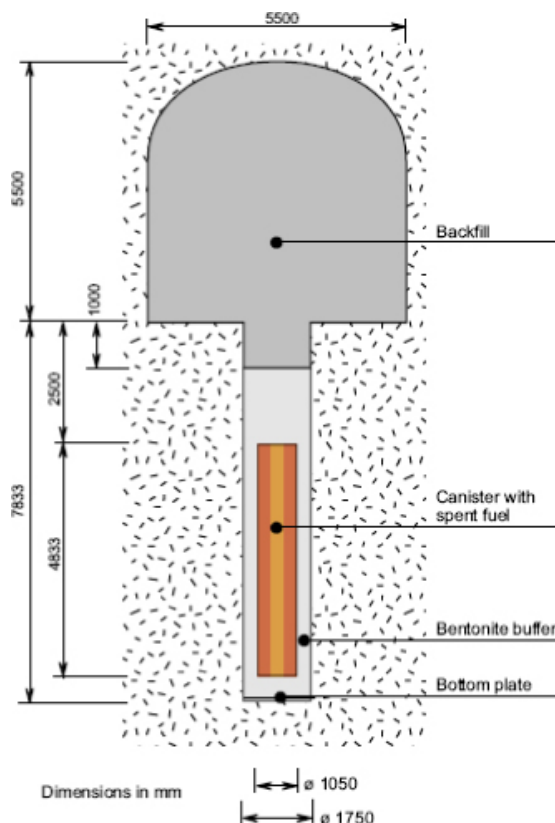


**Figure 1-1.** Conceptual design of a KBS-3V deposition tunnel and borehole showing the dimensions and relative position of the buffer and canister /SKB 2006/.



a)



b)

**Figure 1-2.** Examples of rock shear in vertical boreholes: a) on fractures induced by Mine-by test tunnel excavation following drilling of the borehole, and b) induced on an existing fracture by heating of the rock mass in the Heated Failure Tests at AECL's Underground Research Laboratory /Read 2004/.

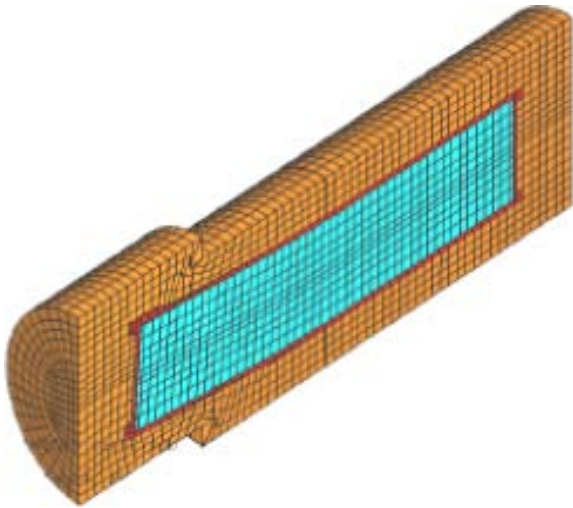


**Figure 1-3.** ABAQUS model simulation of the possible effects of rock shear causing bending and strain in the deposition canister /Börgesson et al. 2004/.

To improve confidence in the understanding of earthquake induced rock shear and its potential effects on containment system integrity, /Börgesson et al. 2004/ proposed the full-scale Rock Shear Experiment (ROSE) to be conducted in situ at the Äspö Hard Rock Laboratory (HRL) in Sweden (Appendix A). Given the scope of the proposed in situ experiment, development of a complementary large-scale laboratory testing program was initiated by SKB in 2006. One purpose of this program was to gain insight into potential rock shear effects that might influence the design or execution of ROSE. The laboratory testing program was also anticipated to produce supplementary data against which to validate numerical models. The purpose of this report is to describe work conducted to date in relation to laboratory testing of rock shear effects, and to present a proposed laboratory testing plan. This plan is expected to provide a basis for preliminary cost estimates and selection of a suitable testing facility to conduct the laboratory testing program, and for guiding implementation of the testing program.

## 2 Synopsis of activities

As part of a collaborative agreement between Ontario Power Generation (OPG) and SKB, RSRead Consulting Inc. (RSRCI) was engaged in 2006 to begin planning a laboratory scale rock shear testing program. A preliminary laboratory testing plan involving a combination of standard laboratory tests, new constant volume tests, and scaled analogue tests using existing specialised testing apparatus (referred to as BORE-SHEAR apparatus) owned and operated by Japan Atomic Energy Agency (JAEA) was developed. The details of the testing plan were presented at a meeting with SKB on December 6, 2006 at the Äspö Hard Rock Laboratory (HRL) in Sweden.

Under a subsequent collaborative agreement between Nuclear Waste Management Organization (NWMO) and SKB, the testing facility at JAEA's Tokai Research Center in Tokai, Japan was visited on June 25/26, 2007 to examine the BORE-SHEAR rock shear testing apparatus and other testing equipment (Appendix B), and to assess its suitability for scaled analogue tests based on the KBS-3V design. The findings from the site visit and discussions with JAEA staff were summarised and reported to NWMO and SKB.

Limitations in the dimensions of the JAEA testing apparatus, the number of available testing vessels, the testing schedule, and availability of JAEA resources were identified during the 2007 visit to Tokai. These limitations were discussed at a meeting with SKB on May 21, 2008 in Oskarshamn, Sweden, and were subsequently summarised and submitted to NWMO and SKB. Based on the information discussed at that meeting, a decision was taken by SKB to identify other testing facilities and options to develop new testing apparatus to conduct the laboratory testing program.

Three prospective testing facilities were visited in 2008 to assess capabilities and interest in undertaking the preliminary laboratory testing program. Contact information for the various laboratory facilities is provided in (Table 2-1). Staff at each facility was given an overview of the key technical issues, the proposed in situ experiment, and the preliminary laboratory testing program. A letter of expression of interest and statement of qualifications was requested from staff at each facility as a starting point for further detailed discussions regarding work scope, schedule and estimated costs to develop testing apparatus and undertake the testing program.

**Table 2-1. Contact information for testing facilities.**

C-CORE Captain Robert A. Bartlett Building Morrissey Road St. John's, Newfoundland Canada A1B 3X5	Contact: Phone Fax Email	Dr. Ryan Phillips (709) 737-8371 (709) 737-4706 Ryan.Phillips@c-core.ca
C-FER Technologies 200 Karl Clark Road Edmonton, Alberta Canada T6N 1H2	Contact: Phone Fax Email	Mr. Duane DeGeer (780) 450-3300 (780) 450-3700 d.degeer@cfertech.com
European Laboratory for Structural Assessment (ELSA), European Commission, Joint Research Centre (JRC) TP 480, Via E. Fermi, 2749 I-21027 Ispra (VA) Italy	Contact: Phone Fax Email	Dr. Georges Magonette +39-0332-789368 +39-0332-789049 georges.magonette@jrc.it

Based on discussions with staff of the prospective testing facilities and review of SKB publications on previous laboratory testing and numerical modeling efforts, the preliminary laboratory testing plan was refined, and a preliminary testing program was developed. The preliminary testing program was discussed with SKB in Stockholm, Sweden and with Clay Technology AB in Lund, Sweden in April, 2010.

In parallel with the development of the preliminary testing plan, SKB undertook additional investigations into sodium and calcium bentonite buffer behaviour /Dueck et al. 2010/, refinement of the material model for shearing of bentonite buffer /Börgesson et al. 2010/, verification of the material model through modeling of 1:10 scale analogue tests of rock shear /Börgesson and Hernelind 2010/, and application of the calibrated numerical model to analyse canister and buffer response under earthquake and glacial loading /Hernelind 2010/. The findings of these four investigations were incorporated into an updated rock shear laboratory testing plan (this report).

## 3 Laboratory testing and numerical modeling review

In order to refine the preliminary rock shear laboratory testing plan, a review of SKB reports related to laboratory testing and numerical modeling of buffer material and buffer/canister systems was undertaken. A list of relevant reports was provided by SKB's librarian. Electronic copies of available reports were downloaded from SKB's website. Copies of older reports not available on-line were provided in hardcopy by SKB. JAEA also provided relevant reports on the same topics /Takaji and Suzuki 1999/; /Takaji et al. 2004/; /Hirai et al. 2003/; /Hirai et al. 2004/, but these reports were in Japanese and therefore of limited use in the literature review. Translated abstracts from the JAEA reports are contained in Appendix C.

### 3.1 Functional requirements of the buffer

Buffer material properties and behaviour in relation to the KBS-3V concept have been studied by SKB and associated investigators for almost 30 years. Some of the key functional requirements identified for the bentonite buffer /Pusch 1983a/ are as follows:

- Chemical stability of the buffer to ensure adequate performance over one million years.
- Sufficient buffer strength to prevent rock fragments from falling, and to minimise canister settlement.
- Sufficient buffer ductility to dissipate stresses induced by tectonically-driven rock displacements.
- Low buffer hydraulic conductivity to minimise groundwater flow between the rock and the canister.
- Low buffer diffusivity to retard ion migration from the rock and from the canister.
- Sufficient buffer heat conductivity to maintain the temperature below critical levels associated with the buffer and the canister.
- Sufficient swelling potential of the buffer to fill any empty spaces between the canister and the rock, and to establish close contact at the buffer-rock and buffer-canister interfaces.
- Buffer adsorption potential through ion exchange mechanisms to retain radionuclides emerging from the canister.

The hydro-mechanical properties of the bentonite buffer listed above are related in large part to the degree of saturation of the material, buffer composition, water chemistry, and bulk density. These aspects are discussed in the next section.

### 3.2 Bentonite buffer properties and stress-strain behaviour

Considerable work has been done in Sweden in assessing properties and stress-strain behaviour of bentonite buffer materials. Results of available testing were used to develop material models and to perform model simulations to support SR-Can /SKB 2006/, a safety assessment for the application to build an encapsulation plant. Additional testing was undertaken to support SR-Site, a safety assessment for the application to build the repository.

#### 3.2.1 Laboratory testing on buffer material to support SR-Can

Significant testing of buffer materials has been ongoing in Sweden for over 30 years. /Pusch 1980a/ presented results from about 90 oedometer swelling tests on two bentonites of different composition (Wyoming MX-80 sodium bentonite and Erbslöh calcium bentonite). Tests were conducted under a range of conditions: different water chemistries (0.6 M NaCl solution, 0.3 M CaCl<sub>2</sub> solution, artificial 'Allard' groundwater, and distilled water), bulk density ranging from 1,750 to 2,195 kg/m<sup>3</sup>, and

temperatures ranging from 20 to 90°C. Empirical relations between swelling pressure and bulk density for saline and fresh water conditions were developed on the basis of these tests as follows:

$$p_s = e^{11.5(\rho-1.87)} \quad (\text{saline water, bulk density between 1.8 and 2.1 t/m}^3) \quad (3-1)$$

and

$$p_s = e^{11.5(\rho-1.81)} \quad (\text{fresh water, bulk density between 1.75 and 2.1 t/m}^3) \quad (3-2)$$

where  $\rho$  is bulk density (t/m<sup>3</sup>), and  $p_s$  is swelling pressure (MPa).

Based on these tests, bentonite composition had minimal effect on the relation between swelling pressure and bulk density. For buffer with bulk density less than 2,050 kg/m<sup>3</sup>, saline conditions (represented by the NaCl and CaCl<sub>2</sub> solutions) reduced swelling pressure by between 30 and 50% compared to fresh water conditions (represented by distilled water and ‘Allard’ groundwater) at a given bulk density. Temperature increase from 20 to 90°C was also shown to reduce swelling pressure by up to 50%. Plots of swelling pressure versus time for 16 of the oedometer tests are contained in an appendix to the report by /Pusch 1980a/. The findings of this study provided an initial basis for estimating the swelling pressure expected at target buffer bulk densities required to mitigate the effects of rock shear displacement, and to minimise canister settlement.

Further study of bentonite properties by /Börgesson 1986/ led to a refined relation between swelling pressure and bentonite saturated bulk density as follows:

$$p_s = 2.86 \cdot (B_c + 0.2)^{10/3} \cdot e^{\left(\frac{\rho-2.0}{0.095}\right)} \quad (3-3)$$

where  $B_c$  is bentonite content (dry bentonite mass/total dry mass),  $\rho$  is bulk density (t/m<sup>3</sup>), and  $p_s$  is swelling pressure (MPa). This relation was originally proposed by /Börgesson and Pusch 1986/ and was applied to tests saturated with distilled water. The various relations for swelling pressure are shown in Figure 3-1. The reason for the apparent discrepancy between the relations represented by Equations 3-2 and 3-3 for fresh water was not investigated as part of this literature review.

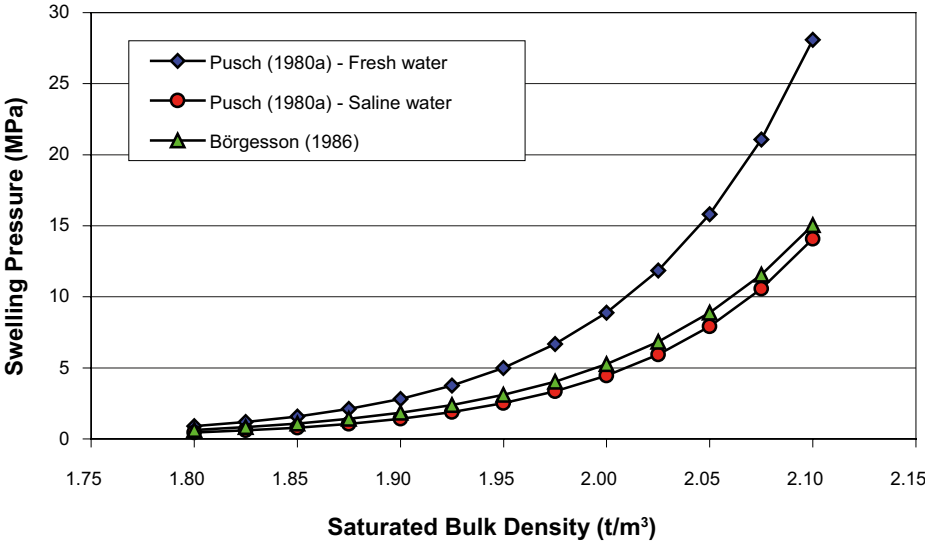


Figure 3-1. Comparison of relations between swelling pressure and saturated bulk density for MX-80 sodium bentonite buffer.

The hydraulic conductivity of highly compacted bentonite was investigated by /Pusch 1980b/. Percolation tests were conducted on bentonite samples of different composition (Wyoming MX-80 sodium bentonite and Erbslöh calcium bentonite) using a swelling pressure oedometer. Seven tests on MX-80 sodium bentonite samples with densities ranging from 1,900 to 2,150 kg/m<sup>3</sup> at temperatures of 20°C (four tests) and 70°C (three tests) were performed. An additional five tests on calcium bentonite samples with densities ranging from 1,870 to 2,210 kg/m<sup>3</sup> at temperatures of 20°C (two tests) and 70°C (three tests) were also completed. All of the tests were conducted using ‘Allard’ groundwater typical of conditions at 500 m depth in the Swedish crystalline bedrock.

Results indicated that measured hydraulic conductivity decreased with increasing buffer bulk density, and increased by a factor of between three and seven with a temperature increase of 50°C. Calcium bentonite was found to have higher hydraulic conductivity than sodium bentonite under given density and temperature conditions. Table 3-1 provides a summary of predicted hydraulic conductivity values as a function of bulk density for Na and Ca bentonite.

Given the very low hydraulic conductivity values, groundwater migration in the buffer material is dominated by diffusion. /Börgesson 1986/ reported a coefficient of water diffusion of  $0.3 \cdot 10^{-9} \text{ m}^2/\text{s}$  for MX-80 sodium bentonite buffer. This value was used to estimate time to saturate samples used in 1:10 scale shear tests to investigate the effects of rock shear (described in Section 3.3).

/Pusch 1983a/ summarised the characteristics and potential use of different types of clays as buffers and backfill in a KBS-3V repository. High density water-saturated bentonite was considered well suited as a buffer due to its low hydraulic conductivity. Strength and stiffness of this material were found to be related to both swelling pressure and bulk density. To limit swelling pressure to a practical maximum of about 10 MPa, an estimated upper bound on bulk density was 2,000 to 2,100 kg/m<sup>3</sup> depending on montmorillonite content of the bentonite. At this density, the matured bentonite mechanical properties were considered sufficient to limit settlement to a fraction of a centimetre in one million years /Pusch 1983b/. The optimum bulk density for this material was considered to be between 1,900 and 2,000 kg/m<sup>3</sup> to limit effects of rock shear and to maintain sufficient bearing capacity to limit settlement. At a density of 2,000 kg/m<sup>3</sup>, the undrained shear strength of MX-80 sodium bentonite was estimated to be between 0.4 and 4 MPa depending on the rate of strain, and its elastic modulus was in the range 100 to 1,000 MPa. These parameters were considered to be of primary importance in evaluating the canister stress state in the event of rock shear. Values for other properties such as viscosity, diffusivity, thermal conductivity, and heat capacity for bentonite buffer were also provided by /Pusch 1983a/.

**Table 3-1. Predicted hydraulic conductivity of bentonite buffer /Pusch 1980b/.**

Bulk Density (kg/m <sup>3</sup> )	Predicted Hydraulic Conductivity (m/s)			
	Early Stage		Final Stage	
	Na Bentonite	Ca Bentonite	Na Bentonite	Ca Bentonite
2,100	$1.5 \cdot 10^{-13}$	$2.0 \cdot 10^{-13}$	$1.5 \cdot 10^{-14}$	$8.0 \cdot 10^{-14}$
2,000	$2.0 \cdot 10^{-13}$	$4.0 \cdot 10^{-13}$	$2.0 \cdot 10^{-14}$	$1.0 \cdot 10^{-13}$
1,900	$5.0 \cdot 10^{-13}$	$8.0 \cdot 10^{-13}$	$3.0 \cdot 10^{-14}$	$2.0 \cdot 10^{-13}$
1,800	$8.0 \cdot 10^{-13}$	$1.0 \cdot 10^{-12}$	$5.0 \cdot 10^{-14}$	$5.0 \cdot 10^{-13}$
1,700	$1.0 \cdot 10^{-12}$	$5.0 \cdot 10^{-12}$	$8.0 \cdot 10^{-14}$	$8.0 \cdot 10^{-13}$

Note: Early stage – 70°C, relatively high hydraulic gradient. Final stage – low temperature, very low hydraulic gradient.

/Pusch 1983b/ investigated the rheological properties of highly compacted bentonite with particular emphasis on settlement and rock shear effects. Three drained and five undrained triaxial tests were conducted on MX-80 sodium bentonite saturated with 'Allard' groundwater to assess creep behaviour and mechanical properties. The bentonite material used was 80–90% clay of which 80–90% was montmorillonite. The undrained tests were conducted at 22°C, and bulk densities of 2,000 kg/m<sup>3</sup> (three tests) and 1,900 kg/m<sup>3</sup> (two tests). The drained tests were conducted at a bulk density of 1,900 kg/m<sup>3</sup>, and temperatures of 22°C (two tests) and 93°C (one test). Plots of strain rate versus time for the tests are included in the original report /Pusch 1983b/. For the undrained tests, strain rate ranged from about 5·10<sup>-9</sup> to 5·10<sup>-8</sup> s<sup>-1</sup> at a time of 5·10<sup>4</sup> s for the various tests. At a time of 1·10<sup>6</sup> s, the strain rate decreased to between 1·10<sup>-9</sup> and 2·10<sup>-9</sup> s<sup>-1</sup> for the various tests. The drained tests displayed more variability and generally higher strain rates relative to the undrained tests. The strain rate in the heated drained test increased by a factor of between three and six relative to the ambient temperature tests. It was noted that pore pressure gauges unexpectedly malfunctioned during the undrained creep tests.

The stress-strain response of dense bentonite measured by /Pusch 1983b/ exhibited strong work-hardening, with an initially high deformation modulus that decreased to a substantially lower value once strain exceeded about 2%. The deformation modulus was estimated from the initial loading portion of the stress-strain curves derived from the creep tests conducted at 22°C. Creep tests on samples with a bulk density of 2,000 kg/m<sup>3</sup> had modulus values of 117, 369, and 533 MPa (average 340 MPa). For samples with a bulk density of 1,900 kg/m<sup>3</sup>, the modulus values estimated from creep tests were 41, 46, and 31 MPa (average 39 MPa). Rapid uniaxial compression tests at constant strain rate on 50% saturated sodium bentonite with a bulk density of 2,050 kg/m<sup>3</sup> /Pusch 1978/ indicated an average modulus value of 270 MPa, and shear strength of 8 MPa. At 100% saturation, the elastic modulus value was estimated to be about 200 MPa. Uniaxial compression testing at a strain rate of 1% per minute on a sample with bulk density of 2,000 kg/m<sup>3</sup> indicated shear strength of 1.1 MPa and elastic modulus of 100 MPa. The relatively large variability in values of these mechanical properties introduced some uncertainty into the calculation of stress and strain induced in the canister by rapid rock shear loading.

/Börgesson et al. 1988/ presented a summary of laboratory test results used to determine rheological properties for bentonite of different types, densities, mixtures and pore water compositions. The influence of temperature, rate of strain, and testing techniques on the measured properties was also considered. The summary included measurements of hydraulic conductivity, undrained stress-strain-strength properties, creep properties, compression and swelling properties in drained and undrained conditions, and undrained thermo-mechanical properties of buffer materials. Mechanical properties of pore water were also investigated. These basic data were used as inputs to material models for long-term performance calculations.

The MX-80 sodium bentonite proposed for buffer material was described in general terms by /Börgesson et al. 1988/ as having a liquid limit of 550% and a plasticity limit of 70% when saturated with distilled water. The liquid limit was observed to decrease dramatically with increasing NaCl content. In the unsaturated state, sodium bentonite was shown to have a high suction potential and water uptake could be simulated as a diffusion process. Hydraulic properties were measured in a triaxial cell and in an oedometer; the latter method was preferred to avoid high pressure differential required to create a gradient across the sample. Relations between hydraulic conductivity and saturated density were provided in the original report for a range of sodium bentonite-sand mixtures at different salt content, and for different types of bentonites. Investigations of possible anisotropy in properties showed that the hydraulic conductivity was isotropic, and that swelling pressure was slightly anisotropic.

Shear properties of sodium bentonite have been investigated using triaxial shear tests, simple shear tests, and direct shear tests /Börgesson et al. 1988/. Eight triaxial tests were conducted to find the general undrained stress-strain-strength relation for clay and to investigate the influence of quick undrained total stress changes on this relation, among other effects. The stress-strain plots of these triaxial tests are included as an appendix to the report by /Börgesson et al. 1988/. The results were used to derive a failure envelope by plotting shear stress at failure versus effective confining stress. The failure envelope was slightly curved, and was affected very little by quick changes in total pressure. This inferred that the stress-strain relation was unique at a given density provided that the same

stress history of the soil was considered. Straight line approximations were applied to the failure envelope above and below 1 MPa to derive Mohr-Coulomb effective strength parameters. Above 1 MPa, effective friction angle was 7° and effective cohesion (i.e. the y-intercept on the effective stress plot) was 150 kPa. Below 1 MPa, effective friction angle was 13° and effective cohesion was 0 kPa. Temperature increase to 60°C had an insignificant effect on shear strength. The shear strength of sodium bentonite was found to exceed that of calcium bentonite at high confining stress.

Three simple shear tests using incremental strain rates ranging from 0.025 to 25%/h were conducted on samples of sodium bentonite to assess the influence of strain rate on shear strength. In addition, four direct shear creep tests and eight triaxial creep tests were conducted to derive parameters required for a creep model to assess longer term effects. The plots from these tests are included as an appendix to the report by /Börgesson et al. 1988/. The results of the shear tests indicated that shear strength increased with strain rate and could be expressed by the following relation:

$$\tau_f = m \left( \frac{\dot{\gamma}}{\dot{\gamma}_o} \right)^n \quad (3-4)$$

where

$\tau_f$  = shear strength

$\dot{\gamma}$  = rate of shear strain ( $s^{-1}$ )

$\dot{\gamma}_o$  = reference rate of shear strain = 1.0 ( $s^{-1}$ )

$m$  = shear strength at reference rate of shear strain

$n$  = slope in double logarithmic space of shear strength (kPa) versus strain rate (%/h)

The exponent  $n$  in Equation 3-4 was found to have an average value of 0.065, which is of the same order as for other clays.

In addition to these tests, five undrained compression/expansion tests were completed to characterise compression and swelling properties. Bulk modulus values for sodium bentonite at bulk density values of 1.8, 2.0 and 2.1  $t/m^3$  were calculated to be 2.3, 5.0 and 6.0 GPa, respectively. Thermal expansion coefficients for sodium bentonite at bulk densities of 1.8, 2.0 and 2.1  $t/m^3$  were calculated to be  $3.1 \cdot 10^{-4}$ ,  $3.0 \cdot 10^{-4}$ , and  $3.1 \cdot 10^{-4} K^{-1}$ , respectively.

/Börgesson et al. 1995/ provided an overview of laboratory tests conducted to characterise bentonite behaviour at various void ratios and temperatures using different bentonite and pore water compositions (i.e. natural sodium-bentonites, calcium-bentonite, sodium converted calcium-bentonite using distilled and saline water). Testing included:

- Triaxial tests to derive stress-strain-strength relations – these tests were conducted at very slow loading rates to avoid excess pore pressures. Undrained tests took 20–30 days and drained tests took 50–70 days. Both loading and unloading tests were performed. Plots of 18 tests from a larger suite of triaxial tests are included in an appendix to the report by /Börgesson et al. 1995/.
- Swelling pressure and hydraulic conductivity tests using a swelling pressure oedometer – no new tests were reported, just a summary of previously conducted tests.
- Swelling/compression tests to evaluate volume change caused by a change in mean stress – results from a series of new tests, along with those from previously conducted tests, were summarised. Eight void ratio versus swelling pressure diagrams showing the effects of loading and unloading were presented. Results from new tests are included in an appendix to the report by /Börgesson et al. 1995/.
- Creep tests including deviatoric creep and volumetric creep tests to develop creep models – these tests were performed and results reported by /Börgesson et al. 1988/.
- Shear tests on interfaces between bentonite and adjacent materials including copper, stainless steel, and granite rock – these tests were performed and reported by /Börgesson 1990/. The results showed that the shear resistance between these materials and bentonite was about 60% of the shear strength of bentonite itself. Interfaces between bentonite and concrete were shown to have the same shear strength as bentonite given a chemical bonding between the clay and concrete.

- Thermal expansion tests – these tests were performed and reported by /Börgesson 1990/. The dominant thermal-mechanical effect was thermal expansion of pore water. Compressibility of pore water and degree of saturation were also studied.
- Thermal conductivity tests – these tests were performed and results reported by /Börgesson et al. 1994/. The average thermal conductivity for a void ratio of 0.7, representing conditions after water saturation, was 1.25 W/m·K.

These test results were used to develop new material models for the bentonite buffer, as described later in this report.

/Börgesson et al. 2004/ investigated the issue of earthquake induced rock shear through a deposition hole, and its effect on the canister and the buffer. Two types of material models for bentonite were used in previous calculations: a total stress model and an effective stress model. The total stress model was considered well-suited for investigating rapid rock shear effects. The shear strength of the buffer was identified as a key input to these models.

As shown in previous studies, the shear strength of buffer material after complete water saturation is a function of swelling pressure (controlled by bulk density of bentonite), and the rate of shear. Bulk density can be expressed in terms of void ratio. Several refined relations developed for buffer material /Börgesson et al. 2004/ follow.

The relation between swelling pressure and void ratio is given by:

$$p = p_0 \left( \frac{e}{e_0} \right)^{\frac{1}{\beta}} \quad (3-5)$$

where  $e$  is void ratio,  $e_0$  is reference void ratio (1.1),  $p$  is swelling pressure at the given void ratio,  $p_0$  is reference swelling pressure (1,000 kPa) at  $e_0$ , and  $\beta$  is  $-0.19$  for MX-80 buffer.

The relation between shear strength and swelling pressure is given by:

$$q_f = q_{f0} \left( \frac{p}{p_0} \right)^b \quad (3-6)$$

where  $q_f$  is the deviatoric stress at failure at the swelling pressure  $p$ ,  $q_{f0}$  is the deviatoric stress at failure (500 kPa) at the swelling pressure  $p_0$ , and  $b$  is 0.77 for MX-80 buffer based on triaxial compression tests conducted at a very low shear rate.

The relation between shear strength and shear rate is given by:

$$q_{fs} = q_{fs0} \left( \frac{v_s}{v_{s0}} \right)^n \quad (3-7)$$

where  $q_{fs}$  is the deviatoric stress at failure at a shear rate  $v_s$ ,  $q_{fs0}$  is the deviatoric stress at failure (2,000 kPa) at the reference shear rate  $v_{s0}$  of  $5 \cdot 10^{-8}$  m/s, and  $n = 0.065$  for MX-80 buffer. It is noted that previous relations were based on shear strain rate rather than shear displacement rate.

Taking these relations together, shear strength for any combination of shear rate and density (or void ratio) can be determined. These relations were based originally on relatively slow triaxial tests. To check the validity of these expressions at very high shear rates, /Börgesson et al. 2004/ performed a series of 34 uniaxial compression tests on MX-80 buffer material. Each cylindrical sample was 20 mm in diameter and 40 mm in height. Three different densities (approximately 1,860, 1,960 and 2,000 kg/m<sup>3</sup>) were tested at shear rates ranging from 0.0001 to 6.0 m/s.

Tests with shear rates between 0.0001 and 0.3 m/s were conducted using a very fast precision compression machine capable of measuring deformation and compression force versus time (Figure 3-2). To achieve higher shear rates, a fall hammer apparatus comprising a hammerhead and weight fixed to the end of a 2 m-long pendulum arm was constructed (Figure 3-3 and Figure 3-4). The speed of the hammerhead at impact was calculated from the drop height. This device was used to shear samples at shear rates between 1.3 and 6.0 m/s. For this apparatus, the sample was placed on a pedestal attached to the frame via a force transducer. Deformation was measured with a displacement transducer placed close to the sample. A rubber block was used to limit shear deformation to about 20 mm to avoid damaging the transducers. Force and displacement were recorded with an oscilloscope.

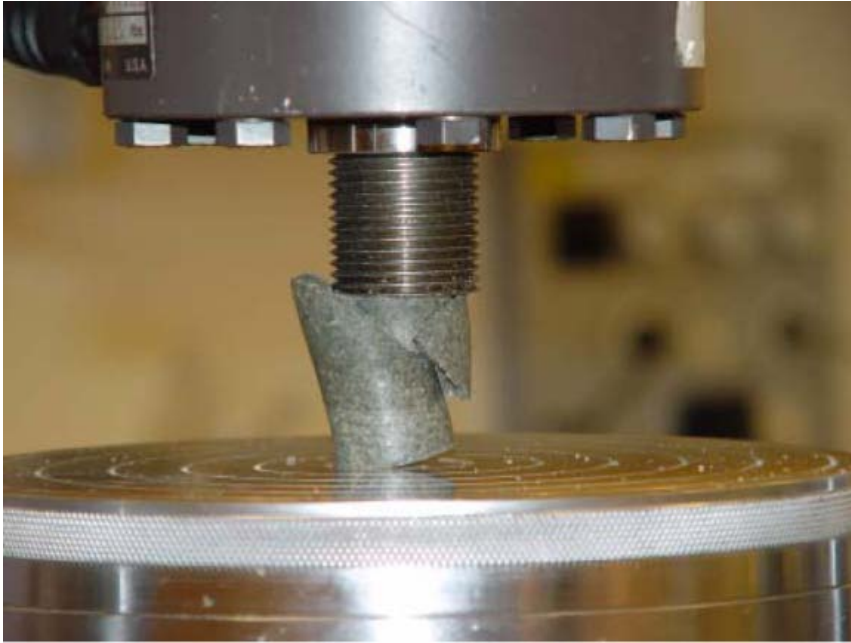


**Figure 3-2.** Precision compression machine used to shear unconfined buffer cylinders (from /Börgesson et al. 2004/).



**Figure 3-3.** Fall hammer device for shearing samples at high shear rates (from /Börgesson et al. 2004/).

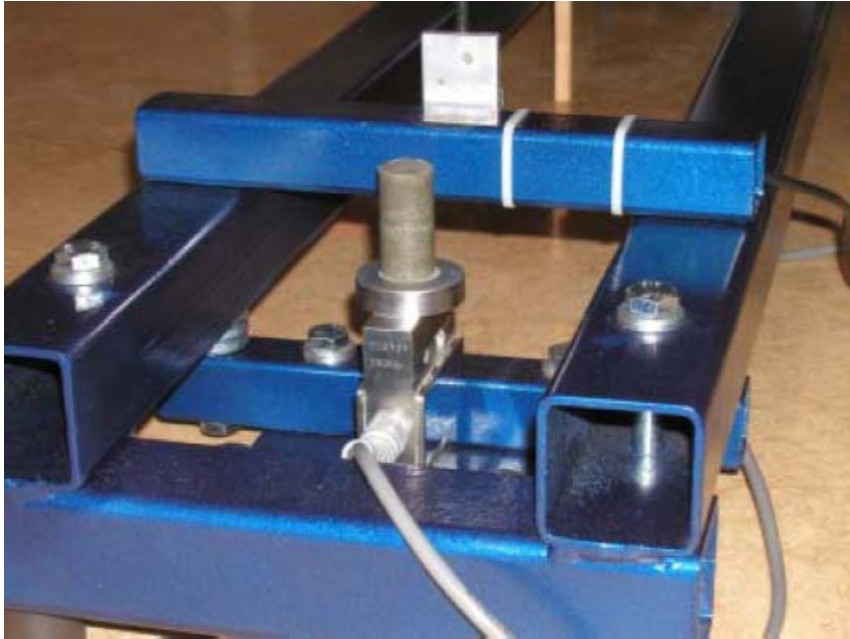


**Figure 3-4.** Details of the pedestal and force and displacement transducers on the fall hammer device (from /Börgesson et al. 2004/).

Samples for these tests were compacted to the target densities and water-saturated in oedometers in confined conditions by wetting from the end faces of the samples. Following each test, density and water ratio for each sample were measured. The maximum deviatoric stress<sup>1</sup>, calculated as the maximum load divided by the area of the sample, was taken as a measure of the strength of the sample. Typical plots from these tests include deformation and deviatoric stress versus time, and deviatoric stress versus strain (calculated as displacement divided by the original length of the sample). A summary of results showing calculated deviatoric strength as a function of shear rate is presented in Figure 3-5. Results from the slow triaxial tests are included as circled values on the plot, along with the trend lines predicted from relations established from previous testing.

In reviewing these earlier reports, there is considerable scatter in the data in Figure 3-5. Values at a shear rate of between 1 and 10 mm/s agree reasonably well with predictions, but at higher shear rates the model over-predicts the measured strength. The trend in results from the two testing methods appear to be different, with the fall hammer device producing a larger change in deviatoric strength with increasing deformation rate on the double logarithmic plot. These discrepancies were thought to be a result of end platen effects (lack of planarity of the sample faces, deviation from a right cylinder in shape) or scale effects (number and size of flaws in specimens). Further investigation of these effects and the scatter in the data was considered warranted.

In addition to these reports on laboratory testing, other studies have been conducted to understand the long-term stability of montmorillonite. The report by /Karnland and Birgersson 2006/ describes an investigation into the processes of montmorillonite transformation to illite and other compounds. Results suggest that only a small fraction (i.e. 1%) of montmorillonite in the buffer will undergo this type of transformation in the conditions expected in a repository. Nonetheless, over long time periods it is considered possible that ion exchange processes may transform sodium bentonite to calcium bentonite, so investigation of both types of bentonite was considered warranted /SKB 2006/.

<sup>1</sup> This value is actually the uniaxial compressive strength and is twice the shear stress in an undrained test.

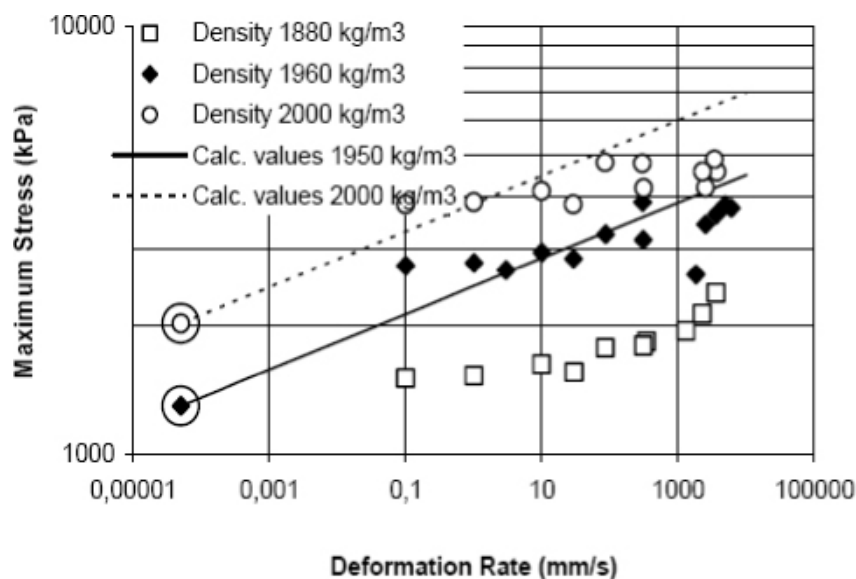


**Figure 3-5.** Results from rapid uniaxial compression tests on samples of compacted buffer material. Circled values are from slow triaxial loading tests (from /Börgesson et al. 2004/).

### 3.2.2 Laboratory testing on buffer material to support SR-Site

In order to derive a material model for SR-Site modeling of rock shear scenarios to support canister design analyses, additional laboratory testing of buffer materials was undertaken /Dueck et al. 2010/. Testing considered new conditions relative to the previous reference buffer case, particularly exposure to high pore water pressure, ion-exchange of Na to Ca in the MX-80 buffer, and influence of strain rate on buffer behaviour. Materials tested were MX-80 buffer, including specimens previously exposed to very high pore water pressure representative of glacial loading conditions; Deponit CaN, a Ca dominated bentonite; and MX-80Ca and MX-80Na, MX-80 ion-exchanged to Ca and Na, respectively. One test series was conducted on purified Wyoming bentonite materials, WyCa and WyNa, to study the difference in behaviour between calcium and sodium bentonite, respectively.

Testing involved a suite of swelling pressure tests, triaxial compression tests and unconfined compression tests (Table 3-2), as well as some measurements of relative humidity to estimate suction and swelling pressure. The report by /Dueck et al. 2010/ describes the various sample preparation and testing techniques, the process for ion exchange of MX-80, and the relation between relative humidity, suction and swelling pressure. Various sample preparation techniques were used for the MX-80, Deponit CaN, and the other bentonite samples. These techniques included preparing a specimen from a block of bentonite by rough sawing and trimming, compaction of a specimen from powder in the laboratory, and compaction of multiple cylindrical specimens to construct a single specimen of specific size for certain tests. Most samples for unconfined compression tests, for example, were constructed by stacking two 20-mm-diameter cylindrical specimens to create a 40 mm high specimen for testing. Some samples were taken from a block of MX-80 bentonite previously exposed to high water pressure to assess glacial loading effects /Harrington and Birchall 2007/.

**Table 3-2. Test matrix for laboratory testing of buffer material /Dueck et al. 2010/.**

Test type (abbreviation)	MX-80	Deponit CaN	MX-80Ca	MX-80Na	WyNa	WyCa
Relative humidity (RH)	2		7	1		
Swelling pressure (SP)	6	1	4			
Triaxial compression (T)	3	2*	3	1		
Unconfined compression at 21°C (UC)	6	3			2	4
Unconfined compression at 12°C (UC)	2	3				
Fast unconfined compression (UC)	8	19				

\* Three special measurements of swelling pressure were made during triaxial testing in addition to the SP test listed.

Basic specimen data including density ( $\rho$ ) and degree of saturation ( $S_r$ ) were estimated for different buffer materials assuming a water density of  $1,000 \text{ kg/m}^3$ , and particle densities of  $2,780 \text{ kg/m}^3$  for MX-80 and ion-exchanged MX-80, and  $2,750 \text{ kg/m}^3$  for Deponit CaN bentonite. Specimens of MX-80 had relatively consistent density and saturation values: laboratory compacted specimens ( $\rho = 2,010 \text{ kg/m}^3$ ,  $S_r = 99\%$ ), block specimen before water pressure ( $\rho = 2,010 \text{ kg/m}^3$ ,  $S_r = 97\%$ ), and block specimen after water pressure ( $\rho = 2,020 \text{ kg/m}^3$ ,  $S_r = 100\%$ ). Deponit CaN specimens were prepared from powder to various densities.

Relative humidity measurements were taken on samples of MX-80, and ion-exchanged MX-80Ca and MX-80Na (four of these from triaxial test specimens). Measured suction values were  $11,540$  and  $9,830 \text{ kPa}$  for MX-80 blocks before and after application of water pressure, respectively. Suction values for MX-80Ca ranged from  $6,320$  to  $18,953 \text{ kPa}$ . A value of  $4,460 \text{ kPa}$  was measured on a specimen of MX-80Na. These values were used to estimate swelling pressure.

Swelling pressure tests were conducted on MX-80, Deponit CaN, and ion-exchanged MX-80Ca specimens using a constant volume apparatus instrumented with a load cell. Specimens were  $35 \text{ mm}$  in diameter and  $13$  or  $20 \text{ mm}$  high. Swelling pressure values of  $4,700$  and  $4,021 \text{ kPa}$  were recorded for MX-80 block specimens before and after water pressure application at respective densities of  $1,970$  and  $1,960 \text{ kg/m}^3$ , and  $101\%$  saturation. Swelling pressure measured on a specimen of Deponit CaN using the swelling pressure test apparatus was  $18,930 \text{ kPa}$  ( $\rho = 2,070 \text{ kg/m}^3$ ,  $S_r = 100\%$ ); other values measured during triaxial tests were  $8,030 \text{ kPa}$  ( $\rho = 1,970 \text{ kg/m}^3$ ,  $S_r = 97\%$ ),  $14,990 \text{ kPa}$  ( $\rho = 2,040 \text{ kg/m}^3$ ,  $S_r = 98\%$ ), and  $12,710 \text{ kPa}$  ( $\rho = 2,020 \text{ kg/m}^3$ ,  $S_r = 100\%$ ). Measured swelling pressure for specimens of MX-80 ion-exchanged to MX-80Ca (expressed as MX-80 swelling pressure/MX-80Ca swelling pressure) were  $5,820/6,570 \text{ kPa}$  ( $\rho = 1,970 \text{ kg/m}^3$ ,  $S_r = 100\%$ ),  $6,150/7,090 \text{ kPa}$  ( $\rho = 1,980 \text{ kg/m}^3$ ,  $S_r = 99\%$ ),  $16,360/19,520 \text{ kPa}$  ( $\rho = 2,090 \text{ kg/m}^3$ ,  $S_r = 100\%$ ), and  $13,900/16,750 \text{ kPa}$  ( $\rho = 2,080 \text{ kg/m}^3$ ,  $S_r = 100\%$ ).

Triaxial compression tests on specimens of MX-80, Deponit CaN, and ion-exchanged MX-80Ca and MX-80Na used a high pressure triaxial cell instrumented with deformation transducer, load cell and pore- and cell-pressure transducers. Specimens were  $35 \text{ mm}$  in diameter and  $70 \text{ mm}$  high. A constant shearing rate of  $5 \cdot 10^{-6} \text{ mm/s}$  was used for tests on MX-80 specimens, resulting in maximum deviator stress values of  $2,170$ ,  $2,835$ , and  $2,704 \text{ kPa}$  for lab compacted ( $\rho = 1,980 \text{ kg/m}^3$ ,  $S_r = 101\%$ ), block before water pressure ( $\rho = 1,990 \text{ kg/m}^3$ ,  $S_r = 101\%$ ), and block after water pressure ( $\rho = 2,020 \text{ kg/m}^3$ ,  $S_r = 101\%$ ) specimens. For Deponit CaN specimens, two tests at shearing rates of  $4.25 \cdot 10^{-6}$  and  $4.5 \cdot 10^{-6} \text{ mm/s}$  produced maximum deviator stress values of  $2,879$  and  $4,349 \text{ kPa}$ , respectively, for fully saturated specimens with densities of  $1,970$  and  $2,030 \text{ kg/m}^3$ . Three tests on MX-80Ca at shearing rates of  $9.1 \cdot 10^{-6}$ ,  $4.7 \cdot 10^{-6}$  and  $5.2 \cdot 10^{-6} \text{ mm/s}$  resulted in maximum deviator stress values of  $2,310$ ,  $2,580$  and  $3,740 \text{ kPa}$  for specimens T1 ( $\rho = 1,990 \text{ kg/m}^3$ ,  $S_r = 100\%$ ), T2 ( $\rho = 2,010 \text{ kg/m}^3$ ,  $S_r = 99\%$ ), and T3 ( $\rho = 2,050 \text{ kg/m}^3$ ,  $S_r = 98\%$ ), respectively. One test on MX-80Na at a shearing rate of  $4.4 \cdot 10^{-6} \text{ mm/s}$  produced a maximum deviator stress of  $2,410 \text{ kPa}$  for specimen T1 ( $\rho = 2,010 \text{ kg/m}^3$ ,  $S_r = 101\%$ ).

Unconfined compressive tests were conducted under various conditions: at relatively low deformation rates at ambient temperature ( $21^\circ\text{C}$ ) and at a reduced temperature ( $12^\circ\text{C}$ ) using a mechanical press, and at high shearing rates under ambient temperature conditions using a very fast precision compression machine (capable of shearing rates between  $0.1 \text{ mm/s}$  and  $300 \text{ mm/s}$ ). Test results (corrected for seating effects between the platen and specimen) follow.

- Ambient temperature unconfined compressive tests on MX-80 specimens were conducted at a constant shearing rate of  $5 \cdot 10^{-3} \text{ mm/s}$ . Maximum deviator stress values of  $2,580$  and  $2,400 \text{ kPa}$  were measured for lab compacted specimens ( $\rho = 2,010 \text{ kg/m}^3$ ,  $S_r = 98\%$ ). Block specimens with  $96\%$  saturation before water pressure application had maximum deviator stress values of  $3,250$  and  $3,150 \text{ kPa}$  ( $\rho = 2,020$  and  $2,010 \text{ kg/m}^3$ , respectively). Values for block specimens after water pressure application were  $2,860$  and  $2,850 \text{ kPa}$  ( $\rho = 2,020$  and  $2,030 \text{ kg/m}^3$ ,  $S_r = 100$  and  $101\%$ , respectively).
- Ambient temperature unconfined compressive tests on DeponitCaN at a shearing rate of  $5 \cdot 10^{-3} \text{ mm/s}$  resulted in maximum deviator stress values of  $2,260$ ,  $3,340$  and  $5,250 \text{ kPa}$  for specimens UC11 ( $\rho = 1,970 \text{ kg/m}^3$ ,  $S_r = 102\%$ ), UC13 ( $\rho = 2,000 \text{ kg/m}^3$ ,  $S_r = 102\%$ ), and UC15 ( $\rho = 2,050 \text{ kg/m}^3$ ,  $S_r = 101\%$ ), respectively.

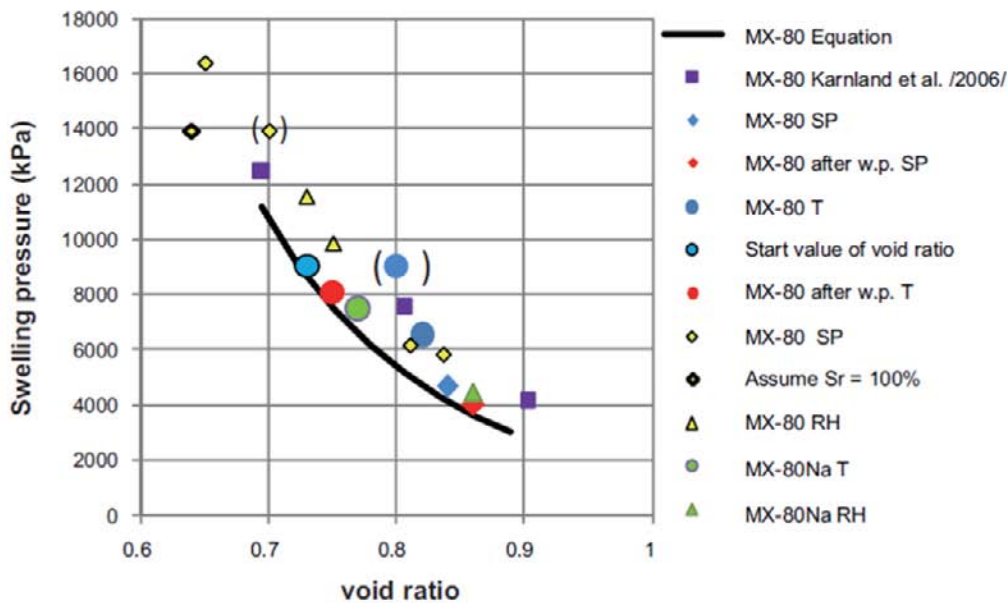
- Ambient temperature unconfined compressive test on purified MX-80 (WyNa and WyCa) were conducted at a shearing rate of  $3 \cdot 10^{-3}$  mm/s on 20-mm-diameter specimens with height to diameter ratio of unity. Maximum deviator stress values from tests on WyNa were 2,540 and 1,990 kPa for specimens UC1 ( $\rho = 2,020 \text{ kg/m}^3$ ,  $S_r = 100\%$ ) and UC2 ( $\rho = 2,010 \text{ kg/m}^3$ ,  $S_r = 101\%$ ), respectively. Values for tests on WyCa were 2,422, 3,400, 3,520 and 2,540 kPa, respectively, for specimens UC3 ( $\rho = 1,970 \text{ kg/m}^3$ ,  $S_r = 101\%$ ), UC4 ( $\rho = 2,020 \text{ kg/m}^3$ ,  $S_r = 100\%$ ), UC5 ( $\rho = 2,010 \text{ kg/m}^3$ ,  $S_r = 101\%$ ), and UC6 ( $\rho = 1,960 \text{ kg/m}^3$ ,  $S_r = 100\%$ ).
- Reduced temperature unconfined compression tests on MX-80 specimens resulted in maximum deviator stress values of 2,098 and 2,744 kPa for two specimens ( $\rho = 1,980$  and  $2,020 \text{ kg/m}^3$ ,  $S_r = 98$  and  $99\%$ , respectively).
- Reduced temperature unconfined compression tests on Deponit CaN produced maximum deviator stress values of 2,185, 2,931, and 4,863 kPa for specimens UC5 ( $\rho = 1,960 \text{ kg/m}^3$ ,  $S_r = 102\%$ ), UC7 ( $\rho = 1,990 \text{ kg/m}^3$ ,  $S_r = 101\%$ ), UC9 ( $\rho = 2,040 \text{ kg/m}^3$ ,  $S_r = 101\%$ ). Some problems with slipping were noted in one test likely due to slightly tilting end surfaces.
- Fast unconfined compressive tests were conducted on MX-80 and Deponit CaN at deformation rates ranging from 0.003 to 269 mm/s. Results are summarised in Table 3-3. Specimens designated DT or ET were compacted from high water content material to almost full saturation. Specimens designated ESP were drilled from saturated specimens from the swelling pressure device. The other specimens were compacted from powder.

**Table 3-3. Summary of fast unconfined compression tests /Dueck et al. 2010/.**

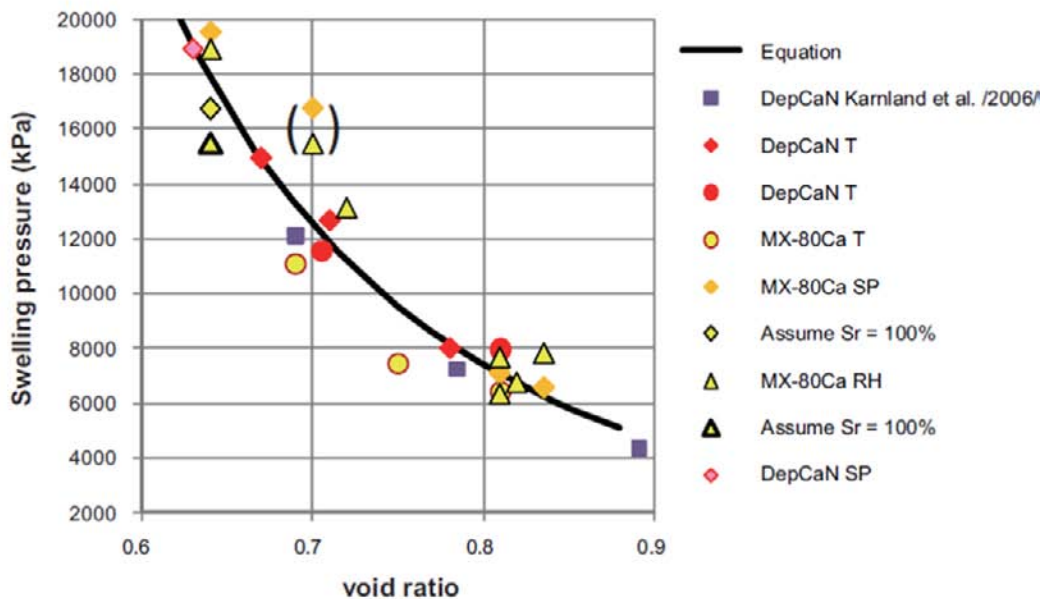
Ref.	Shearing Rate (mm/s)	Density (kg/m <sup>3</sup> )	Saturation (%)	Max. Deviator Stress (kPa)
<b>MX-80</b>				
D01	0.003	2,050	97	3,803
D02	0.1	2,040	97	3,909
D03	10	2,030	97	4,094
D04	98	2,030	97	4,391
D05	268	2,030	97	4,979
D06	271	2,040	97	5,136
DT1	192	2,080	98	6,171
DT2	218	2,070	96	6,978
<b>Deponit CaN</b>				
E01	0.003	2,060	101	4,959
E02	0.003	2,050	100	4,837
E03	0.1	2,040	100	5,091
E04	1	2,050	102	5,685
E05	10	2,050	101	6,551
E06	98	2,050	102	6,841
E07	218	2,050	101	6,607
E08	269	2,040	100	6,631
E09	0.1	2,050	101	5,405
E10	1	2,060	101	6,239
E11	10	2,060	101	6,245
E12	97	2,050	101	6,578
E13	275	2,050	101	6,800
E14	266	2,050	100	7,409
ET1	105	2,070	97	8,268
ET2	0.1	2,070	97	6,456
ET3	226	2,060	97	7,852
ESP1	239	2,070	99	8,693
ESP2	236	2,070	100	9,169

Based on these new laboratory test results, relations between swelling pressure, void ratio (or density), shear strength and strain rate for MX-80 buffer used for SR-Can were revised and extended to other buffer materials /Börjesson et al. 2010/.

The relation between swelling pressure and void ratio is expressed by Equation 3-5. The constants used in this equation for MX-80 buffer were a reference void ratio of 1.1, reference swelling pressure of 1,000 kPa, and an exponent  $\beta$  value of  $-0.19$ . This relation is plotted in the upper chart in Figure 3-6 along with results from laboratory tests conducted on MX-80 and MX-80Na /Dueck et al. 2010/. The relation and parameters used for SR-Can under-estimate the swelling pressure by about 1–2 MPa for the data shown. For Ca-bentonites (including Deponit CaN and MX-80Ca), derived constants in Equation 3-5 are reference void ratio of 1.33, reference swelling pressure of 1,000 kPa, and an exponent  $\beta$  value of  $-0.254$ . This relation is plotted in the lower chart in Figure 3-6 along with laboratory test results /Dueck et al. 2010/.



a) MX-80 and ion-exchanged MX-80Na



b) Deponit CaN and ion-exchanged MX-80Ca

**Figure 3-6.** Results from swelling pressure tests (SP), triaxial tests (T) and relative humidity measurement (RH) compared to empirical relation between swelling and void ratio /Börjesson et al. 2010/.

The relation between shear strength (expressed as maximum deviator stress) and swelling pressure is shown by Equation 3-6. The constants used in this equation for MX-80 buffer were a reference swelling pressure of 1,000 kPa, a deviator stress at failure of 500 MPa at the reference swelling pressure, and an exponent  $b$  value of 0.77. As shown in Figure 3-7, new laboratory tests on MX-80 /Dueck et al. 2010/ confirm the relation for MX-80 used for SR-Can. For other bentonites (including Deponit CaN, MX-80Ca and Moosburg Ca), the derived reference swelling pressure and exponent  $b$  in Equation 3-6 are the same as for MX-80, but the values for maximum deviator stress at failure at the reference swelling pressure for Deponit CaN, MX-80Ca and Moosburg Ca are 610, 540, and 750 kPa, respectively. These relations are also plotted in Figure 3-7, along with results from the laboratory tests /Dueck et al. 2010/.

The relation between shear strength (expressed as maximum deviator stress) and shear rate is given by Equation 3-7. The constants used in this equation for MX-80 buffer were a reference shear rate of  $5 \cdot 10^{-8}$  m/s, a deviator stress at failure of 2.0 MPa at the reference shear rate, and an exponent  $n$  value of 0.065. To improve the utility of this expression, /Börgesson et al. 2010/ redefined the parameters  $v_s$ , and  $v_{s0}$  as strain rate and reference strain rate, respectively, with units of  $s^{-1}$ . This formulation was considered more relevant for finite element modeling. Applying the new expression to triaxial and unconfined compression test results on Deponit CaN /Dueck et al. 2010/ at the dimensioning density of  $2,050 \text{ kg/m}^3$ , the derived constants are a reference strain rate of  $10^{-6} \text{ s}^{-1}$ , a deviator stress at failure of 4.27 MPa at the reference strain rate, and an exponent  $n$  value of 0.038. This relation is plotted in Figure 3-8 along with results from the laboratory tests /Dueck et al. 2010/. The new test results for MX-80 shear strength at a density of  $2,040 \text{ kg/m}^3$  fall very close to those from previous tests at a density of  $2,000 \text{ kg/m}^3$ . The reason for this is not obvious but may relate to subtle differences in specimen preparation or planarity/orthogonality of end faces of specimens.

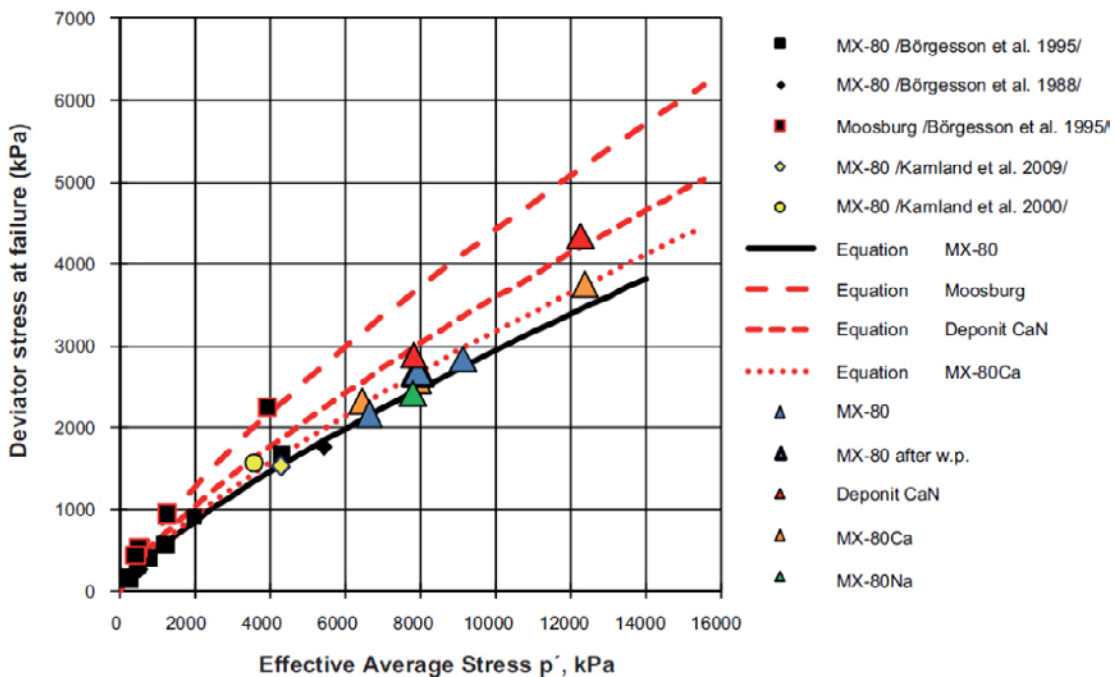


**Figure 3-7.** Results from triaxial tests on various bentonite materials showing the relation between deviator stress at failure and effective average stress /Börgesson et al. 2010/.

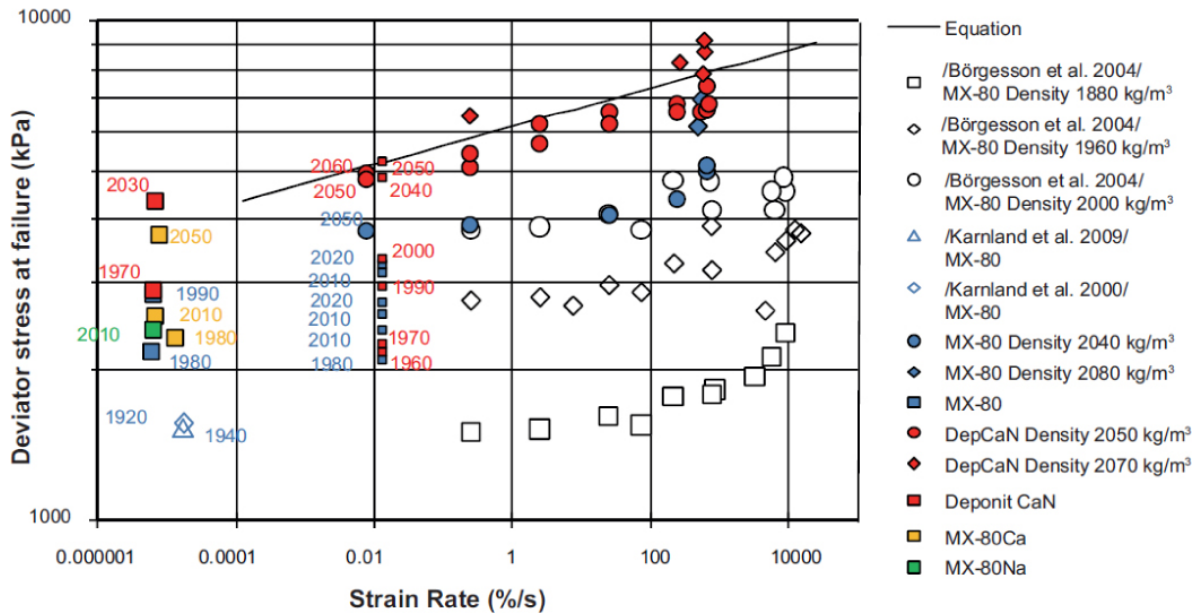


**Figure 3-8.** Results from triaxial and unconfined compression tests on various bentonite materials. Coloured symbols represent new test results from /Dueck et al. 2010/ and uncoloured symbols are from previous tests recast in terms of strain rate /Börgesson et al. 2010/.

Based on laboratory testing results, /Börgesson et al. 2010/ observed that the stress-strain behaviour of a range of bentonite materials is similar. The deviator stress increases linearly to about half of the maximum deviator stress at failure, then starts to yield to reach a maximum value at 3 to 10% strain. Post-peak behaviour is almost perfectly plastic with some exceptions. A generalised model was developed with an initial linear elastic rise to 1% strain at a stress equal to 58% of the maximum deviator stress at failure, plastic hardening between 1% and 5.3% strain to the maximum deviatoric stress determined using the relations described above, and almost ideally plastic behaviour in the post-peak region /Börgesson et al. 2010/. A typical stress-strain curve relation for a density of 2,050 kg/m<sup>3</sup> at a strain rate of 10 s<sup>-1</sup> is shown in Figure 3-9. This relation scales with maximum deviator stress.

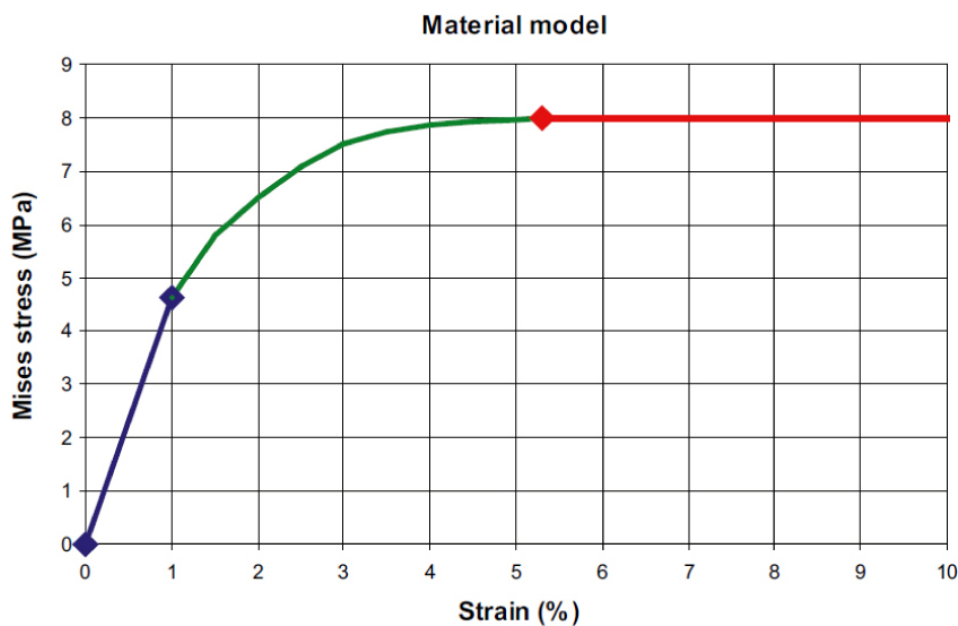


**Figure 3-9.** General stress-strain relation used for the material model of bentonite /Börgesson et al. 2010/.

The material model was implemented in the finite element code Abaqus with elastic and plastic properties defined as a function of strain rate and density /Börgesson et al. 2010/. Young's modulus values specified for Deponit CaN at density values of 2,050 and 2,000 kg/m<sup>3</sup> were 462 and 347 MPa, respectively. A Poisson's ratio of 0.49 was specified for use in model simulations. According to /Börgesson et al. 2010/, the model is considered an improvement over that used for SR-Can because the bentonite Deponit CaN is used as the reference buffer material, rate dependence in the model is more realistic, and the maximum Mises stress is rate dependant which reduces stiffness in parts of the buffer that do not experience significant strain. Review of laboratory tests at reduced temperature and on specimens previously subjected to high water pressure suggested that these effects are relatively minor and do not affect the applicability of the buffer model /Börgesson et al. 2010/.

### **3.3 Scaled buffer/canister shear tests**

#### **3.3.1 Description of scaled laboratory tests**

To provide a basis for refining models of bentonite behaviour under shearing conditions, /Börgesson 1986/ designed and conducted 1:10 scale shear tests on a simulated copper canister with buffer overpack. The buffer was water-saturated MX-80 sodium bentonite, and the simulated canister was a solid HPOF copper rod with similar average stiffness as a real canister. Shaped buffer components to construct the sample were created from a mass of pre-compacted buffer with a bulk density of 2.14 t/m<sup>3</sup> and a water ratio of 9%. The permeable rock was simulated by a cylindrical bronze filter 20 mm thick, comprising small bronze pellets to produce a maximum pore size of 12 µm, installed inside a cylinder made of acid proof stainless steel 2333. The filter was permeable enough to allow unlimited water supply to the buffer without buffer penetration into the filter, and was stiff enough to resist swelling pressure and stress concentrations during shearing. To ensure a perfect fit between the filter and the stainless steel cylinder, the cylinder was made 0.2 mm smaller than the outer diameter of the filter, then expanded through heating to accommodate the filter. A tight fit was obtained upon cooling.

The test cylinder comprised two cylindrical halves forming a central shear plane orthogonal to the cylinder axis. The cylinder halves were rigidly mounted in a steel frame during saturation, with one half freed to shear during the shearing phase of the test. Stiffness of the frame and cylinder was a primary consideration to avoid unwanted deformation of the system. Filters were mounted at the top and bottom ends of the cylinder to provide distilled water to saturate the sample. To ensure a water-tight frictionless contact between the two halves of the test cylinder, opposing end faces of the test cylinders and inner filters were each covered by a ring-formed plate with an O-ring seal to prevent leakage. The plates had holes and channels to allow passage of water from one half to the other, and a smooth lubricated surface to minimise friction during shearing. A second smooth lubricated plate at the top of the sliding half of the cylinder was used to restrain the sample once the two halves of the cylinder were disengaged for the shearing phase. Axial restraint was provided by threaded reaction bars through the end plate. The elasticity of the bars allowed narrow annular gaps to open at the ends of the shearing cylinder upon bentonite swelling. These gaps prevented direct contact between the shearing cylinder, the end plate, and the fixed cylinder, but were small enough to prevent bentonite from swelling out through the gap. The filter in contact with the end plate was also lubricated. The testing apparatus is shown in Figure 3-10.

Saturation with distilled water was predicted to take about 60 days, but was generally complete after about 40 days. Swelling pressure was monitored using six pressure transducers during saturation. The measured swelling pressure generally agreed with that predicted using Equation 3-3 (i.e. 8.9 MPa at a bulk density of 2.05 t/m<sup>3</sup>), although some anomalies in swelling pressure were attributed to variations in density in the sample following saturation. The test cylinder was positioned vertically during the saturation phase.

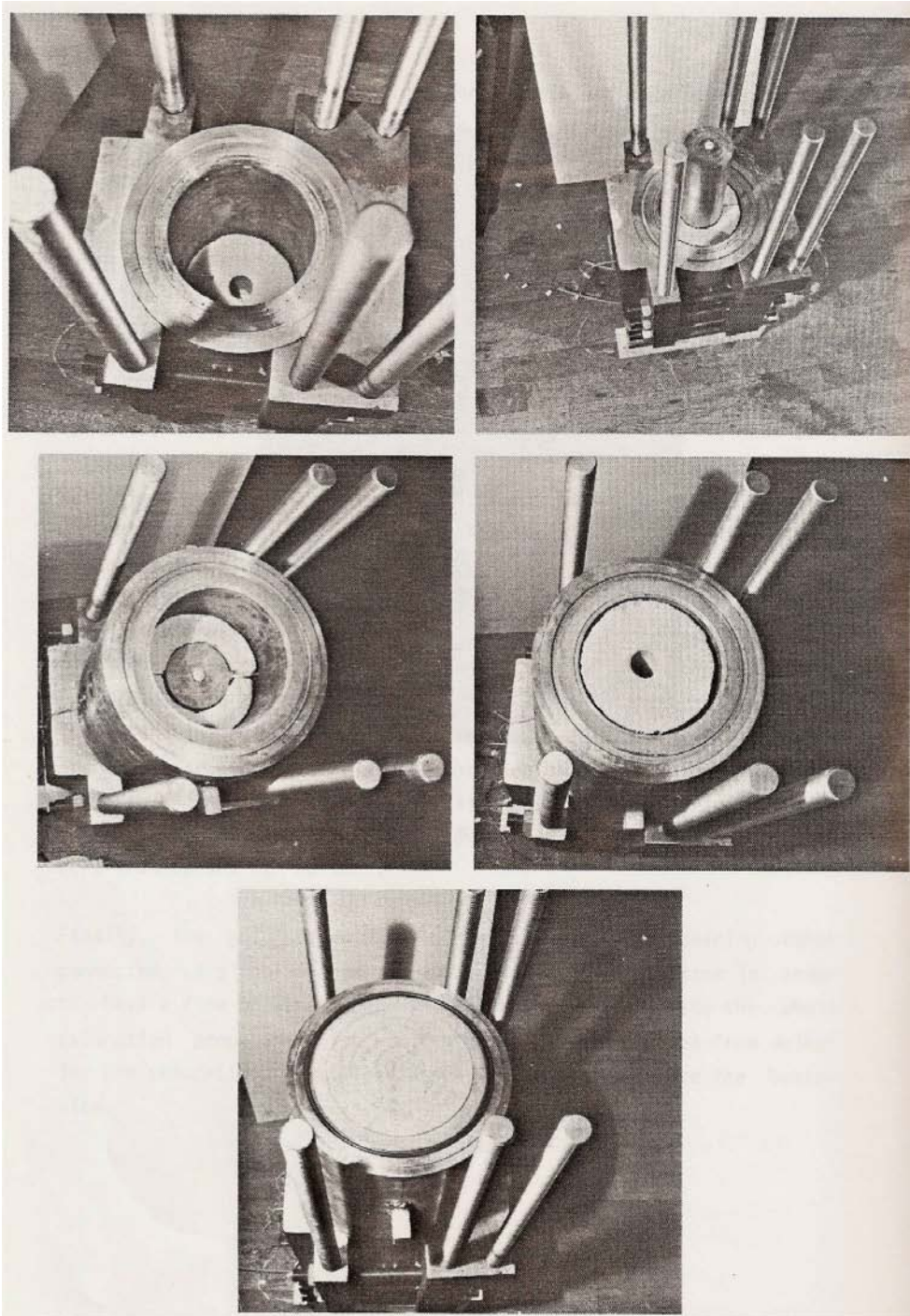


*Figure 3-10. Apparatus used for 1:10 scale shear testing of buffer-canister system at various stages of sample preparation (from /Börgesson 1986/).*

During the shearing phase, eighteen instruments were monitored. These included four force transducers (later reduced to three during the tests) and two displacement transducers to measure the applied load/displacement response at the loading platen, six pressure transducers to measure earth pressure at three opposing points on the buffer-canister and buffer-filter interfaces, five strain gauges on the surface of the simulated copper canister arranged in an anti-symmetric pattern relative to the pressure sensors, and a displacement transducer housed in a copper tube penetrating the stainless steel test cylinder to measure the position of the canister relative to the wall of the test cylinder. The instrumentation layout is shown in Figure 3-11. The test cylinder was positioned horizontally during the shearing phase.

Following a pilot test using an unsaturated sand-bentonite mixture and an iron tube to simulate the canister, three shear tests were conducted on MX-80 bentonite with a simulated copper canister at different shear displacements and shear rates:

- Test 1: 28 mm displacement at 0.032 mm/s.
- Test 2: 30 mm displacement at 1.9 mm/s.
- Test 3: 21 mm displacement at 160 mm/s.

The first two tests used a large compression machine at the Technical University of Lund, Sweden. The third test required a very large compression machine at Alfa Laval in Lund, Sweden to achieve the high shear rate.

Sample characterisation followed testing to determine density, water content, degree of saturation, homogenisation, and effect of shear on the bentonite and canister. Initial characterisation after the first test identified problems with free swelling of the buffer before sampling could be completed, necessitating modified sampling and characterisation procedures to minimise these effects. Sampling showed that the buffer was not completely homogenised at the time of testing despite full development of swelling pressure. Values used for densities of solids and water in the calculations of bulk density were 2.87 and 0.965 t/m<sup>3</sup>, respectively. Test results were used to validate numerical models, comparing measured force, pressure change, canister strain, relative displacement, canister bending, and axial deformation of the shear plane to model predictions (discussed further in the next section).

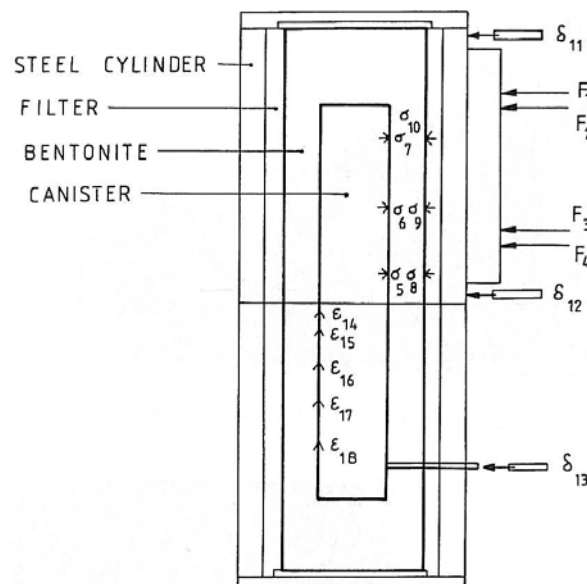


**Figure 3-11.** General instrumentation layout for 1:10 scale model shear tests (from /Börgesson 1986/).

The results from the three tests indicated that the force required to shear the sample 15 mm was shear rate dependent, increasing from about 145 kN at the lowest shear rate to almost 200 kN at the highest shear rate. The ratio of canister shear deformation to total shear deformation increased from about 50% to almost 100% over the same range of shear rates. High strain and axial stress were generated in the 450-mm-long canister at a distance of about 60 to 120 mm from the imposed shear plane. Specific observations from the tests are as follows:

- Test 1 was conducted at an average swelling pressure of 9.4 MPa. The shear test results indicate possible rotation of the shearing cylinder during testing, with the displacement transducer furthest from the shearing plane registering 6 mm higher displacement than the transducer near the shear plane. Pressure change ranged from about -3 to 14 MPa at the various pressure sensors during the test. Canister strain measured by two of the strain gauges reached as high as 1.4% compression at about 20 mm displacement. Total force reached about 150 kN at this same displacement. About 1.6 mm movement of the canister end relative to the shear cylinder wall was recorded during the test, with about 1.2 mm occurring at 20 mm shear displacement. Measurements of the position and shape of the canister following testing indicated symmetrical deformation in relation to the shear plane, with bending localised in the central half of the canister. The canister experienced about 14 mm of shear deformation, or 50% of the total shear displacement of the test.
- Test 2 was conducted at an average swelling pressure of 8.9 MPa. Pressure change ranged from about -5 to 22 MPa at the various sensors during the test. Canister strain measured by one of the strain gauges (the others malfunctioned during testing) reached as high as 3% compression at about 30 mm displacement. Total force reached about 180 kN at this same displacement. Measurements of the position and shape of the canister following testing indicated a similar deformation pattern as Test 1, but the canister experienced about 18.5 mm of shear deformation, or 62% of the total shear displacement of the test.
- Test 3 was conducted at an average swelling pressure of 9.3 MPa. The shear test results indicate possible rotation of the shearing cylinder during testing, with the displacement transducer furthest from the shearing plane registering 4 mm higher displacement than that near the shear plane. Some difficulties were encountered in maintaining a constant shear rate during the latter part of this test, so only the first 15 mm of displacement was considered in the analysis. The resulting force/displacement response showed a rapid increase in force during the first 3 mm of displacement, then a non-linear work hardening plastic response for the remainder of the test. Pressure change ranged from about -5 to 11 MPa at the various sensors during the test. Canister strain measured by the strain gauges reached as high as 2.6% compression at about 15 mm displacement. Total force reached about 197 kN at this same displacement. Measurements of the position and shape of the canister following testing indicated a non-symmetrical deformation pattern, with 20 mm of shear deformation at one end and 14 mm at the other end. Based on end face positions, the estimated canister shear deformation was 18 to 20 mm, which was close to 100% of the total shear displacement of the test. Measurements of axial displacement of the buffer at the shear plane following the test showed that bentonite had moved from the compressed part of the sample to the expanded part near the shear plane. The contours associated with this plane of axial deformation were used in subsequent comparisons with predicted model results.

The author concluded that stress-strain properties of the bentonite and canister must be related to the applied strain rate to achieve an appropriate result. The models used in the initial analysis of these tests did not predict the measured responses very well, illustrating the need to develop more representative material models that included non-linear stress-strain relations and viscous (i.e. rate dependent) behaviour. Despite some issues with instrumentation, particularly the strain gauges and some pressure gauges, the tests provide a useful basis for validating numerical models. Further testing of this type was recommended to consider other material compositions and densities.

As part of numerical model simulations (described in the next section), test results were reviewed by /Börgesson and Hernelind 2010/. Using a density of solids value of 2,780 kg/m<sup>3</sup> rather than the value of 2,700 kg/m<sup>3</sup> used by /Börgesson 1986/, the calculated densities at saturation were 2,017, 2,035, and 2,053 kg/m<sup>3</sup> for Tests 1, 2 and 3, respectively. Corresponding swelling pressures were calculated to be 9.4, 8.6 and 10.0 MPa, respectively.

### 3.3.2 Numerical simulation of scaled laboratory tests

/Börgeßon 1988/ presented results of three-dimensional finite element modeling using Abaqus and various material models to simulate effects of rock shear, settlement and swelling. A non-linear stress-strain relation and elasto-plastic total stress model was selected to simulate sudden rock shear, using the results of 1:10 scale testing /Börgeßon 1986/ for comparison. The stress-strain relation simulated elastic behaviour to about 1% strain followed by non-linear yielding under work hardening. Peak strength was reached at about 5% strain. The stress-strain relation for the buffer was shown to be density and strain-rate dependent, and was therefore adjusted to account for initial density of the buffer, applied strain rate, and variations in strain rate within different parts of the model. The copper behaviour was simulated using a non-linear elasto-plastic model, with the plastic state reached at 50 MPa deviatoric stress and 0.3% strain. The material behaviour of the copper exhibited strong strain-hardening even after 25% strain.

/Börgeßon 1988/ noted that, for the rock shear scenario simulated at 1:10 scale, the strain rate of the clay buffer ranged from several hundred percent at the shear plane to less than one percent in the top corners. Comparison of simulation results using the strain-rate dependent stress-strain relations to those from the 1:10 scale rock shear tests showed good agreement in terms of the total force versus deformation response, strain-rate dependent shear resistance, bending of the canister, axial displacement of the clay, total pressure in the clay in the shear direction, and strain in the canister. The author concluded that the selected material models for MX-80 buffer and copper adequately simulated the measured responses. Given that the stress-strain response was found to be dependant on both strain rate and density, a range of density-strain rate combinations could be simulated using a single strain rate and varying material density, mapping responses at other strain rates into an intermediate density response. Based on this approach, a sensitivity study of the 1:10 scale model tests was conducted using the material models in eight different constant volume shearing scenarios at an assumed strain rate of 0.6%/h. The key results from the study are as follows:

- Density of the buffer significantly affected the amount of strain experienced by the canister. At a bulk density of 2.14 t/m<sup>3</sup>, the canister already experienced plastic strain at 3 mm displacement, and as much as 75% of the canister symmetry plane was plasticised up to 4% plastic strain at 12 mm displacement. For a bulk density of 1.9 t/m<sup>3</sup>, no plastic strain was evident in the canister up to a displacement of 8.7 mm, just rotation of the canister within the buffer.
- Thickness of the buffer did not significantly affect the strain in the canister based on the maximum Mises stress, the maximum plastic strain, and the percentage of canister at yield for three clay thicknesses (27, 40 and 60 mm) at a bulk density of 2.08 t/m<sup>3</sup>. This finding was attributed to the fact that a large amount of the clay reached its maximum shear resistance at a relatively small displacement, and therefore the canister was surrounded by plasticised clay in all cases. This findings was not considered valid for buffer material at high density or when buffer materials with high shear resistance are used.
- The initiation of plastic behaviour in the copper canister occurred about halfway between the shear plane and the end face as opposed to at the shear plane in a simulation of a hollow steel cylinder. This finding emphasised the need to use representative materials in laboratory tests and model simulations to examine material behaviour.
- By inference, these findings also hold for strain-rate effects given that one stress-strain relation is valid for a number of strain rate-density combinations. A change in shear rate by a factor of 10 corresponds roughly to a change in density of 0.01 t/m<sup>3</sup>.

Using the 1:10 scale tests as a primary basis for model validation, /Börgeßon and Hernelind 2010/ presented modeling results from application of the updated MX-80 bentonite model used for SR-Site /Börgeßon et al. 2010, Dueck et al. 2010/.

The stress-strain relation for MX-80 bentonite used for the three simulations was based on the generalised function shown in Figure 3-9. For the saturated buffer material with a density of  $2,020 \text{ kg/m}^3$  at the reference strain rate of  $10^{-4} \text{ s}^{-1}$ , the calculated elastic modulus is 179 MPa and the maximum Mises stress is 3.10 MPa at a strain of 5.4%. Values of elastic modulus and maximum Mises stress for other strain rates can be determined using Equation 3-7. Stress-strain relations were determined for various material densities spanning those observed in the 1:10 scale tests.

Although actual Poisson's ratio was expected to be 0.5 for MX-80 buffer due to the constant volume configuration of the tests, Poisson's ratio was assumed to be 0.49 in each case to avoid numerical problems with the model. This same approach was used in previous model simulations of rock shear.

The stress-strain properties of copper in the rods used to simulate the canister in the 1:10 scale tests were investigated by several laboratories using samples from one of the original rods (Figure 3-12). Results from three tensile tests conducted at a strain rate of about 5%/s were used to develop a material model for copper. This model is similar to the elastic-plastic model for bentonite, with a constant elastic modulus of 120 GPa, Poisson's ratio of 0.33, and strain-rate dependent plasticity. The maximum Mises stress is reached at 40% plastic strain followed by a sharp drop in strength.

The Abaqus model of the 1:10 scale tests incorporated about 50,000 elements. Plastic properties of each element were made a function of strain rate, and a constant elastic modulus was assigned. Contact elements used at all interfaces between the buffer and the copper canister were characterised by a friction angle of  $5.7^\circ$  and zero cohesion. The contact between buffer and canister was released if swelling pressure was lost. Simulations were conducted using a constant buffer density throughout the model, and with the model subdivided into three zones with different density to match observed density distribution in the original 1:10 scale tests.



**Figure 3-12.** Copper rod used in one of the 1:10 scale rock shear tests just prior to sampling for stress-strain testing (photo taken April 30, 2010 at Clay Technology AB laboratory in Lund, Sweden).

Results from the model simulations were compared to measured test data for total force, pressure change, canister strain, canister bending and axial buffer displacement. Both trends and the ratio of calculated to measured values (C/M ratio) were investigated for each simulation. C/M ratios greater than unity indicate overprediction by the model, and those less than unity indicate underprediction. Based on the three density zone model, key findings were:

- The total force C/M ratio was 1.08, 1.08, and 1.07 for Tests 1, 2 and 3, respectively. The measured force required to shear the specimen in each test was based on values from three to four force transducers. The C/M ratio values and trends suggest that the model slightly overpredicts the applied force required to shear the test specimen in each case. The general trend in the force versus displacement response measured in each case was similar to the modeled response. The measured response from Test 3 indicated that the elastic modulus increased in the first few millimetres of movement. This stiffening effect was not predicted by the model, and could be related to a seating adjustment in the test. Overprediction of the force suggests that the buffer shear strength or stiffness is slightly over-estimated in the model.
- The average pressure change C/M ratio was 0.94, 0.99, and 1.27 for Tests 1, 2 and 3, respectively. The measured values were based on results from four of the six installed pressure transducers. These results indicate that the model overpredicts the average pressure change associated with shearing of the test specimen in Test 3, but otherwise predicts pressure change well in the other tests. The general trends in the radial stress versus displacement responses measured in each case were similar to the modeled responses, with some exceptions related possibly to sensor malfunction or mislabelling. For Tests 2 and 3, the model tended to overpredict the pressure change at sensors experiencing increased radial stress, while those experiencing a reduction in radial stress tended to show better agreement with model predictions. The opposite was true for Test 1. The discrepancy for those sensors in areas of increased compression suggests that the buffer stiffness in the model may be too high.
- The canister strain C/M ratio was 1.28, 1.02, and 1.08 for Tests 1, 2 and 3, respectively. The measured results were based on two of the five strain gauges on the canister surface. These two strain gauges yielded considerably higher strains than the other strain gauges used in the tests. At maximum displacement, the predicted strains tended to exceed the measured strains, but there was better agreement at displacement of about 15 mm. This trend suggests that the buffer stiffness in the model may be too high, or that the actual strain gauges attached to the copper surface may have experienced problems during the tests. This latter possibility is not surprising given the high swelling pressure to which the gauges were exposed. Very little strain was predicted or measured in the central part of the canister.
- The relative displacement C/M ratio of the canister end (indicating tilting of the canister) was about 1.2 at the end of Test 1. This was the only laboratory test for which relative displacement between the canister and the wall of the steel test vessel was successfully measured. The shape of the measured relative displacement versus shear displacement curve and its slope were very similar to the predicted response. The overprediction of tilt in Test 1 suggests that the shear strength at the buffer/canister interface in the model may differ from that in the laboratory test, or that there is compliance in the bentonite buffer, laboratory testing equipment, or measuring system that is not accounted for in the model.
- The canister bending C/M ratio was 0.96, 1.14 and 0.92 for Tests 1, 2 and 3, respectively. The general predicted and measured shape of the canister at the end of each test compared very well. This finding suggests that the material model for copper is representative of the actual copper rod used in each test.
- The buffer axial displacement C/M ratio was 1.04 in Test 3. This was based on the differential axial movement of the buffer at the shear plane on opposite sides of the canister (one area compressed, the other relaxed). This was the only test in which the axial displacement of the buffer was measured. Comparison to the model results showed good agreement in both the general distribution and magnitude of axial displacement over the deformed shear plane.

The findings from this study suggest that the material models and modeling approach used provide very good estimates of the effects of rock shear in the 1:10 scale tests. Results from the single density model showed negligible differences compared to the three zone density model. The authors emphasised that no attempt was made to adjust the models or input parameters from those used for SR-Can and SR-Site modeling, and as such, results were considered sufficient to validate the rock shear scenario modeling conducted for SR-Site.

## 3.4 Numerical modeling of rock shear at field scale

Development and application of numerical models to assess key technical issues such as rock shear has been ongoing in Sweden for many years. This section provides background on model development to simulate buffer material behaviour and use of the models to assess rock shear effects at field scale to support SR-Can and SR-Site applications.

### 3.4.1 Modeling to support SR-Can

Pilot model studies reported by /Pusch 1983b/ provided an initial assessment of the potential impact of rock shear on canister stress. Simulations using an elastic 3D model with properties of 6,000 MPa for buffer elastic modulus, 0.45 for buffer Poisson's ratio, 133 GPa for copper canister elastic modulus, and 0.35 for copper canister Poisson's ratio resulted in 375 MPa tensile stress in the copper container at 10 mm shear displacement. Given the unrealistically high buffer elastic modulus value in the 3D analysis, preliminary 2D finite element analysis using the same canister properties, a buffer elastic modulus of 200 MPa, and assuming plasticity at a shear stress of 8 MPa, resulted in a maximum tensile stress of 20 MPa in the copper canister. This value was below the yield stress of the canister, suggesting that a rock shear displacement of 10 mm could be accommodated by the canister. /Pusch 1983b/ concluded based on the pilot model studies that consideration of the non-linear behaviour of the buffer, and further study of the visco-elasto-plastic nature of clay material, was required to fully understand the potential impact of rock shear displacements on the physical state of the copper canister.

In addition to rock shear modeling, /Börgesson 1988/ used other models to estimate settlement, thermo-mechanical and swelling effects. Settlement was estimated using a creep model defined on the basis of triaxial tests. Thermo-mechanical calculations used the same model as for rock shear with coupled thermal-mechanical effects. Swelling and compression effects were modeled using a Drucker-Prager model with poro-elasticity. The use of different models for different applications was considered a prudent approach to avoid unnecessary complexity in analysis.

/Börgesson 1992/ presented finite element calculations using Abaqus for three different canister types (KBS-3 HIP canister, KBS-3 copper/steel composite canister, and VLH large copper/steel composite canister). The effects considered in the analyses included swelling pressure of the MX-80 bentonite, rock shear through different levels of the canister, and thermo-mechanical effects on the canister including creep and consolidation of the buffer following rock shear. The buffer was modeled as a porous elastic medium exhibiting generalised Drucker Prager plasticity with non-associated flow upon yield. The copper and steel parts of the canister were modeled with traditional elasto-plastic metal models, and the rock was modeled either as a rigid surface or a very stiff porous elastic medium, depending on application. The authors provided parameter values for the various models used in the simulations. Details on canister design and manufacturing are provided in the report by /Andersson 2002/.

As background for the study, the authors summarised results of previous simulations of the 1:10 scale model shear tests /Börgesson 1986/ using a total stress elasto-plastic model. Other calculations based on combined models of porous elasticity and critical state plasticity /Börgesson 1990/ included completely drained buffer material exposed to rock creep displacements or very small intermittent rock displacements, completely undrained buffer material exposed to fairly rapid rock displacements, and partly drained buffer material exposed to rock displacement lasting for years. These latter simulations indicated that the rock shear scenario could be modeled using material models in Abaqus based on effective stress theory, and that even for very slow rock displacement, significant pore pressure would be generated.

Initial conditions of the buffer in rock shear simulations of the various canister designs included a void ratio of 0.65 (corresponding to a bulk density of 2.05 t/m<sup>3</sup>), initial average effective stress (corresponding to the swelling pressure) of 8 MPa, initial pore water pressure of 5 MPa, and a temperature of 15°C. Rock shear effects were assessed for conditions of 100 mm shear displacement in 30 days along a horizontal shear plane intersecting the vertical canister. Results of simulations of the VLH canister, which has a spherical end geometry that is quite different from the other canister designs, were described by /Börgesson 1992/.

For the KBS-3 Hot Isostatic Pressure (HIP) canister, simulations were conducted at a buffer bulk density of  $2.05 \text{ t/m}^3$  with the shear plane intersecting the canister at one quarter the canister length from its end (i.e. the quarter point). Additional simulations were conducted for a mid-height intersection scenario using buffer bulk density values of  $1.93$  and  $2.14 \text{ t/m}^3$ . The rock was assumed to be undrained with no exchange of water between the rock and the buffer. The simulations proceeded stepwise, first calculating the stress and strain in the canister induced by the cooling phase of the HIP process, then the conditions following consolidation of the buffer under drained conditions, and finally the conditions associated with rock shear. Results showed a strong dependence between rock shear effects and buffer density, with a maximum plastic strain of 4% for a buffer density of  $2.14 \text{ t/m}^3$  and no plastic strain for a buffer density of  $1.93 \text{ t/m}^3$ . At a buffer density of  $2.05 \text{ t/m}^3$ , the maximum plastic strain at the canister surface was estimated to be 1.5%, including 0.3% plastic strain induced by the HIP process. Pore pressure increased to 9 MPa in compressed parts of the buffer, and decreased to less than 1 MPa in areas of stress decrease, as a result of shearing. Plastic strain reached 5% in most of the clay, and 50% in the shear zone close to the canister.

For the KBS-3 copper/steel composite canister, rock shear simulations were conducted at a buffer bulk density of  $2.05 \text{ t/m}^3$  with the shear plane intersecting the canister at mid-height and at the quarter point in separate cases. A gap of 1 mm between the empty inner steel and outer copper cylinders was assumed in the simulations. Initial swelling of the buffer prior to rock shear was shown to close this gap except at the edges of the lid, and to generate up to 0.2% plastic strain over a large part of the copper canister.

The symmetric mid-height rock shear case assumed drained rock conditions, allowing some drainage from the bentonite to take place. Results from this case showed a shear-induced increase in pore pressure up to 17 MPa in the compressed buffer, and negative pore pressure in areas of reduced stress (or possibly a gap forming between the canister and buffer under these conditions). Maximum plastic strain in the copper and steel was 1% and 0.4%, respectively, under the simulated conditions. Contact between the steel and copper cylinders was partly lost on the passive side of the canister during rock shear. Post-shear creep calculations showed that maximum total creep strain in the copper cylinder and at the cylinder/lid connection could reach 6% and 36%, respectively, over 100,000 years, although the calculations were viewed to have a high level of uncertainty.

For the asymmetric quarter point rock shear case, the rock was considered completely undrained. Plastic strain in the buffer near the shear plane close to the canister reached 170%, similar to that in the symmetric case. Most of the bending in this case took place near the centre of the canister, but the maximum strain in the copper canister was 2.5% at the shear plane location. The maximum plastic strain in the copper was about twice that in the symmetric shear case. In the steel, the maximum plastic strain was about four times that in the symmetric case.

As concluded by /Börgesson 1992/, these results suggest that, although the composite copper/steel canister designs seem to be slightly more affected by rock shear than the KBS-3 HIP canister design, the most important factor controlling canister strain is buffer density. Rock shear simulations at a buffer density of  $2.05 \text{ t/m}^3$  indicated that intersection of the shear plane at the canister quarter point produced more severe strain in the canister than the mid-height intersection case. For the composite canisters, the initial swelling pressure closed the gap between the copper and steel cylinders, but rock shear reopened this gap in some areas of stress reduction. Pore pressures between 10 and 20 MPa in compressed areas of the buffer, and between  $-1$  and  $-10$  MPa in areas of reduced stress, were predicted for the various scenarios. A gap between the canister and the clay buffer would be expected to develop instead of negative pore pressures being generated. Large changes in void ratio near the shear plane, and axial deformation of the buffer were also evident in the Abaqus plots from these simulations. These findings highlight that a poro-elasto-plastic model offers the possibility of comparing laboratory-measured and model-predicted pore pressure and void ratio distributions as part of model validation.

/Börgesson et al. 1995/ overviewed several generations of material models for bentonite, starting with a total stress model, then an effective stress porous elasticity model with Drucker-Prager plasticity, and finally an elasto-plastic cap model (the Claytech model). This latter model was shown to account for most of the behaviours observed in laboratory testing. It was partly adapted to the material models available in the Abaqus finite element code, and was shown through a number of verification examples to simulate many of the observed THM behaviours of bentonite with some exceptions (e.g. volumetric creep). This new material model implemented in Abaqus featured a curved critical state line (CSL), a curved failure envelope, a cap that defines the limit between elastic and plastic volumetric strain, a porous elastic region with a variable Poisson's ratio, and a plastic region with contractancy on the cap and dilatancy outside the CSL.

The Claytech model was based on effective stress theory and Darcy's law with a variable hydraulic conductivity. Heat flow was modeled assuming thermal conduction with variable heat conductivity. The TM response was linked to the thermal expansion of water and particles. Contact elements with no thickness and undergoing only tangential strain were used to improve simulation of the buffer/canister interface. Although the model produced representative responses, further improvement was considered necessary for general use.

/Börgesson et al. 2003/ conducted additional modeling of earthquake induced rock shear through a deposition hole to assess effects on the canister and the buffer. Relative to previous modeling studies, several changes were taken into consideration. First, the canister design was updated to match the KBS-3 geometry with a copper/cast iron canister. Next, shear displacement up to 200 mm was considered and shear rate up to 1 m/s was applied as a boundary condition. Finally, the bentonite model was updated for very fast shearing.

A total stress model was used in Abaqus for the calculations. Eight simulations were run to consider four densities (1,950, 2,000, 2,050 and 2,100 kg/m<sup>3</sup>) and a shear plane intersecting the full-scale deposition hole at canister mid-height (centric) and at the quarter point (eccentric). An additional case with an eccentric shear plane and buffer density of 2,000 kg/m<sup>3</sup> was run using contact elements with zero tensile strength to allow a gap to form between the canister and the buffer. For compression, the contact elements had a Mohr-Coulomb friction angle of 5.7°. An elastic-plastic stress-strain responses was assumed for the buffer material.

Results from the study showed that, for a reference MX-80 buffer density of 2,000 kg/m<sup>3</sup> and eccentric shear, plastic strain in the cast iron insert started after 20 mm of shear displacement and reached 4.4% plastic strain after 200 mm of shear displacement. The corresponding maximum plastic strain in the copper was about 8% on the canister surface, and locally much higher at the lid. Plastic strain in the cast iron insert and on the copper canister surface was 10 and 24%, respectively, at a buffer density to 2,100 kg/m<sup>3</sup> for the eccentric shear case, also starting at 20 mm shear displacement. At a buffer density of 1,950 kg/m<sup>3</sup>, plastic strain was 2.7 and 6%, respectively for the cast iron insert and the copper canister surface, starting at a shear displacement of 30 mm. The case for a buffer density of 2,050 kg/m<sup>3</sup> produced results intermediate to the cases at densities of 2,000 and 2,100 kg/m<sup>3</sup>.

For the cases with a centric shear plane, there was no plasticisation of the cast iron insert at a buffer density of 1,950 kg/m<sup>3</sup>, and about 4% plastic strain in the copper canister surface at 200 mm shear displacement. A slight increase in plastic strain to 0.2% and 6% for the cast iron insert and the copper canister surface, respectively, was noted at a buffer density of 2,000 kg/m<sup>3</sup>, starting at 40 mm shear displacement. At buffer densities of 2,050 and 2,100 kg/m<sup>3</sup>, plastic strain in the cast iron insert was 11 and 19%, starting at shear displacements of 30 and 20 mm, respectively. Plastic strain on the copper canister surface for these cases was 16 and 26%, respectively. These results showed that the position of the shear plane influences the development of plastic strain in the cast iron insert, and to a much lesser extent in the copper canister surface. A centric plane was shown to be more detrimental to the cast iron insert at higher buffer densities than an eccentric shear plane. The converse was true at lower buffer densities.

The plastic strain in the cast iron insert more than doubled for an increase from 100 to 200 mm shear displacement in all cases except the low buffer density case with a centric shear plane, which indicated no plasticization of the insert. The use of contact elements generally reduced plastic strain in the copper to values similar to the cast iron insert, but had no effect on plastic strain in the cast iron insert due to the gap between the two components.

/Börgesson and Hernelind 2006/ expanded on previous finite element modeling of the rock shear case of 200 mm displacement at a shear rate of 1 m/s along a fracture intersecting the deposition hole. The rock surrounding the deposition hole was included explicitly in the model simulations, and all buffer interfaces with the rock and the canister were modeled using contact elements. This modification was considered an improvement on earlier simulations, although the assumption that contact properties of zero cohesion and a friction angle of  $5.7^\circ$  were representative of interfaces with both rock and copper was considered uncertain. Different shear plane angles ( $90$ ,  $45$  and  $22.5^\circ$ ) were considered for both sodium and calcium bentonite at buffer densities of  $2,000$  and  $2,050 \text{ kg/m}^3$  in 24 simulations. For the cases with a horizontal shear plane, both eccentric and centric shear plane positions were investigated. For the other cases, both tension and compression shear directions along the shear plane were considered (Figure 3-13). Effects of transformation of bentonite to illite and partial cementation of the buffer were also investigated.

The results showed that damage to the canister was influenced by inclination of the intersecting fracture, the shear direction on the fracture (when not horizontal), the location of a horizontal shear plane, magnitude of the shear displacement, bentonite type, bentonite density, and transformation of the buffer to illite or cemented bentonite. Mutual interference was noted between these different effects. In comparison to previous simulations, the use of contact elements at the buffer-rock and buffer canister interfaces appeared to reduce stresses in the buffer and the resulting strain in the cast iron insert and copper canister.

The copper canister in all except one case for calcium bentonite buffer reached or exceeded 1% plastic strain at 100 mm shear displacement, while only half the cases for sodium bentonite had reached or exceeded 1% strain at this displacement owing to the lower relative stiffness and strength of the sodium bentonite. After 200 mm shear displacement, the maximum plastic strain in the copper canister (excluding the lid) was 19% for calcium bentonite and 8% for sodium bentonite. Both cases used a buffer density of  $2,050 \text{ kg/m}^3$ , with a shear plane intersecting the deposition hole at  $45^\circ$ , and a shear direction causing tension in the canister. For plastic strain in the copper lid, the critical cases for both calcium and sodium bentonite involved inclined shear planes, buffer density of  $2,050 \text{ kg/m}^3$ , and shearing in the direction causing compression. Under these conditions, maximum plastic strain in the copper lid was 32% for a shear plane at  $22.5^\circ$  in calcium bentonite, and 23% for a shear plane at  $45^\circ$  in sodium bentonite.

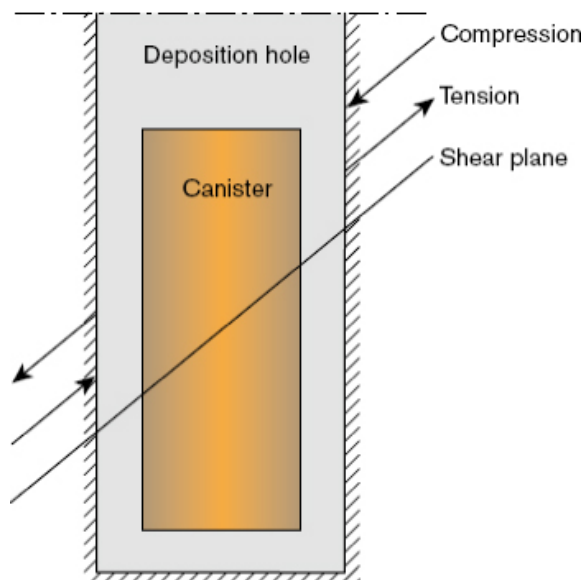


**Figure 3-13.** Illustration of shear directions corresponding to compression and tension in the case of an inclined shear plane (from /SKB 2006/).

In contrast to these results, the maximum plastic strain in the cast iron insert was 13% for high density calcium bentonite and a horizontal centric shear plane, and 3.6% for high density sodium bentonite and a horizontal eccentric shear plane. It is noted that the results for sodium bentonite differ significantly from those presented in /Börgesson et al. 2003/ where plastic strain in the cast iron insert was 6.2 and 11% for an eccentric and a centric shear plane, respectively, at a buffer density of 2,050 kg/m<sup>3</sup> and shear displacement of 200 mm.

Transformation of bentonite to illite was found to reduce damage to the canister in all cases due to a loss of swelling pressure and strength in the illitization process. Cemented bentonite produced more severe effects on the canister owing to the increased stiffness relative to the original sodium bentonite. However, because properties of cemented bentonite were not known, these results were considered qualitative in nature.

The results from /Börgesson and Hernelind 2006/ were used as the basis for numerical modeling of rock shear effects to support the SR-Can application /SKB 2006/. The conditions considered in the site evaluation included a maximum shear velocity of 1 m/s, a maximum shear displacement of 0.1 m, and an upper bound buffer density of 2,050 kg/m<sup>3</sup> to reduce rock shear effects.

### 3.4.2 Modeling to support SR-Site

/Hernelind 2010/ describes a series of numerical simulations of rock shear at field scale under various conditions including glacial loading. Simulations considered two canister designs (BWR and PWR). The reference buffer in these simulations was Ca-bentonite rather than Na-bentonite assumed in previous simulations of this type. Reference density assumed for Ca-bentonite was 2,050 kg/m<sup>3</sup>, but cases using density values of 2,000 and 1,950 kg/m<sup>3</sup> were also analysed. Both the short-term elastic-plastic and long-term creep behaviour of copper were investigated.

Detailed geometric models of the canister components (iron insert, steel insert lid, and copper shell complete with fillets and flange for the lid) were used in the simulations. The material model for the iron insert was based on an elastic-plastic von Mises model, with Young's modulus of 166 GPa and Poisson's ratio of 0.32 for the elastic part. A similar model was used for the steel insert and lid, with Young's modulus of 210 GPa and Poisson's ratio of 0.3. Copper behaviour during short duration rock shear was based on a simplified elastic-plastic material model derived from a creep model developed by the Corrosion and Metals Research Institute (and advanced by Swerea KIMAB), assuming a strain rate of 0.5%/s. This elastic-plastic model differed from that used to simulate 1:10 scale rock shear laboratory tests. Copper behaviour over the long term used the creep model directly in Abaqus as a user supplied subroutine.

Bentonite buffer was modeled using the material model described by /Börgesson et al. 2010/. For density values of 1,950, 2,000 and 2,050 kg/m<sup>3</sup>, corresponding swelling pressure values were 5.3, 8.0 and 12.3 MPa, respectively. Young's modulus values at these densities were 243, 307 and 462 MPa, with Poisson's ratio set to 0.49 for all simulations. A porous-elastic model combined with a Drucker-Prager model was used in Abaqus to simulate consolidation of the buffer material. This combined model required specification of bulk modulus of the soil skeleton and water, permeability and specific weight.

Contact elements with a friction angle of 5.7° and zero cohesion were used at all interfaces between the bentonite buffer, the copper shell, the insert, and the insert lid. Additional sensitivity analyses were conducted using friction angle values of 2.9 and 11.3° to assess the influence of this parameter on results. Contact was released upon loss of swelling pressure. The buffer/rock interface was assumed to be tied, with no opening/closing or sliding permitted.

Initial conditions in the model included a constant temperature of 300 K, total pressure selected to simulate swelling pressure plus 5 MPa water pressure at 500 m depth, effective pressure and pore pressure initially in a state of equilibrium then increased to 5 MPa to simulate glacial loading and groundwater pressure effects. Symmetry conditions were specified such that displacements normal to the symmetry plane were assumed to be zero. Zero displacement was prescribed on the axis of symmetry at one point in the axial direction and two points in the horizontal direction to avoid rigid body motion. Rock shear was simulated by imposing displacements at the outer surface of the buffer (i.e. the rock was not included in the model).

Simulations of short-term rock shear of 10 cm for the reference case with the BWR canister considered a fracture plane intersecting the canister at different heights (mid-height and three-quarter height relative to the bottom of the canister) and angles (perpendicular to the axis of the canister, at 22.5° to the axis of the canister, and horizontally along a vertical plane through the centerline of the canister and one offset halfway between the canister centerline and edge). The reference shear velocity for these simulations was 1 m/s, but a scenario using 0.1 m/s was included in the analyses. Comparative scenarios using the PWR canister were conducted. In addition, a long-term creep scenario representing a period of 100,000 years was analysed. Glacial loading with and without rock shear was also considered in separate analyses. Other sensitivity analyses addressed uncertainty in creep model parameters, the effect of buffer thickness, and the effect of reinforcing the cast iron insert with a surrounding steel cylinder.

*Horizontal shear plane at quarter point* – nine cases were simulated using the BWR canister, reference Ca-bentonite buffer at 2,050 kg/m<sup>3</sup>, shear displacement of 5 and 10 cm, a shearing rate of 1 m/s, and shear plane normal to canister at the quarter point. The reference case produced 1.6 and 2.9% plastic strain in the cast iron insert and steel channels, respectively, at 10 cm shear displacement. Corresponding plastic strain in the copper shell ranged from 0.05% in the bottom fillet to 16% at points of discontinuous geometry in the canister bottom, with a value of 2.0% mid-shell. Compared to these results, findings from the various sensitivity analyses were as follows:

- Creep reduced plastic strain in the cast iron insert and steel channels slightly. In the copper shell, plastic strain was reduced to about 9% at points of discontinuous geometry in the canister bottom, and there was a slight reduction mid-shell.
- Hydrostatic pressure from a simulated ice sheet resulted in significantly reduced plastic strain in the cast iron insert and steel channels. In the copper shell, plastic strain was redistributed and ranged from 0.5% in the bottom fillet to 17% at points of discontinuous geometry in the canister bottom, with a value of 1.4% mid-shell. Plastic strain in the top weld increased to 13% relative to the reference case value of 4.3%.
- Glacial loading following rock shear generally increased plastic strain at all points in the iron insert, steel channel tubes and copper shell. Results showed 2.3 and 4.4% plastic strain in the cast iron insert and steel channels, respectively, at 10 cm shear displacement. Corresponding plastic strain in the copper shell ranged from 0.2% in the bottom fillet to 23% at points of discontinuous geometry in the canister bottom, with a value of 2.7% mid-shell.
- Contact element friction angle was shown to influence plastic strain in the steel channel tubes more significantly than in the cast iron insert. Reducing the friction angle to 2.9° had no effect on plastic strain in the cast iron insert, but reduced plastic strain in the steel channel tubes from 2.9 to 2.1%. Likewise, increasing the contact element friction angle to 11.3° increased plastic strain slightly in the cast iron insert, and resulted in an increase from 2.9 to 3.9% in the steel channel tubes. In the copper shell, reducing the contact element friction angle had no significant effect on plastic strain. Increasing the friction angle resulted in slight redistribution of plastic strain, reducing plastic strain in the top weld, slightly increasing plastic strain at points of discontinuous geometry in the top and bottom, and reducing plastic strain from 3.1 to 0.7% in the top reminding region.
- Shearing velocity was reduced to 0.1 m/s in one simulation. No significant effects on the cast iron insert, steel channel tubes, or copper shell were observed except a very slight reduction in plastic strain in some regions of copper shell and steel channel tubes, and a slight increase in plastic strain in the cast iron insert. These findings suggest that shearing velocity has a relatively weak influence on plastic strain in the canister in the range of velocities considered, consistent with the relatively small exponent associated with Ca-bentonite in Equation 3-7.
- Steel reinforcement of the cast iron insert reduced plastic strain in the iron insert and steel channel tubes to less than 1%, and redistributed plastic strain in the copper shell. The most significant increase in plastic strain in the copper shell was an increase to 21% at points of discontinuous geometry in the bottom of the canister.
- Doubling the buffer thickness to 70 cm decreased plastic strain in the cast iron insert and steel channel tubes to 0.9%, and resulted in minor changes in plastic strain distribution in the copper shell. Plastic strain ranged from 0.8% in the bottom reminding zone to 12% at points of discontinuous geometry in the bottom of the canister, and was 1.4% mid-shell in this scenario.

*Horizontal shear plane at midpoint* – two cases were simulated using the same conditions as the reference case, but with the shear plane normal to the canister at the midpoint. Observations from these cases relative to the reference case were as follows:

- The change in position of the horizontal shear plane reduced plastic strain in the cast iron insert and steel channel tubes to 0.7 and 1.5%, respectively, at 10 cm displacement. Plastic strain in the copper shell increased significantly, ranging from 2.5% at the bottom reminding zone to 29% at points of discontinuous geometry in the bottom of the canister. At mid-shell, plastic strain was 4.4% in this scenario. Significant increases were also noted in the top fillets (plastic strain of 15%) and at points of discontinuous geometry in the top of the canister (plastic strain of 9.6%).
- Allowing creep in this configuration reduced plastic strain significantly at the points of high stress concentration. The maximum plastic strain in the copper shell, for example, was reduced to 7.6% from 29%. Plastic strain in the cast iron insert and steel channel tubes was also reduced.

*Inclined shear plane at quarter point* – two cases were simulated using the same conditions as the reference case, but with the shear plane at 22.5° to the canister axis intersecting the canister at the quarter point. Observations from these cases relative to the reference case were as follows:

- The change in angle of the shear plane reduced plastic strain in the cast iron insert and steel channel tubes to 0.09 and 0.3%, respectively, at 9.2 cm displacement (limited by numerical stability of the model). Plastic strain in the copper shell increased significantly at the top and bottom welds (27 and 12%, respectively), and at the top fillet (13%), with less significant changes in other parts of the canister.
- Results of allowing creep in this configuration were uncertain as the model ran only to 5.1 cm displacement, then stopped. At 5 cm displacement, creep significantly reduced plastic strain in the copper shell with the exception of an increase in plastic strain in the bottom weld.

*Inclined shear plane at midpoint* – two cases were simulated using the same conditions as the reference case, but with the shear plane at 22.5° to the canister axis intersecting the canister at the midpoint. Observations from these cases relative to the reference case were as follows:

- The change in angle and position of the shear plane reduced plastic strain in the cast iron insert and steel channel tubes to 0.2 and 0.6%, respectively, at 10 cm displacement. Plastic strain in the copper shell increased somewhat at the top and bottom welds (14 and 5.9%, respectively), and at the top fillet (3.5%), with minor changes in other parts of the canister.
- Results of allowing creep in this configuration were uncertain as the model ran only to 5.5 cm displacement, then stopped. At 5 cm displacement, creep significantly reduced plastic strain in the copper shell with the exception of an increase in plastic strain in the bottom weld.

*Vertical shear plane offset from centerline* – two cases were simulated using the same conditions as the reference case, but with a vertical shear plane intersecting the canister halfway between the centerline and the canister edge. Observations from these cases relative to the reference case were as follows:

- The change in angle and position of the shear plane reduced plastic strain in the cast iron insert and steel channel tubes to 0.4 and 0.5%, respectively, at 10 cm displacement. Plastic strain in the copper shell was redistributed, ranging from 0.9% mid-shell to 6.9% at the top weld.
- Results of allowing creep in this configuration were uncertain as the model ran only to 6.4 cm displacement, then stopped. At 5 cm displacement, creep increased plastic strain at the top and bottom welds, and redistributed plastic strain elsewhere in the copper shell.

*Vertical shear plane through centerline* – two cases were simulated using the same conditions as the reference case, but with a vertical shear plane intersecting the canister at the centerline. Observations from these cases relative to the reference case were as follows:

- The change in angle and position of the shear plane reduced plastic strain in the cast iron insert and steel channel tubes to 0.6 and 0.8%, respectively, at 10 cm displacement. Plastic strain in the copper shell was redistributed, ranging from 1.1% mid-shell to 9.1% at the point of discontinuous geometry at the bottom of the canister.
- Results of allowing creep in this configuration showed little change in plastic strain in the cast iron insert and steel channel tubes compared to the non-creep case. However, creep resulted in increased plastic strain at the top and bottom welds (6.2 and 7.6%, respectively), and redistributed plastic strain elsewhere in the copper shell.

*Moderate buffer density* – three cases were simulated using the same conditions as the reference case, but with a buffer density of 2,000 kg/m<sup>3</sup>, and various shear plane angles and positions. Observations from these cases relative to the reference case were as follows:

- The change in density of the buffer alone reduced plastic strain in the cast iron insert and steel channel tubes to 1.2 and 1.3%, respectively, at 10 cm displacement. Plastic strain in the copper shell was generally reduced, ranging from 0.3% at the bottom fillet to 14% at the point of discontinuous geometry at the bottom of the canister.
- The change in density of the buffer in combination with a shear plane at 22.5° to the canister axis intersecting the canister at the midpoint reduced plastic strain in the cast iron insert and steel channel tubes to 0.0 and 1.7%, respectively, at 10 cm displacement. Plastic strain in the copper shell was redistributed, ranging from 0.6% mid-shell to 16% at the top weld.
- The change in density of the buffer in combination with a shear plane at 22.5° to the canister axis intersecting the canister at the quarter point reduced plastic strain in the cast iron insert and steel channel tubes to 0.0 and 0.03%, respectively, at 6.6 cm displacement (limited by numerical stability of the model). Plastic strain in the copper shell was redistributed, ranging from 0.7% mid-shell to 30% at the top weld.

*Low density buffer* – three cases were simulated using the same conditions as the reference case, but with a buffer density of 1,950 kg/m<sup>3</sup>, and various shear plane angles and positions as per the cases at a density of 2,000 kg/m<sup>3</sup>. Observations from these cases relative to the reference case were as follows:

- The change in density of the buffer alone reduced plastic strain in the cast iron insert and steel channel tubes to 0.7% at 10 cm displacement. Plastic strain in the copper shell was generally reduced, ranging from 0.5% at the bottom fillet to 14% at the point of discontinuous geometry at the bottom of the canister.
- The change in density of the buffer in combination with a shear plane at 22.5° to the canister axis intersecting the canister at the midpoint reduced plastic strain in the cast iron insert and steel channel tubes to 0.0% at 8.9 cm displacement (limited by numerical stability of the model). Plastic strain in the copper shell was redistributed, ranging from 0.5% mid-shell to 12% at the top weld.
- The change in density of the buffer in combination with a shear plane at 22.5° to the canister axis intersecting the canister at the quarter point reduced plastic strain in the cast iron insert and steel channel tubes to 0.0% at 7.1 cm displacement (limited by numerical stability of the model). Plastic strain in the copper shell was redistributed, ranging from 0.6% mid-shell to 29% at the top weld.

*PWR design canister* – two cases were simulated using the same conditions as the reference case, but with a PWR canister. Observations from these cases relative to the reference case were as follows:

- The change in canister design reduced plastic strain in the cast iron insert and steel channel tubes to 1.5 and 1.2%, respectively, at 10 cm displacement. Plastic strain in the copper shell was similar to the reference case, ranging from 0.1% at the bottom fillet to 17% at the point of discontinuous geometry at the bottom of the canister.
- Results of allowing creep in this configuration showed a slight reduction in plastic strain in the cast iron insert and steel channel tubes compared to the non-creep case. Creep generally decreased plastic strain in the copper shell, ranging from 0% in the bottom fillet to 10% at the point of discontinuous geometry at the bottom of the canister.

*Glacial loading* – finally, three glacial loading cases were run using different creep parameters to simulate effects over a timeframe of 100,000 years. No plastic strain was induced in the insert. Maximum creep strain in the copper shell ranged from 13 to 18% in the three cases, with most of this strain associated with the initial application of the load in the model. The model results indicated that the copper shell will deform to a maximum of about 1 mm when the initial load is applied but will mainly close initial gaps between components. These displacements do not affect the geometry assumed for subsequent earthquake-induced rock shear analysis.

/Hernelind 2010/ drew several conclusions based on the numerical modeling results:

- Stiffness of the bentonite was found to have a great effect on stress and strain levels both for the copper shell and the insert, and was therefore considered an important parameter.
- The use of Ca-bentonite with reference density of 2,050 kg/m<sup>3</sup> resulted in increased strain in both the copper shell and the insert compared to the previous MX-80 reference buffer.
- Localisation of plastic strain was evident in the models in the fillets and flange in the copper shell and at the corner of specific channels in the insert, but severe damage was not expected as a result; global plastic strains were much lower than localised plastic strain values.
- The maximum principal stress in the insert was found to be controlled by bending of the copper shell, which in turn was a function of bentonite buffer properties.
- Rate-dependency associated with creep was found to decrease the maximum strain in the copper shell; creep in bentonite was expected to reduce creep in copper over time.
- Strain-rate dependence was considered in all material models except that for copper which used an estimated strain rate; however, the use of creep models in other simulations accounted for strain-rate dependence in the copper.
- The hydrostatic case considered in the study was not based on the correct bentonite model; however the glacial load case in combination with rock shear was not found to be the most critical one.
- Comparative cases using different canister designs showed that stress and strain in the PWR canister were lower than in the BWR canister.
- Based on the reference Ca-bentonite buffer and BWR canister, rock shear perpendicular to the canister axis at the midpoint produced the largest plastic strains (Figure 3-14).
- Glacial loading was shown to result in relatively low plastic strain in the insert, and maximum creep strain where the lid is welded to the flange in the copper shell; calculated displacements were on the order of 1 mm and tended to produce compression in the insert well below the yield stress.
- Glacial loading followed by rock shear was found to reduce plastic strains in the cast iron insert and steel channels, and in the copper shell (except for very minor increase at one localised spot); the converse was true for the case of earthquake induced rock shear followed by glacial loading, but plastic strain increases were relatively small except a very localised spot where the geometry is discontinuous.

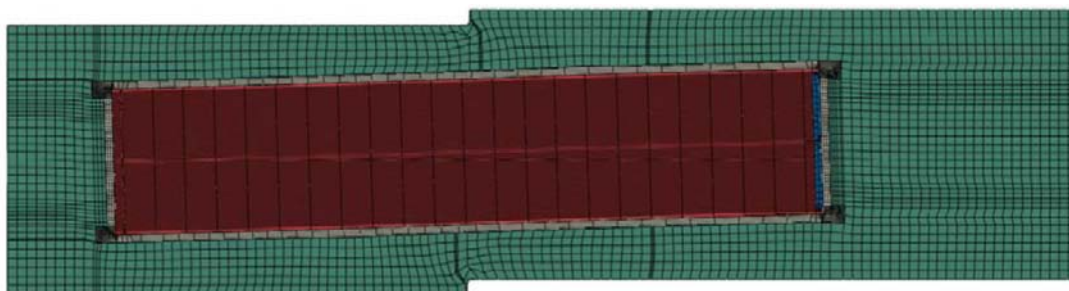


**Figure 3-14.** Abaqus model showing reference case of 10 cm rock shear along a midpoint plane through a deposition hole containing Ca-bentonite buffer and a BWR container (from /Hernelind 2010/).

/Hernelind 2010/ noted several remaining uncertainties associated with the numerical modeling of rock shear. Strain rate effects in the various materials may affect the distribution of stress and strain; despite some uncertainties with the creep model used in the analyses, results indicate that the maximum stress and strain levels may be reduced if creep is considered. Variability in measured properties and conditions in experimental results used for model calibration may also add some uncertainty to the model results, especially given the important relations between swelling pressure, material stiffness and strength. The complex geometry of the canister and its components may require finer discretisation in some parts of the model to better estimate stress and strain, but in general effects of element size in the model were considered minimal. It was also noted that creep analysis in copper was performed at 27°C but the experimental results for the insert were determined at 0°C, resulting in some conservatism in the combined model. Finally, the assessment of rock shear combined with glacial loads used a simplified approach, combining various material models, that may introduce uncertainty in the predicted stresses and strains.

### 3.5 Summary of literature review

The literature review identified the key technical reports associated with laboratory testing to determine basic bentonite properties, 1:10 scale analogue tests to directly assess the effects of rock shear on the buffer and canister, and the evolution of numerical models used to simulate rock shear. In general, the work completed to date in Sweden has provided a wealth of laboratory test data on various bentonite materials that has been used effectively to develop models of material behaviour. The use of the developed numerical models in the assessment of rock shear for SR-Can /SKB 2006/ and SR-Site applications was supported by model validation based on the 1:10 scale analogue tests conducted in 1986. The total stress model used provided a good approximation of rock shear effects observed in the analogue tests.

Given the shift in emphasis to Ca-bentonite buffer, confidence in the developed numerical models and simulation results could be enhanced through additional laboratory testing to address specific issues identified in the literature review, as follows:

- Buffer strength and stiffness under constant volume conditions – there appears to be some uncertainty regarding the behaviour of bentonite buffer under constant volume conditions. Model simulations of the 1:10 scale analogue tests tended to overestimate force and relative displacement of the canister end, which could imply that the buffer material in the laboratory tests was more compliant than the model would predict. In addition, the 1:10 scale analogue tests were conducted on the MX-80 reference buffer; no such tests have been conducted using Ca-bentonite buffer. A combination of standard tests, constant volume tests, and analogue tests would help address these discrepancies or deficiencies.
- Buffer interfaces with other materials – the model simulations of the 1:10 scale analogue tests used frictional contact elements along all interfaces between the buffer and copper canister; the buffer/rock interface was not modeled. Likewise, in the field scale simulations the buffer/rock interface was treated as tied. Sensitivity analyses showed that, under these assumptions, contact element friction angle had a relatively small effect on calculated plastic strains and stresses.

Discrepancies between the predicted and measured strain and deformation of the canister in the 1:10 scale analogue tests may be related in part to the simulated interface conditions, including the conditions on the buffer/rock interface. Specialised constant volume tests to determine interface properties and behaviour during shearing are expected to help confirm or refine the interface model.

- Buffer density and strain rate effects – the models developed to date assume that the general stress-strain curve for bentonite buffer can be scaled in terms of stress to match specific buffer density and strain rate conditions. This model assumes that plastic behaviour starts at 1% strain and 58% of peak deviator stress, and that the peak shear strength is reached at about 5% strain. The elastic modulus is therefore assumed to be directly correlated to peak deviator stress or shear strength. The normalised shape of the stress-strain curve is assumed to be constant for a range of density-strain rate combinations. The 1:10 scale analogue tests conducted in 1986 considered a single target material density and three shear rates for MX-80 reference buffer. Additional analogue tests at different densities and shear rates for Ca-bentonite would provide further evidence against which to evaluate the various assumptions inherent in the bentonite material model, and to validate assumptions about the relation between elastic modulus and shear strength.
- Scale effects – the analogue tests conducted to date have been at 1:10 scale. The possible influence of scale on model validation results could be addressed by conducting analogue tests at a different (preferably larger) scale. This would provide a broader basis against which to validate models. It is also noted that earlier material models for MX-80 bentonite included scaling relations for shear strength based on shear strain rate, while later material models scaled shear strength on the basis of shear rate. The former is a scalable parameter based on the scale of the specimen being tested while the latter is independent of specimen size. To cover the possibility that shear strength is a function of shear rate, the maximum shear rate used in scaled tests should match the upper bound shear rate possible at full-scale (i.e. 1 m/s).
- Position of orthogonal shear plane – the various model simulations of the full-scale rock shear scenario provide conflicting results on the critical position of an orthogonal shear plane depending on material density and the approach to simulate interfaces. Previous analogue tests were conducted with a midpoint shear plane orthogonal to the canister axis. The full-scale ROSE setup was based on a quarter point shear plane. Numerical modeling of Ca-bentonite at a density of 2,050 kg/m<sup>3</sup> confirmed that the midpoint shear plane orthogonal to the canister axis is most critical for plastic strain. A midpoint shear plane arrangement in laboratory tests offers some advantages in terms of exploiting the symmetry (or antisymmetry) of the setup to place instruments.
- Instrument performance and recorded responses – there were several identified issues with instrumentation used in the 1:10 scale analogue tests, particularly strain gauges and pressure sensors. In addition, the load-deformation response and associated instrumentation responses were relatively erratic, and in some cases appeared to indicate slack in the measuring system, compared to predicted responses from model simulations. Improvements in instrumentation and load control systems would improve the accuracy and consistency of monitoring results, and may reduce some discrepancies between calculated and measured responses. Testing of instrumentation as part of two-component constant volume tests is considered prudent before deploying instruments in additional scaled analogue tests.
- Equipment design – The testing apparatus manufactured for the 1:10 scale analogue tests incorporated a number of key design features such as stiff bronze filters to allow saturation, and frictionless sealed end plates to maintain pressure and avoid friction during shearing. There was evidence of out-of-plane rotation of the sliding test cylinder during shearing in a couple of the analogue tests. Design improvements to prevent this type of rotation and better control displacement during shearing would reduce uncertainty in the test results. Other design solutions to ensure frictionless sealed sliding interfaces between components may be available.
- Numerical models and comparison basis – The total stress model used to compare predicted and measured responses has been shown to perform well, and is relatively simple in its formulation. An effective stress model based on poro-elasticity and Drucker Prager plasticity with non-associated flow was also shown to produce reasonable results in previous model simulations. A benefit of using the effective stress model is the ability to compare predicted and measured pore pressure responses before and during shearing, as well as density (or void ratio) and moisture content distributions within the buffer before and after shearing. Adoption of both numerical models for different aspects of test back analysis would make better use of the post-test characterisation data, and would justify the addition of pore pressure sensors to future laboratory tests.

## 4 Rock shear laboratory testing program

### 4.1 General

As part of a collaborative agreement between SKB and NWMO, a preliminary laboratory testing plan to investigate rock shear effects and to support the design of ROSE was developed. The preliminary plan was subsequently updated with new information from laboratory visits, and new laboratory and modeling work reported by SKB in 2010. The detailed literature review in this report reflects this progression. The updated rock shear laboratory testing plan includes three suites of tests:

- Standard single component tests – new uniaxial compression tests at two scales to determine the undrained shear strength and stress-strain response of Ca-bentonite buffer material at different densities and shear rates, and to assess possible scale effects.
- Two-component constant volume tests – new concentric cylinder tests to investigate stress-strain behaviour of Ca-bentonite buffer under constant volume conditions in compression (and optionally in shear), and stress-strain behaviour of Ca-bentonite buffer at bentonite/rock and bentonite/copper interfaces under constant volume conditions in shear. These tests also offer the opportunity to test new instruments under representative loading conditions.
- Analogue tests – new 1:5 or 1:10 scale rock shear analogue tests to investigate containment system interactions and effects of rapid shear displacement along a midpoint orthogonal shear plane using Ca bentonite and scaled canisters.

The three test suites are expected to provide a basis to validate and/or refine material models used to simulate Ca-bentonite buffer behaviour. The test suites are independent of one another, so can be undertaken in parallel at one or more facilities. However, the results from all three suites are required to undertake model validation or refinement. Completion of the single and two-component tests prior to the analogue tests would permit an iterative approach to model refinement, with discrepancies between model predictions and measured laboratory results diagnosed and reconciled to the extent possible as testing progresses.

### 4.2 Standard single component tests

Upon review of previous laboratory testing conducted in Sweden, the suite of standard single component tests was reduced from its original scope to focus strictly on uniaxial compression tests of Ca-bentonite buffer material. The objective of these tests is to validate or refine the relations between undrained shear strength, displacement rate, and bulk density of Ca-bentonite buffer. These tests are similar to those performed using a precise compression machine /Börgesson et al. 2004, Dueck et al. 2010/, and are intended to supplement the existing data set. General specifications and requirements for this test suite are as follows:

- Specimen specifications – tests will be conducted on cylindrical specimens prepared from MX-80Ca bentonite buffer saturated to 100% with distilled water. Each specimen will be a perfect right cylinder with a length-to-diameter ratio of 2:1, and precise end geometry to avoid eccentric loading effects. Specimen diameters to be tested will be 20 and 40 mm. Specimens will be prepared and tested in a timely fashion to avoid potential free swelling effects of the bentonite material.
- Test conditions – tests will be conducted on samples of two sizes (20 and 40 mm diameter) and three bulk densities (1,950, 2,000, 2,050 kg/m<sup>3</sup>) at three constant displacement rates (0.01, 0.1 and 1.0 m/s) to at least 60% strain relative to the original sample length. Of the 18 possible combinations of testing parameters, there are 10 primary sensitivity cases. Duplicate testing for these primary sensitivity cases would require 20 individual tests. If significant discrepancies between results from duplicate tests are evident, supplemental tests may be required.
- Equipment requirements – a precise compression machine with load and displacement control capable of a constant displacement rate of up to 1 m/s is required for this test suite. The maximum stress recorded from previous tests of this type on 20 mm diameter samples of MX-80 buffer was about 5 MPa. Fall hammer tests conducted by /Börgesson et al. 2004/ lack the control required to ensure precise loading of the end face orthogonal to the specimen axis, and to ensure a constant displacement rate throughout the test.

- Monitoring – tests will be monitored using force and displacement transducers to produce a detailed record of force and displacement versus time. A data acquisition system with high frequency reading capabilities is required to capture the complete monitoring responses over these very short duration tests. Displacement is to be ceased once the specified engineering strain is reached. A high-speed digital video of each test is to be recorded to document the testing procedure and results.
- Characterisation – pre- and post-test characterisation is required to determine initial and final density and water content of each specimen. Standard laboratory procedures will be used to determine these parameters. Specimens will be photographed before and after testing.
- Data management and analysis – results from monitoring sensors used in each test and meta-data (e.g. sample description, date of testing, characterisation data, etc) will be captured using a custom EXCEL workbook template. From this data set, plots of force versus time, displacement versus time, force versus displacement, and stress versus engineering strain will be produced. Data will be reviewed immediately following testing to diagnose any anomalies in results.
- Reporting – a brief data report will be prepared for each test to summarise the results and document any observations taken during the test. A final summary report will be produced once all testing in this suite is completed.

### 4.3 Two-component constant volume tests

Early in the program development, specialised two-component tests were proposed to assess the behaviour of bentonite buffer under conditions of constant volume. These tests were to be conducted at 1:10 scale to reduce buffer maturation time. Three types of tests were envisioned:

- Hollow cylinder compression tests – the purpose of these tests is to directly measure the stress-strain response, as well as strength and deformation characteristics, of buffer material compressed between two concentric cylinders under constant volume conditions (Figure 4-1). These tests would involve the preparation of MX-80Ca buffer samples inside an open-ended thick-walled steel cylindrical test vessel with a central thick-walled pipe extending past the ends of the test vessel. Over-sized flanged end plates would be secured to the central pipe to provide lateral constraint to the buffer-filled annulus. The contact between the flanged end plate and the test vessel would be sealed to prevent pressure loss during testing, and would be designed so as to create a frictionless interface between the end plate and the test vessel. The central pipe would rest on two fixed supports equipped with load cells to record applied load. The outer vessel would be loaded vertically down at a constant velocity by a custom loading platen. Force and displacement would be measured at the top of test vessel. The central pipe would be checked for deflection during loading. Additional instrumentation would include total pressure and pore pressure sensors on the central pipe interface with the buffer, and on the inner wall of the outer vessel to measure pressure change during the test. From the measured force, displacement and pressure versus time data, stress-strain relations for Ca-bentonite buffer would be derived, along with material stiffness and strength properties.

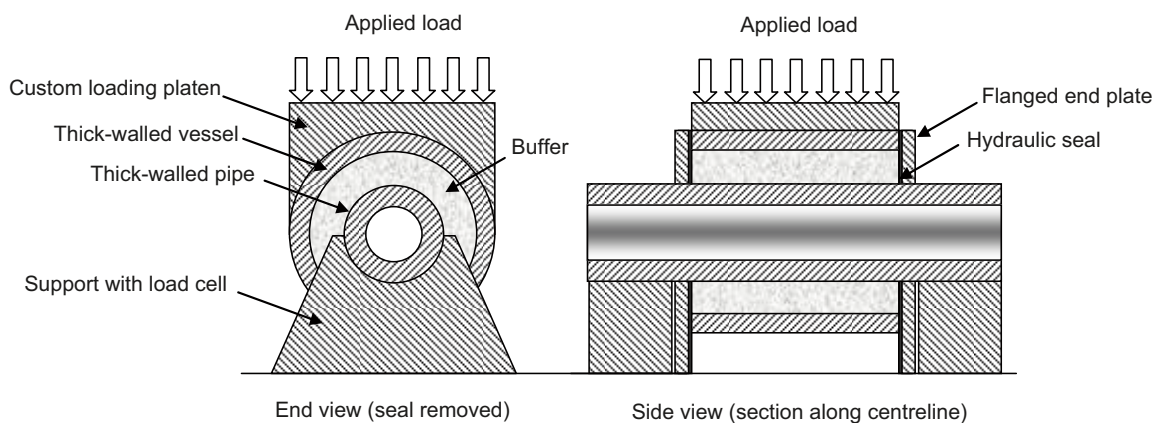


**Figure 4-1.** Conceptual drawing of hollow cylinder compression testing apparatus.

- Hollow cylinder interface shear tests – the purpose of these tests is to determine the shear strength of the rock/buffer and the buffer/canister interfaces. An MX-80Ca bentonite buffer specimen would be prepared inside an outer thick-walled test vessel with a central cylinder (solid or hollow) of the appropriate material to be tested (either copper or rock). The test would involve loading the central cylinder axially at a constant displacement rate while constraining the buffer annulus and outer vessel against a bottom plate with a central hole (Figure 4-2). The axial load would extrude the central cylinder from the specimen through the hole in the plate, shearing along the interface with the buffer. The force and displacement on the central cylinder would be monitored to develop a stress-strain curve, and estimate shear strength. Additional instrumentation would include total pressure and pore pressure sensors on the central pipe interface with the buffer, and on the inner wall of the outer vessel to measure pressure change during the test.
- Hollow cylinder buffer shear test – the purpose of these tests is to measure the shear strength of an annulus of buffer material sheared along an orthogonal plane without the influence of a rigid structure crossing the shear plane. These tests would involve the preparation of an MX-80Ca bentonite buffer specimen inside a two-part cylindrical test vessel, each part with a central pipe (Figure 4-3). Both parts of the test vessel would be flanged to allow sliding along the interface formed by the opposing flanges. The two central pipe pieces would each be capped, and would rest against one another in a horizontal alignment. The interface between the two pipe ends would be designed to be frictionless. Axial restraint would be applied to the test setup to offset swelling pressure, and to maintain a seal between the two halves of the test vessel. The right half of the test vessel would be secured, and the left half sheared at a constant velocity. The applied force and shear displacement would be monitored during the test, from which the shear strength along the shear plane would be derived. The stress-strain response would also facilitate validation of material models of Ca-bentonite buffer. These tests are similar to direct shear tests previously conducted on MX-80 bentonite buffer, and are considered optional. However, they present an opportunity to test instrumentation in a configuration similar to scaled analogue tests.

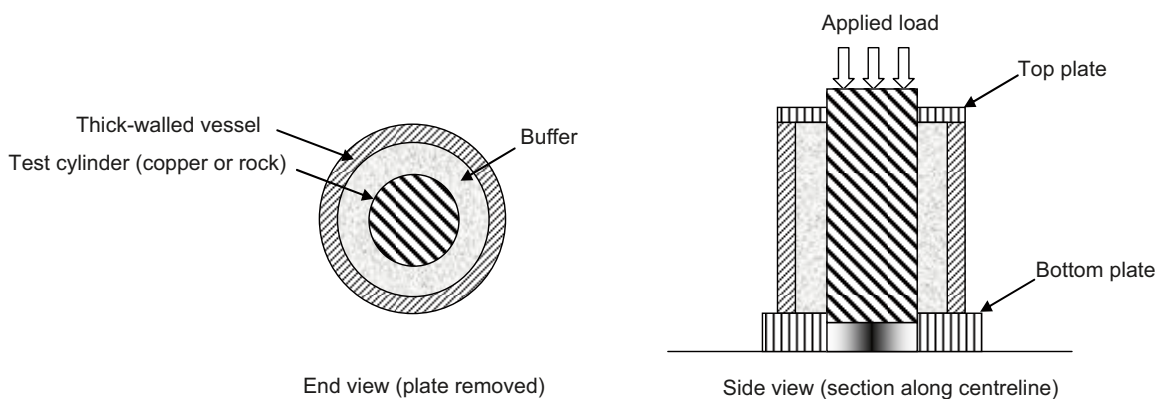


**Figure 4-2.** Conceptual drawing of hollow cylinder interface shear testing apparatus.

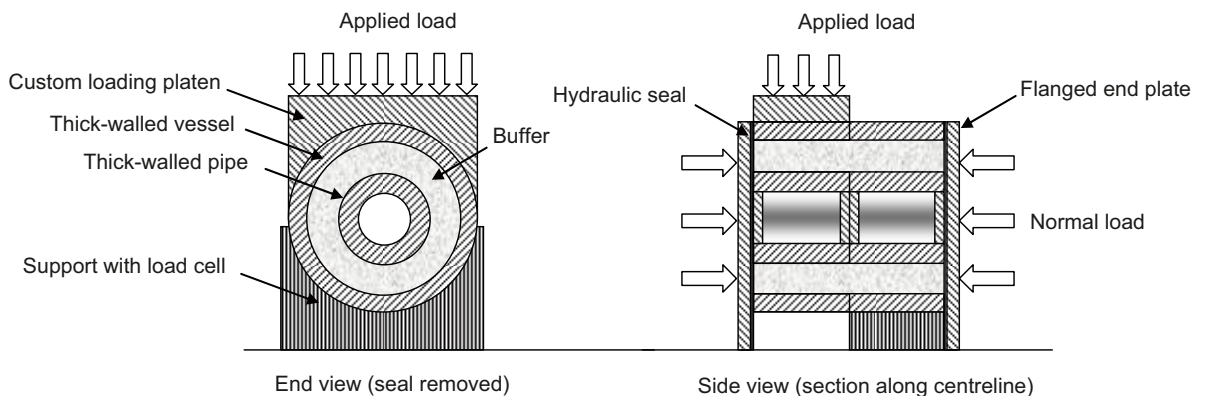


**Figure 4-3.** Conceptual drawing of hollow cylinder buffer shear testing apparatus.

These constant volume test configurations address specific issues identified in the literature review. The compression tests are meant to resolve the outstanding issues with the stress-strain response of Ca-bentonite buffer under constant volume conditions, and associated issues with selection of appropriate buffer stiffness and strength values for model simulations. The interface shear tests are intended to address the outstanding issues concerning the use and properties of contact elements at model interfaces between clay buffer and other materials. The optional buffer shear tests are meant to provide additional validation data for the numerical models under constant volume conditions if deemed necessary. General specifications and requirements for this test suite are as follows:

- Specimen specifications – tests will be conducted on 100% water-saturated specimens prepared from MX-80Ca bentonite buffer. Annular specimens will be produced from blocks of pre-compacted bentonite of known density and moisture content that will be exposed to distilled water under pressure and allowed to mature over a period of time. Sample preparation procedures for analogue tests described by /Börgesson 1986/ provide a general guideline to prepare specimens for these tests. In each case, the surface of the central pipe in the test setup is either copper or rock, depending on the test type.
- Test conditions – tests will be conducted on samples at three bulk densities (1,950, 2,000, 2,050 kg/m<sup>3</sup>) at three constant displacement rates (0.01, 0.1 and 1.0 m/s). One constant volume compression test and two different constant volume interface tests (one using copper and the other using rock) will be conducted at select combinations of density and displacement rate. Of the 27 possible combinations of test parameters, there are 15 primary cases to be tested. If significant anomalies are evident in these specific test results, supplemental tests may be required.
- Equipment requirements – a precise compression machine with load and displacement control capable of a constant displacement rate of up to 1 m/s is required for this test suite. In addition, specialised test vessels, loading platens and associated reaction frames are required as per the schematic drawings in Figure 4-1 and Figure 4-2. The test cylinders are to be designed to 1:10 scale in cross section orthogonal to the cylinder axis, with the length of the outer test cylinder twice its diameter to reduce end effects. The inner and outer cylinder walls are to be thick enough to prevent undesirable deformation during shearing, and all sliding surfaces are to be frictionless and water-tight. Stiff filters along the inner surface of the test vessel, and a water control system, are required to facilitate specimen saturation with distilled water. Given the long sample preparation time, two compression and two interface shear test vessels will be required to accommodate a reasonable test schedule and provide redundancy in the event of equipment malfunction.
- Monitoring – tests will be monitored using force and displacement transducers to produce a detailed record of force and displacement versus time. Displacement in the compression test is to be ceased after 20 mm in the tests (i.e. 60% of the buffer annulus thickness). Axial displacement in the interface shear test will depend on the test vessel design, but at a minimum should be 20 mm. Additional instrumentation will include total pressure and pore pressure sensors on the central pipe interface with the buffer, and on the inner wall of the outer vessel to measure conditions prior to and during the test. A data acquisition system with high frequency reading capabilities is required to capture the complete monitoring responses over these very short duration tests. A high-speed digital video of each test is to be recorded to document test performance.
- Characterisation – pre- and post-test characterisation is required to determine initial and final density and water content of each specimen. Standard laboratory procedures are to be used to determine these parameters. Specimens are to be photographed before and after testing. In addition, post-characterisation observations (e.g. gaps at interfaces, extent of visible shearing, etc) will be made, and forensic sampling of the buffer material to determine density and moisture variations within the sample will be undertaken. The use of X-ray CT scanning or similar imaging technology will be explored to capture the density and moisture distributions in the post-test sample for comparison with model predictions.
- Data management and analysis – results from monitoring sensors used in each test and meta-data (e.g. sample description, date of testing, characterisation data, etc) will be captured using a standard EXCEL workbook template. From this data set, plots of force, total pressure, pore pressure, and displacement versus time; force, total pressure and pore pressure versus displacement; and stress versus engineering strain will be produced. Data will be reviewed immediately following testing to diagnose any anomalies in results.
- Reporting – a brief data report will be prepared for each test to summarise the results and document any observations taken during the test. A final summary report will be produced once all testing in this suite is completed.

## 4.4 Scaled analogue tests

A proposed suite of nine scaled analogue tests was based on using JAEA's existing BORE-SHEAR apparatus at the Tokai Research Centre in Japan. Due to issues with dimensions of the test vessel and other considerations, the proposed suite of tests was modified. The refined suite of tests covers a range of bentonite buffer densities, shear rates, and shear displacements. A significant part of this testing suite involves equipment design, fabrication and testing (Figure 4-4 and Figure 4-5).

- Specimen specifications – tests will be conducted on 100% water saturated specimens prepared from MX-80Ca bentonite buffer. Specimens will be prepared from pre-compressed disks and rings of MX-80Ca buffer to a specified density to achieve desired final bulk density upon saturation with distilled water and swelling. Sample maturation at 20°C will take place in the test vessel using distilled water under a constant pressure. Non-deformable filters in the test vessel are required to provide water flow to the specimen. Sample preparation procedures for analogue tests described by /Börgesson 1986/ provide a general guideline to prepare specimens. In each case, the central canister will comprise an outer copper shell and an inner cast iron insert with properties comparable to an actual canister. The KBS-3 canister to be scaled down for the analogue tests is shown in Figure 4-6.
- Test conditions – tests will be conducted on bentonite samples at three bulk densities (1,950, 2,000, 2,050 kg/m<sup>3</sup>), three constant displacement rates (0.01, 0.1 and 1.0 m/s), and two shear displacements (approximately 30% and 60% of buffer annulus). The tests would ideally be conducted at 1:5 scale, although 1:10 scale is also acceptable. At 1:10 scale, the target shear displacements would be 10 and 20 mm; at 1:5 scale they would be twice these values. Of the 18 possible combinations of parameters, there are 10 primary cases to be tested, with provision for prototype tests to aid in equipment and instrumentation development and testing. If significant anomalies are evident in specific test results, supplemental tests may be required.
- Equipment requirements – a large precise compression machine with load and displacement control capable of a constant displacement rate of up to 1 m/s is required for this test suite. Loads in previous 1:10 scale tests were as high as 200 kN at a relatively fast shear rate. At full-scale, the applied shearing force was estimated to be 20 MN for the ROSE test setup. Specialised test vessels and associated reaction frames are required as per previous analogue tests (see /Börgesson 1986/). The test cylinder walls are to be designed thick enough to prevent undesirable deformation during shearing, and all sliding surfaces are to be frictionless and water-tight. The data acquisition system is required to capture data at a very high frequency given the potentially short duration of these tests. Given the long sample preparation time, four test vessels are required to accommodate a reasonable test schedule. A scaled canister is required for each of the primary test cases, and for each prototype test.
- Monitoring – tests will be monitored using force and displacement transducers to produce a detailed record of force and shear displacement versus time. Displacement is to be ceased at displacement equivalent to 30 or 60% of the buffer annulus thickness, depending on the specified test conditions. Additional instrumentation will include total pressure sensors on the canister interface with the buffer, and on the inner wall of the test vessel to measure total pressure change during the test. Pore pressure sensors will also be installed to allow comparison of pore pressure with results from effective stress models. Water uptake and swelling pressure are to be monitored to confirm completion of maturation and measure swelling pressure, and to calculate density. Strain gauges on the inner surface of the copper container may be used to provide additional information. Two relative displacement sensors will be installed between the copper canister and the test vessel to measure canister tilt during the test. Canister position and shear deformation are to be measured at the end of each test through careful disassembly of the test specimen. A high-speed digital video of each test is to be recorded to document test performance.
- Characterisation – pre- and post-test characterisation is required to determine initial and final density and water content of each specimen. Standard laboratory procedures are to be used to determine these parameters. Post-test characterisation will include non-destructive X-ray CT scanning of samples, or use of alternative imaging technology if available, to determine density and moisture distribution within specimens for comparison to model predictions. In addition, post-characterisation observations (e.g. gaps at interfaces, extent of visible shearing, canister geometry, axial displacement of buffer on the shear plane, etc) will be made, and forensic sampling of the buffer material to determine density and moisture variations within the sample will be undertaken. Sampling procedures are required to ensure that the sampling process is conducted efficiently to avoid effects of free swelling of the bentonite. Specimens are to be photographed before and after testing.

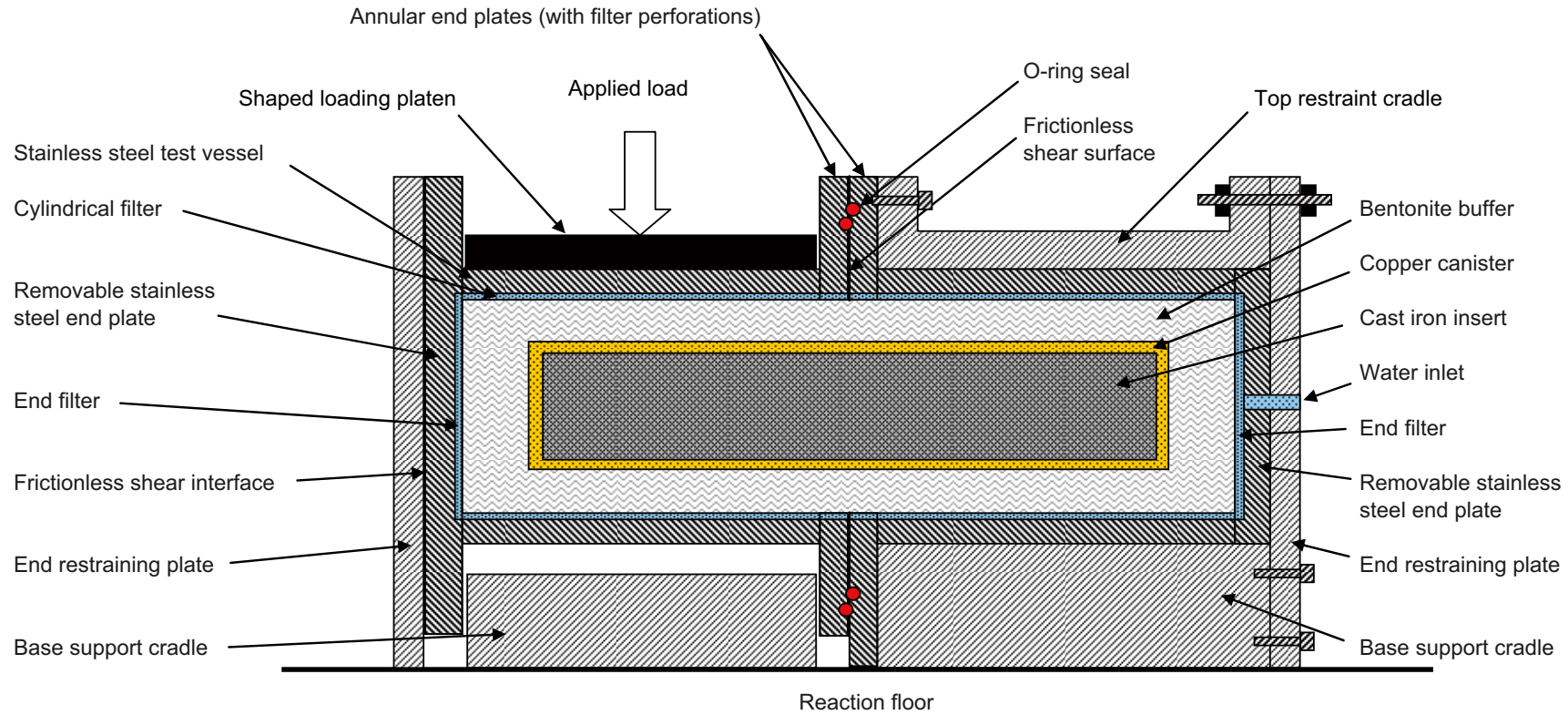


**Figure 4-4.** Conceptual drawing of scaled rock shear analogue testing apparatus (side view, vertical central cross section).

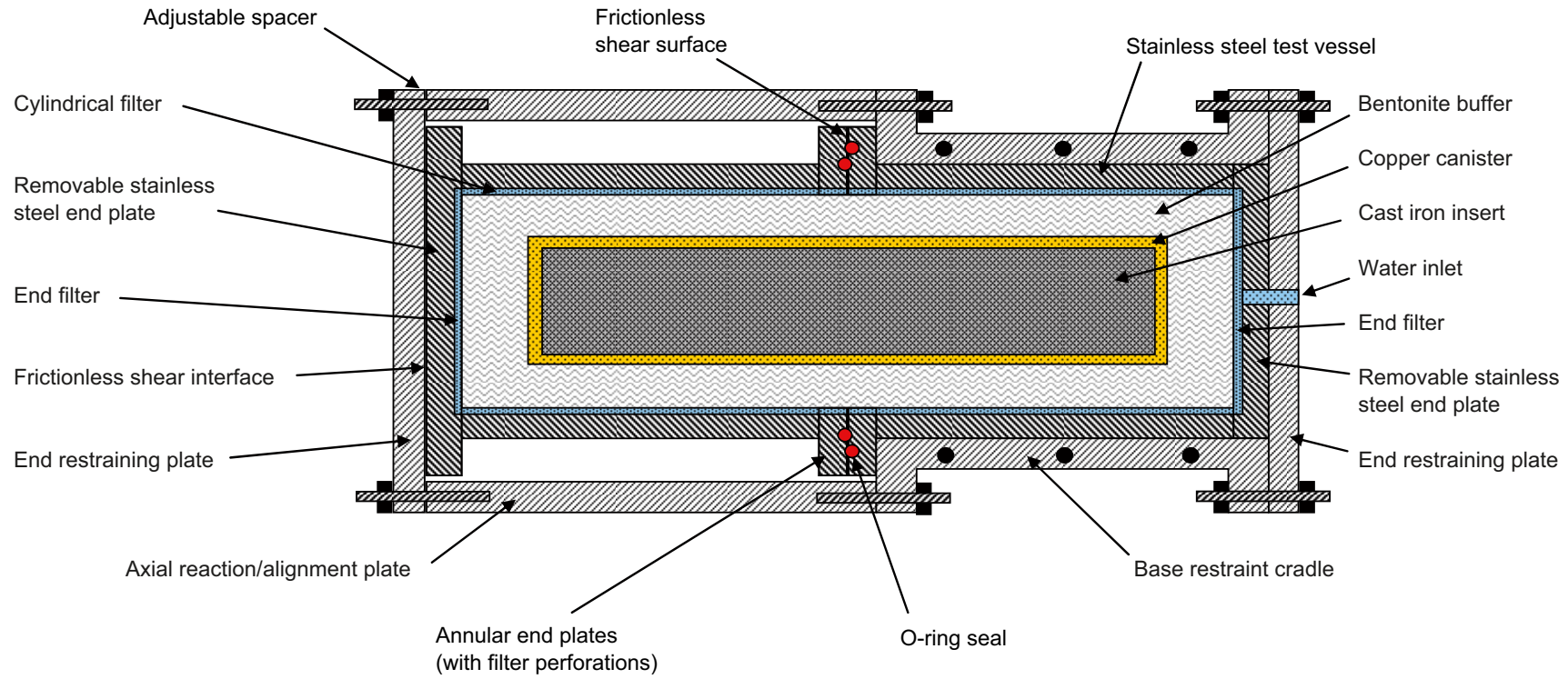
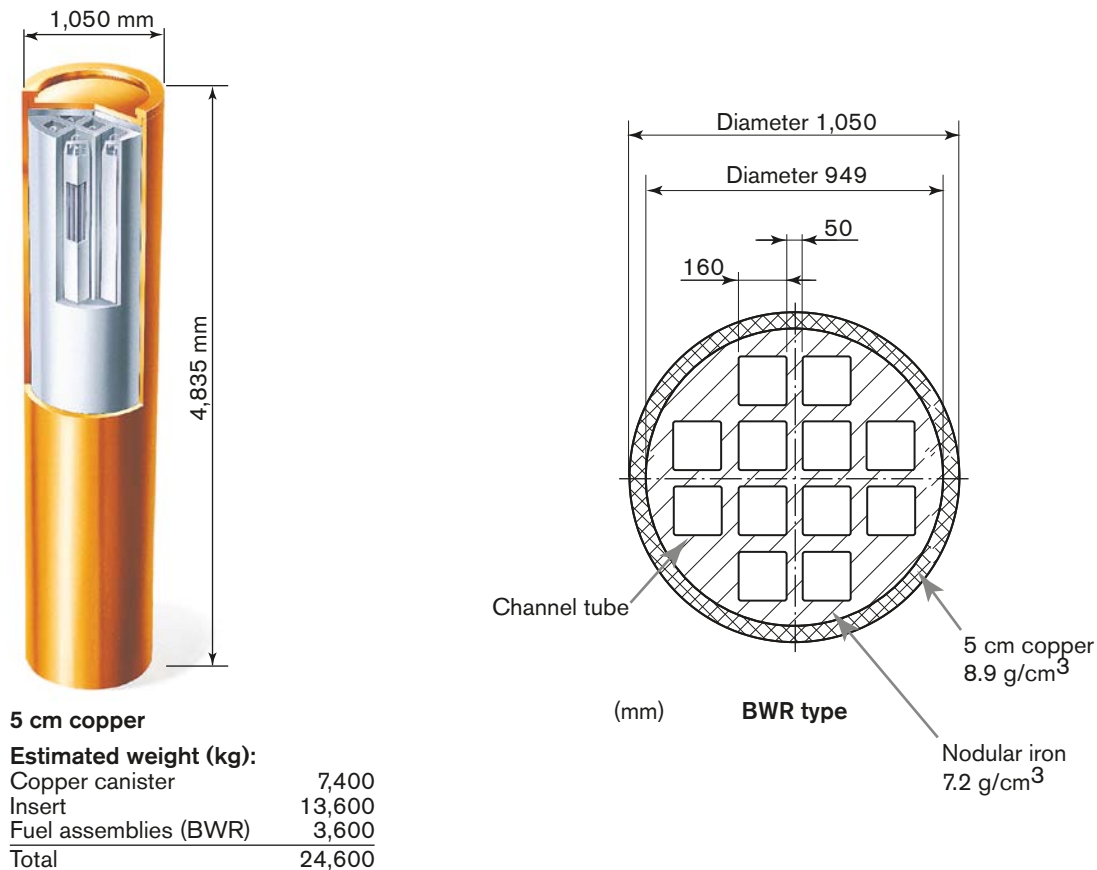


Figure 4-5. Conceptual drawing of scaled rock shear analogue testing apparatus (top view, horizontal central cross section).



**Figure 4-6.** Illustration of the KBS-3 BWR composite copper/cast iron canister to be simulated in scaled analogue tests (from /SKB 2006/).

- Data management and analysis – results from monitoring sensors installed in each test and meta-data (e.g. sample description, date of testing, characterisation data, etc) will be captured using a custom EXCEL workbook template. From this data set, plots of force, total pressure, pore pressure, shear displacement, relative displacement and strain (if strain gauges are used) versus time; force, total pressure, pore pressure, relative displacement and strain (if strain gauges used) versus shear displacement; and stress versus engineering strain will be produced. In addition, plots of density, moisture content, axial displacement across the shear plane, and post-test canister geometry will be produced as supplemental points of comparison to model simulation results. Data are to be reviewed immediately following testing to diagnose any anomalies in the results.
- Reporting – a brief data report will be prepared for each test to summarise the results and document any observations taken during the test. A final summary report will be produced once all testing in the suite is completed.

## 4.5 Technical considerations

Based on previous testing and laboratory visits, several technical considerations in designing and fabricating testing apparatus, and in conducting the tests, were identified. Key considerations are:

- Dimensions of test vessels – the test vessels required for the analogue tests will be designed to a preferred scale of 1:5, or optionally to 1:10 scale. The scaled dimensions of the buffer and canister based on the KBS-3V design are shown below in Table 4-1. The length of buffer in this design is different above and below the canister (1.5 and 0.5 m, respectively, at full-scale). A key technical issue to be resolved is whether or not to simulate the full thickness of the buffer above the canister, or to reduce this dimension to match the thickness below the canister. This latter approach will reduce time required to saturate the buffer and will retain symmetry conditions for the test, but may introduce non-representative end effects. Design scoping analyses are required to resolve this issue. The inner diameter of the steel test vessels (including inner filter) for both the analogue tests and the two-component tests will be designed to match the scaled buffer diameter, and the inner hollow cylinders or replica canisters in these tests will match the scaled canister diameter. The length of the buffer specimens used in the two-component and single component tests will be twice their outside diameter. Design scoping analyses are required to select the composition and thickness of test apparatus components to prevent deformation and deterioration. Use of available dimensioned tubes may reduce test vessel costs.
- Testing apparatus – aside from the large precision compression machine (or custom built loading frame and actuators) to be used for these tests, a reaction system is required to secure the fixed components of the analogue test vessel and prevent movement. As shown in Figure 4-4 and Figure 4-5, this system would comprise an upper and lower cradle connected by threaded bars to hold the cylindrical test vessel, and secured to a reaction floor to prevent movement. The test vessel would be horizontal during shearing to take advantage of the reaction floor. Previous scaled analogue tests experienced some out-of-plane rotation of the sliding cylinder during shearing. A means of controlling displacement direction of the sliding cylinder to prevent rotation is critical to avoid biasing the results of the tests. Control of axial displacement due to swelling of the buffer is another important consideration. Precise control of displacement rate is also critical to ensure the specimen experiences a constant velocity boundary condition with ‘instantaneous’ deceleration to zero velocity.
- Canister design – for the analogue tests, a scaled replica canister comprising a copper outer sheath and a cast iron (or steel) core will be used. It is anticipated that this component will be fabricated by SKB to match the properties of the materials in BWR canister design (Figure 4-6). Previous analogue tests used a solid copper rod. Design scoping analyses are required to ensure structural integrity of the scaled canister is maintained under high hydrostatic load. The use of a composite canister with channels between the copper and cast iron insert offers the possibility of installing internal strain gauges or other instrumentation. Wire leads from any internal instruments would require routing through the buffer and test vessel, ensuring a watertight seal and enough slack in the leads to avoid damage during shearing.

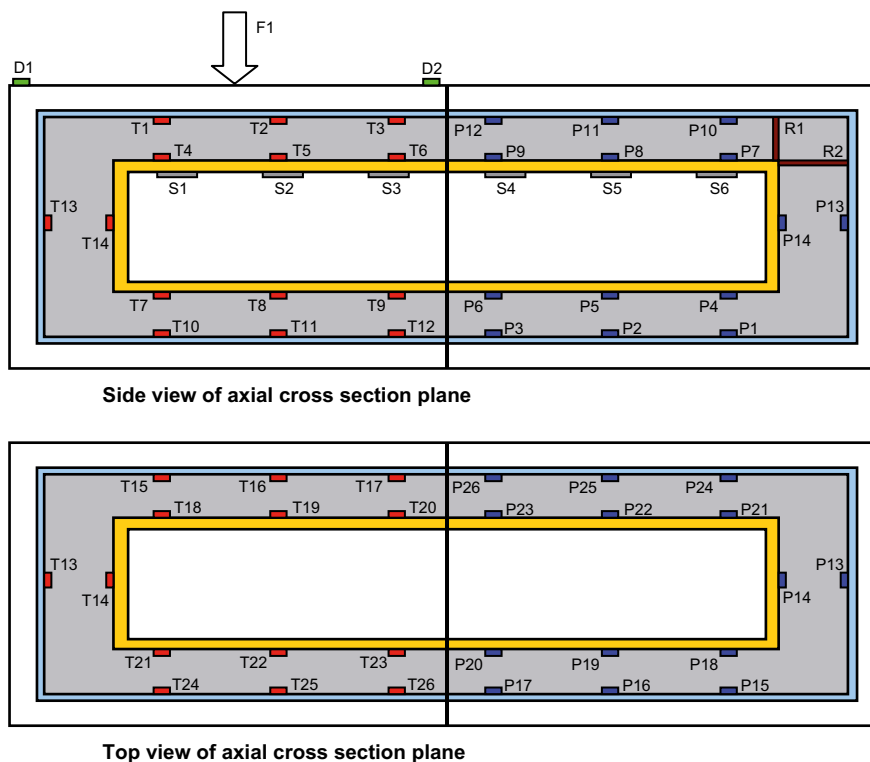
**Table 4-1. Summary of scaled dimensions for the KBS-3V design.**

Design Element	Scale	Dimensions (mm)	
		Diameter	Length
Buffer above canister	1:1	1,750	1,500
	1:5	350	300
	1:10	175	150
Canister	1:1	1,050	4,833
	1:5	210	967
	1:10	105	483
Buffer around canister	1:1	1,750	4,833
	1:5	350	967
	1:10	175	483
Buffer below canister	1:1	1,750	500
	1:5	350	100
	1:10	175	50

- Instrumentation – instrumentation of the analogue tests will include a force transducer (or load cell) to measure applied load at the loading platen, two displacement transducers to measure displacement of the shearing cylinder, two displacement transducers installed inside the test vessel to measure relative displacement between the canister and the test vessel, 13 total pressure and 13 pore pressure sensors installed on the inner surface of the test vessel/filter, 13 total pressure and 13 pore pressure sensors installed on the outer surface of the canister, and possibly 6 strain gauges installed on the inner copper surface of the canister. The approximate positions of these sensors are shown in Figure 4-7. For the two-component tests, the instrumentation inside the test vessel will include 12 total pressure sensors and 8 pore pressure sensors on the inner wall of the test vessel/filter, and 12 total pressure sensors and 8 pore pressure sensors on the outer surface of the inner test cylinder. Force and displacement will also be measured in these tests using appropriate transducers. Figure 4-8 shows a conceptual layout of instruments for the two-component tests.

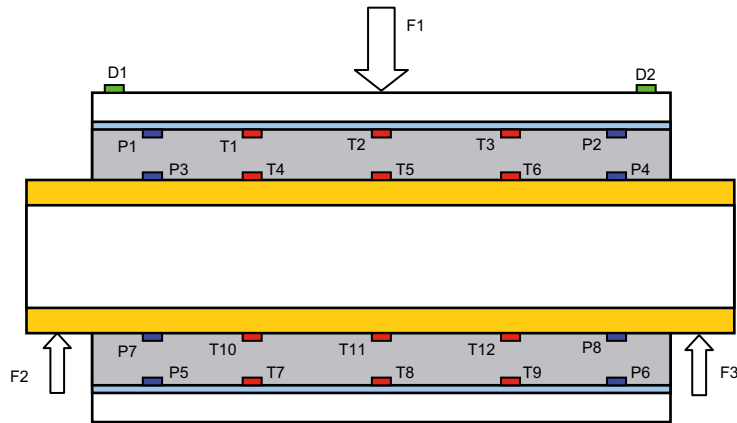
Related technical considerations for instrumentation include measurement range, sensitivity, robustness/durability, ease of replacement, longevity/survivability and compatibility with very high sampling frequencies. Experience from JAEA's BORE-SHEAR tests indicates that particular attention is required in the selection of pore pressure monitoring sensors. Furthermore, the instrumentation system should be designed to facilitate instrument replacement as needed. Given the long durations for buffer saturation/maturation, instruments must be stable and reliable for long periods of time over which they are inaccessible.

As there are many instruments shown in the conceptual drawings, routing of instrument wiring is another consideration. Routing along channels inside the canister in the analogue tests, then passage through a sealed port in the side of the canister and test vessel is envisioned for instruments on the canister. For the two-component tests, wiring can be run internally through the central cylinder if it is hollow. For interface shear tests using a solid cylinder, the instrumentation on the cylinder shown in Figure 4-8 may not be feasible. In both the analogue and two-component tests, wiring from instruments on the outer test vessel is expected to be routed in specially-designed channels in the test cylinder, accounting for the shear plane and the separate end plates on the steel test cylinder.

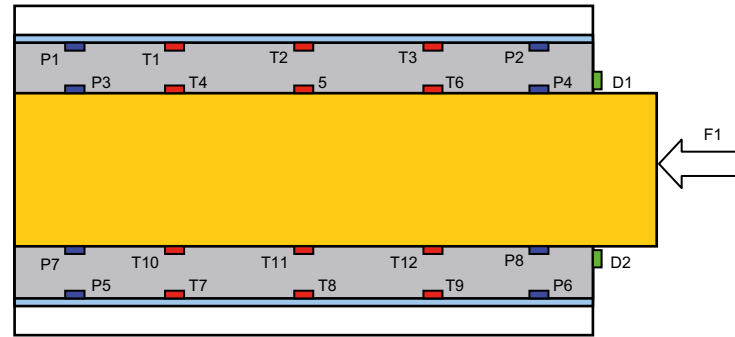


Note: The fixed part of the test cylinder is on the right of these diagrams. Sensor symbols are as follows: T – total pressure, P – pore pressure, S – strain, R – relative displacement, D – displacement, and F – force. The scaled replica canister (gold) is surrounded by MX-80Ca bentonite buffer (grey), a filter (light blue), and the test cylinder (white). The core of the copper canister is occupied by a cast iron insert.

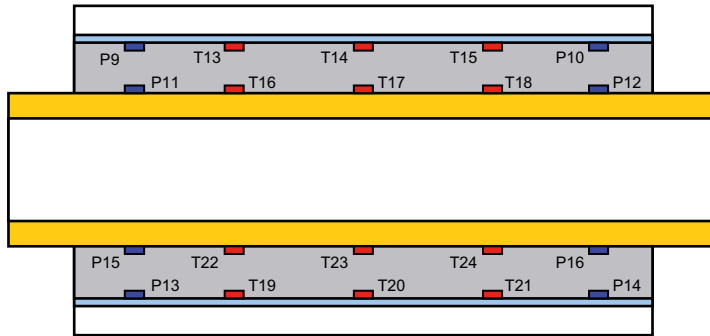
**Figure 4-7.** Conceptual instrumentation layout for a typical scaled analogue test.



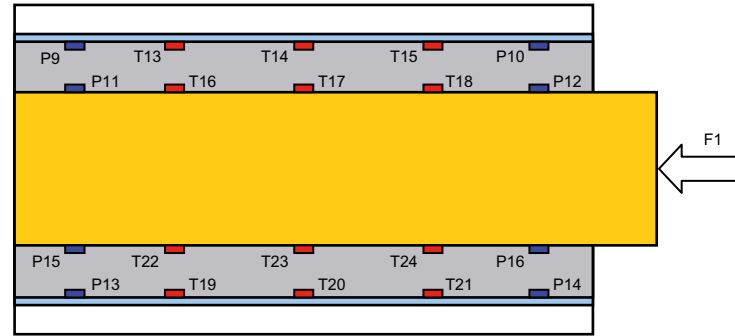
Side view of axial cross section plane



Side view of axial cross section plane



Top view of axial cross section plane



Top view of axial cross section plane

Note: Sensor symbols are as follows: T – total pressure, P – pore pressure, D – displacement, and F – force. The central cylinder (gold) is surrounded by MX-80Ca bentonite buffer (grey), a filter (light blue), and the test cylinder (white). The interface shear test (right) is shown in a rotated view for comparison.

Figure 4-8. Conceptual instrumentation layout for two-component compression (left) and interface shear (right) tests.

- Saturation time – the time for a specimen to mature and develop a uniform swelling pressure can be estimated using a coefficient of water diffusion of  $0.3 \cdot 10^{-9} \text{ m}^2/\text{s}$  for MX-80 sodium bentonite buffer, or an alternate value for MX-80Ca bentonite. This process may take 2–4 months at 1:10 scale based on previous analogue tests, and was estimated to take 2 years at full-scale for the ROSE test setup using filter mats. Design of a suitable filter system to supply water to the buffer is a critical design issue. The filter must be stiff enough to prevent deformation during shearing, and smooth enough to represent the rock mass. Monitoring of this stage of sample preparation is required to ensure pore pressure and/or total pressure equilibrate prior to testing.
- Swelling pressure – in the two-component and analogue tests, the test vessel will experience internal swelling pressure generated by the maturing buffer. For Ca-bentonite buffer bulk densities of 1,950, 2,000 and 2,050  $\text{kg}/\text{m}^3$ , swelling pressures are expected to reach 5.2, 8.2 and 12.9 MPa, respectively, based on Equation 3-5 using a specific gravity of 2.78 for bentonite particles and 1.0 for water. Test vessels must be designed to accommodate these pressures without deformation. End plates and facing plates on testing vessels must be restrained to offset this swelling pressure and maintain a watertight seal. It is imperative that all contact surfaces on the apparatus subjected to shearing are frictionless to avoid influencing the test results.
- Applied load and shear rates – based on previous testing, the applied load required to shear the 1:10 scale analogue test specimens was as high as 200 kN for the densities and shear rates used. The required load for the full-scale ROSE test arrangement is estimated to be 20 MN. The 1:5 scale analogue tests are estimated to require an applied load of about 800 kN. Shear rates of 0.01, 0.1 and 1.0 m/s were selected to cover the range of values considered possible at full-scale. This approach addresses the possibility that shear strength is shear rate dependent rather than strain rate dependent.
- Target shear strain – the buffer annulus in the KBS-3V design is 350 mm thick. Total shear displacement considered at full-scale has ranged from 0.1 to 0.2 m. At 1:10 scale, these values would be 10 and 20 mm, respectively. At 1:5 scale, they would be 20 and 40 mm, respectively. These values represent 28.6 and 57.1% shear strain, respectively, relative to the thickness of the buffer annulus in each case.
- Test duration – the planned displacement rates to be used in the various tests are 0.01, 0.1 and 1.0 m/s. For the single component tests, total displacements range from 11.4 to 45.7 mm for the two specimen lengths (40 and 80 mm) and target strains (28.6 and 57.1%). Test durations range from 4.6 to 0.01 seconds at the selected displacement rates. For the two-component tests, 20 mm displacement will take between 2.0 and 0.02 seconds at these displacement rates. For the analogue tests, displacements of 10, 20 or 40 mm (depending on scale and final specified strain) will take between 4.0 and 0.01 seconds. These short durations require a data acquisition system with very high data sampling frequency to capture the complete monitoring responses. Likewise, sensor selection will need to take these durations and sampling rates into account.
- Post-test characterisation – characterisation of the buffer specimen after testing requires detailed procedures and protocols in order to capture the required information in an efficient manner without compromising specimen integrity. The testing apparatus should be designed to accommodate handling of the sheared specimen. A base support at the appropriate height to support the shear cylinder is shown in the conceptual drawings (Figure 4-4). The apparatus also allows removal of the specimen from the test cylinder by taking the end plates off of the test cylinder, and extruding the soil mass. Once removed as a single piece, the specimen is to be photographed, and subjected to X-ray CT scanning or similar technology to obtain a 3D image of the density and moisture distribution within the specimen. This type of technology has been used by JAEA but has some limitations associated with embedded metal objects. Investigation of this and other technology is required to determine the feasibility of conducting such imaging non-destructively on a recovered buffer overpack specimen. Forensic sampling following imaging provides a complementary basis for defining density and moisture distributions.

- Testing procedures and checklists – as part of detailed design of the testing apparatus and experimental setup, a series of detailed procedures and checklists is required to ensure tests are conducted consistently. Procedures will cover sample preparation, sample saturation/maturation monitoring, instrumentation installation and calibration, equipment operation including a step-by-step process to prepare for the analogue tests prior to shearing, and other relevant processes or operations.
- Numerical modeling – refinement of material models will be advanced in conjunction with the laboratory testing program, or at junctures where a suite of tests is available for calibration purposes. Existing material models will be used for this component of the program, the goal being to identify required adjustments, if any, to the models to minimise discrepancies between laboratory test results and outputs from model simulations. SKB’s fit-for-purpose approach to developing numerical models has been successful and is amenable to model refinement, given the relative simplicity of the total stress and effective stress models used to date to model rock shear. Model validation will draw on monitoring results from installed instruments as well as observations from post-test characterisation (density and moisture distributions), and measurements of the post-test canister and shear plane geometry.
- Number of test vessels – given the long duration to saturate and mature buffer specimens and the relatively large number of tests envisioned, the only practical means of completing the tests in reasonable time-frame of a few years is to construct multiple test vessels for the various test types. By modularizing the system design so that individual test cylinders are self-contained in terms of instrumentation and can be saturated outside of the testing apparatus as individual test cartridges, testing will proceed in overlapping cycles of specimen preparation, saturation/maturation, test execution, and post-test characterisation. In order to ensure that a particular design is adequate, it is envisioned that an initial period of time will be required to develop and test prototype equipment and instrumentation/data acquisition systems before fabricating multiple test cylinders. For the hollow cylinder tests, two compression and two interface shear vessels are required. Four scaled analogue test vessels are required. In addition, twelve scaled composite copper/cast iron canisters, two thick-walled hollow cylinders with an outer copper surface, two copper cylinders and two rock cylinders (hollow or solid) will be required.
- Analysis and reporting – ongoing analysis and reporting is imperative to ensure that adjustments to the testing schedule or conditions can be made in a timely manner. Communication between laboratory personnel and SKB investigators is a vital element of the testing program. Reporting requirements will be streamlined to the extent possible using custom EXCEL workbook templates and standard data reporting formats. Technical meetings will be held at specific intervals as required to keep SKB apprised of progress.

## 4.6 Work scope

The scope of work envisioned for the laboratory testing program (Table 4-2) includes a number of sub-tasks under the general task headings of Management, Systems Development, Testing, Analysis, and Reporting. The specific laboratory tests included in the laboratory testing program are itemised in Table 4-3 through Table 4-5, inclusive.

**Table 4-2. Summary of laboratory program tasks.**

---

**Task 1: Management**

---

- 1.1 **Project management** – this task covers the project management and technical coordination aspects of the laboratory testing program including teleconferences and meetings with SKB investigators, generation of presentations on interim results, and associated administrative activities. This task will involve collaboration between SKB investigators and laboratory facility staff to steer the project to successful completion.
- 

**Task 2: Systems Development**

---

- 2.1 Laboratory testing apparatus development – this task involves design, fabrication and testing of laboratory testing apparatus for the rock shear scaled analogue tests (preferably at 1:5 scale, but optionally at 1:10 scale relative to the KBS-3V design), and for two-component constant volume compression and interface shear tests at 1:10 scale. It also involves selection of appropriate loading machines to conduct the various tests (including the standard uniaxial compression tests). Conceptual drawings for the two-component and analogue tests are contained in Sections 4.3 and 4.4. Fabrication and testing of alternate designs and prototypes is envisioned as part of this task prior to production of multiple test vessels for the various test types. Development of procedures and checklists related to operation of testing apparatus is also part of this task. It is assumed that the composite copper/cast iron canisters required for multiple scaled analogue tests, and hollow and solid cylinders required for two-component tests, will be fabricated by SKB in Sweden using representative materials.
- 2.2 Instrumentation systems development – this task involves detailed design of the instrumentation systems for the various test types, including selection and testing of data acquisition components and instruments to monitor force, displacement, total pressure, pore pressure and strain under expected test conditions. Completion of prototype tests to verify instrument performance and to finalise the instrument arrangement in each test type is envisioned as part of this task. Scoping analyses using existing numerical models are anticipated to help optimise the arrangement of instruments. Conceptual instrumentation layouts are provided in Figures 4-7 and 4-8. Development of procedures and checklists related to instrumentation installation, calibration, operation and replacement is included in this task.
- 

**Task 3: Testing**

---

- 3.1 Specimen preparation – this task involves developing a process and associated procedures and checklists for preparing specimens of MX-80Ca bentonite buffer to a specified density at 100% water saturation for the various test types (i.e. uniaxial compression tests, two-component constant volume compression and interface shear tests, and rock shear scaled analogue tests). For the two-component and analogue tests, this process includes water saturation of the buffer material under a specified pressure, and associated monitoring of the saturation/maturation process. Equipment to create compressed rings and disks of bentonite is to be acquired, or arrangements are to be made to utilise equipment available to SKB. Prototype specimens will be prepared to demonstrate the reliability of the developed procedures and equipment. Once developed, the procedures will be followed to produce test specimens over the course of the testing program.
- 3.2 Test execution – this task covers the execution of the various single component, two-component, and scaled analogue tests as outlined in Tables 4-3, 4-4 and 4-5, respectively. Test execution includes all activities that occur once a specimen has reached maturation, and is ready for testing. Development and implementation of a step-by-step procedure for loading the specimen into the testing apparatus, ensuring all instruments are positioned properly and are connected correctly to the data acquisition system, activating the loading machine, checking the status of collected data, disengaging the instrumentation and preparing the specimen for post-test characterisation are the main activities associated with this task. Organization of all test results into a customised EXCEL workbook template, and review of test results with SKB investigators, are both part of this task.
- 3.3 Post-test characterisation – this task covers the development and application of post-test characterisation procedures. Specimen characterisation will involve non-destructive x-ray CT scanning (or similar) technology after testing to assess 3D changes in the distribution of density, moisture and possibly other conditions useful for model validation. In addition, systematic forensic disassembly to determine density and moisture content of samples from the original specimen following non-destructive scanning will be completed on all specimens. Standard laboratory tests for these physical measurements are included in this task, along with organisation of the information in a custom EXCEL workbook template.
- 3.4 Data reporting – this task involves the preparation of a data report for each individual test conducted. Each report will include details on sample preparation, test execution and post-test characterisation. Data plots from the customised EXCEL workbook templates and photographs will be included in these data reports. An electronic copy of the related EXCEL workbooks and digital video of the test will be attached to the report on DVD.
- 

**Task 4: Analysis**

---

- 4.1 Material model refinement – this task involves using existing material models in Abaqus to simulate the various single-component, two-component and scaled analogue tests. Results from these simulations will be compared directly with measured instrument responses, characterisation data, and observations from each test (e.g. analogue test shear plane geometry and canister geometry, two-component test plasticised zone and gaps, and uniaxial specimen failure geometry). Simulation results will be organised in a custom EXCEL workbook template identical to that used for the laboratory test results. Comparative plots will be generated based on the two data sets to identify differences. Based on the observed differences, refinements to the material models will be made in consultation with SKB to improve the fit between the two data sets. The step-wise modifications to the material model parameters will be documented as specific simulation cases. The final best-fit parameters for the material models will be documented for use in full-scale model predictions.

- 4.2 Numerical model prediction – this task involves using the refined material models in Abaqus to predict the full-scale response of a canister subjected to rock shear of 0.1 and 0.2 m displacement at a shear rate of 1 m/s for a buffer density of 2,050 kg/m<sup>3</sup> (the 0.1 m displacement case is considered in SR-Can and SR-Site, although the analyses are concentrated on 0.05 m displacement in the latter). These two cases provide the basis for direct comparison of the refined material model results to those from previous simulations using the existing material models.

---

**Task 5: Reporting**

---

- 5.1 Summary reporting – this task involves the generation of data summary reports for each of the three suites of laboratory tests, and a final summary report that includes the results from material model refinement, and full-scale prediction of rock shear effects. This report will be written jointly by SKB investigators and laboratory personnel using an SKB report format template.
- 

**Table 4-3. Updated laboratory testing schedule (single component tests).**

Test Ref.	Test Type					Buffer Density			Shear rate			Scale		Comment
	UC	HCC	HCIR	HCIC	Analogue	Low	Medium	High	Low	Medium	High	1:10	1:5	
S01	✓							✓			✓	✓		Initial test
S02	✓							✓		✓		✓		Initial test
S03	✓							✓	✓			✓		Initial test
S04	✓						✓				✓	✓		Initial test
S05	✓					✓					✓	✓		Initial test
S06	✓							✓			✓		✓	Initial test
S07	✓							✓		✓			✓	Initial test
S08	✓							✓	✓				✓	Initial test
S09	✓						✓				✓		✓	Initial test
S10	✓					✓					✓		✓	Initial test
S11	✓							✓			✓	✓		Duplicate test
S12	✓							✓		✓		✓		Duplicate test
S13	✓							✓	✓			✓		Duplicate test
S14	✓						✓				✓	✓		Duplicate test
S15	✓					✓					✓	✓		Duplicate test
S16	✓							✓			✓		✓	Duplicate test
S17	✓							✓		✓			✓	Duplicate test
S18	✓							✓	✓				✓	Duplicate test
S19	✓						✓				✓		✓	Duplicate test
S20	✓					✓					✓		✓	Duplicate test

**Legend**

Test Type	Density (kg/m <sup>3</sup> )	Shear Rate (m/s)
UC – Unconfined compression	Low – 1,950	Low – 0.01
HCC – Hollow cylinder compression	Medium – 2,000	Medium – 0.1
HCIR – Hollow cylinder interface shear (rock)	High – 2,050	High – 1.0
HCIC – Hollow cylinder interface shear (copper canister)		
Analogue – Scaled analogue test on buffer and canister		

**Table 4-4. Updated laboratory testing schedule (two-component tests).**

Test Ref.	Test Type					Buffer Density			Shear rate			Scale		Comment
	UC	HCC	HCIR	HCIC	Analogue	Low	Medium	High	Low	Medium	High	1:10	1:5	
T01		✓						✓			✓	✓		Max. disp. 20 mm
T02		✓						✓		✓		✓		Max. disp. 20 mm
T03		✓						✓	✓			✓		Max. disp. 20 mm
T04		✓					✓				✓	✓		Max. disp. 20 mm
T05		✓				✓					✓	✓		Max. disp. 20 mm
T06			✓					✓			✓	✓		Min. disp. 20 mm
T07			✓					✓		✓		✓		Min. disp. 20 mm
T08			✓					✓	✓			✓		Min. disp. 20 mm
T09			✓				✓				✓	✓		Min. disp. 20 mm
T10			✓			✓					✓	✓		Min. disp. 20 mm
T11				✓				✓			✓	✓		Min. disp. 20 mm
T12				✓				✓		✓		✓		Min. disp. 20 mm
T13				✓				✓	✓			✓		Min. disp. 20 mm
T14				✓			✓				✓	✓		Min. disp. 20 mm
T15				✓		✓					✓	✓		Min. disp. 20 mm

**Table 4-5. Updated laboratory testing schedule (scaled analogue tests).**

Test Ref.	Test Type					Buffer Density			Shear rate			Scale		Comment
	UC	HCC	HCIR	HCIC	Analogue	Low	Medium	High	Low	Medium	High	1:10	1:5	
A01					✓			✓			✓		✓	Max. strain 30%
A02					✓			✓		✓			✓	Max. strain 30%
A03					✓			✓	✓				✓	Max. strain 30%
A04					✓		✓				✓		✓	Max. strain 30%
A05					✓	✓					✓		✓	Max. strain 30%
A06					✓			✓			✓		✓	Max. strain 60%
A07					✓			✓		✓			✓	Max. strain 60%
A08					✓			✓	✓				✓	Max. strain 60%
A09					✓		✓				✓		✓	Max. strain 60%
A10					✓	✓					✓		✓	Max. strain 60%

**Legend**

**Test Type**

UC – Unconfined compression  
HCC – Hollow cylinder compression  
HCIR – Hollow cylinder interface shear (rock)  
HCIC – Hollow cylinder interface shear (copper canister)  
Analogue – Scaled analogue test on buffer and canister

**Density (kg/m<sup>3</sup>)**

Low – 1,950  
Medium – 2,000  
High – 2,050

**Shear Rate (m/s)**

Low – 0.01  
Medium – 0.1  
High – 1.0

## 4.7 Schedule

The five-year schedule envisioned for the specified scope of work involves six months to seek detailed proposals and cost estimates, and select qualified testing laboratories; 18 months to design, fabricate and test equipment and undertake single component tests; two years to complete the various two-component and scaled analogue tests; and a final year to complete analysis, numerical modeling and reporting. The three test suites are independent and can therefore be carried out in parallel if feasible. The completion of standard single-component tests in the first year in parallel with systems development is expected to improve understanding of material behaviour for the design and execution of the other tests. A tentative schedule for the testing program is shown in Figure 4-9. This schedule assumes a duration of 3 months for tasks related to each two-component test, and 7 months for tasks related to each scaled analogue test. These durations will need to be confirmed through scoping analyses and prototype testing. On this basis, it is estimated that three test vessels (one compression and two interface shear) will be needed for the two-component tests, with one extra compression test vessel as backup, and four test vessels will be required for the scaled analogue tests, to meet this schedule. A total of twelve scaled canisters, two copper-surfaced hollow cylinders, one rock cylinder and one copper cylinder, along with associated testing apparatus, will need to be manufactured in the first year of the program. This number of test vessels and associated testing components provides redundancy in the event of equipment malfunction.

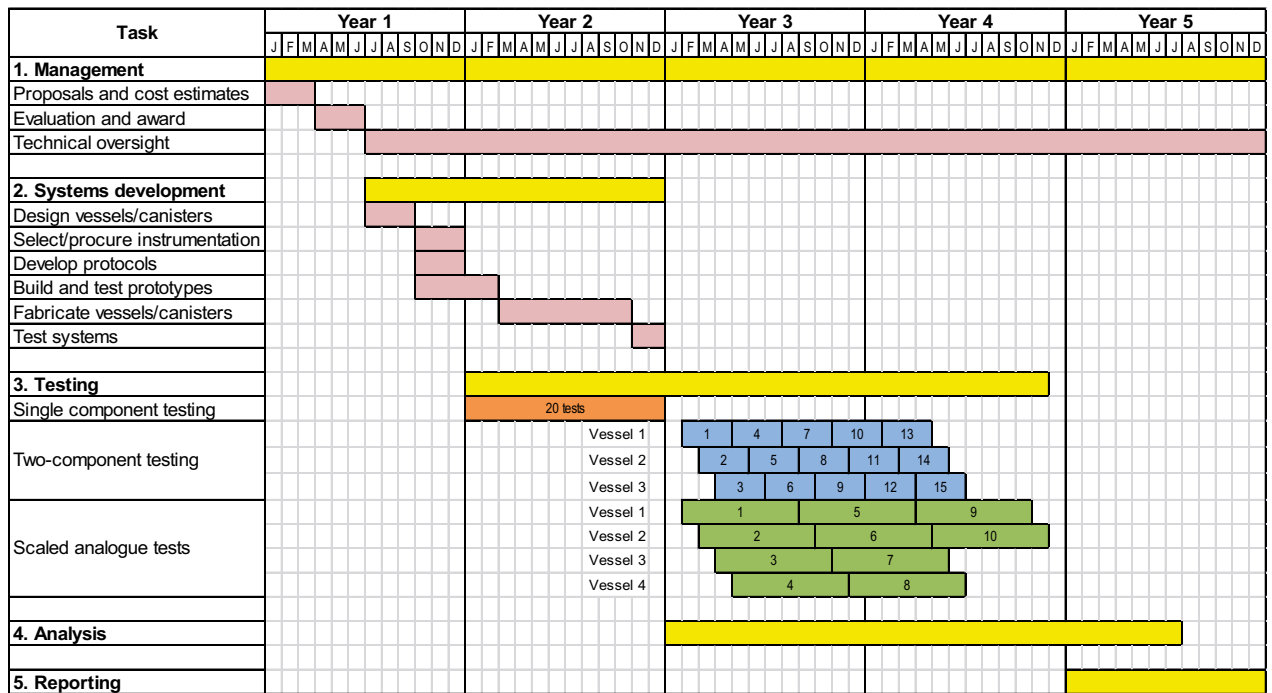


Figure 4-9. Tentative schedule for the testing program.

## 5 Conclusions and recommendations

### 5.1 Conclusions

Earthquake induced rock shear, and its effects on containment system integrity, is a key technical issue for concepts involving deep geologic isolation of spent nuclear fuel. Significant work related to this issue has been undertaken by SKB over the past 30 years in characterising material behaviour, developing material models, and performing numerical modeling simulations. This work has successfully supported SR-Can and SR-Site safety assessments in Sweden.

Much of the previous laboratory testing conducted in Sweden was focused on MX-80 sodium bentonite as the reference buffer material, although other materials were also tested. The adoption of calcium bentonite as a new reference buffer warrants additional standard single component laboratory tests to verify unconfined compressive strength and stress-strain behaviour. In addition, a suite of two-component and scaled analogue tests is proposed to develop a framework for numerical model calibration and prediction of rock shear effects at full-scale. The number of tests specified in this report is considered a minimum to build confidence in the testing results and subsequent model calibration and predictions. Additional tests may be required depending on equipment and instrumentation performance, and quality of test results.

Based on a detailed review of previous testing and modeling, a five year rock shear testing program is proposed to develop testing equipment, undertake laboratory testing, conduct numerical modeling, and deliver a report addressing the issue of rock shear effects on containment system integrity. The modularisation of the testing program into three testing suites offers the possibility of using multiple facilities to conduct the testing. The uniaxial compression tests may be best suited for testing at facilities in Sweden where other tests of this type have been conducted on bentonite buffer material. The two-component and analogue tests may benefit from being designed and conducted at a single facility as the instrumentation and other design issues in each case are similar. However, the testing schedule may need to be adjusted if a single compression machine is to be used for both test suites.

The preferred use of scaled composite copper/cast iron canisters for the analogue tests will require direct involvement of SKB to design and fabricate these components. The canisters should have the same stiffness characteristics as the full-scale canister. In addition, the test cylinders for the two-component constant volume tests will require SKB involvement to ensure the materials selected are comparable to those to be used in the KBS-3 design.

The information provided in this report is considered to be a sufficient basis for a preliminary cost estimate and feedback on technical issues from staff at qualified testing facilities.

## 5.2 Recommendations

Based on the information contained in this report, the following recommendations are made:

- A five-year rock shear testing program should be established to provide an avenue for addressing this key technical issue. In the initial stage of this program, SKB should reaffirm qualifications and interest of the three testing facilities identified in this report, and potentially others involved in previous testing. Once the qualification process is completed, SKB should seek proposals and cost estimates from qualified testing laboratories to implement the various components of the proposed testing plan. Evaluation and selection criteria should be established by SKB at the outset of this stage.
- Following selection of one or more qualified laboratories, equipment and instrumentation design, fabrication and testing should be undertaken, including prototype testing to develop and test sample preparation, instrumentation, monitoring, testing and post-test characterisation protocols. Information from JAEA on existing testing equipment and procedures may facilitate this development step. SKB should acquire available information from JAEA. The preparation of bentonite samples in Sweden will require expertise at SKB, Clay Technology AB, and/or other organisations.
- Single component testing should be conducted as soon as possible in the schedule once suitable testing facilities are identified and procedures established. The scope of the testing plan is considered a minimum therefore consideration should be given to additional tests using a standard experimental design approach (e.g. factorial experiment) to check for repeatability and other factors. Strict control of sample and loading platen geometry is essential to ensure representative test results.
- Two-component and scaled analogue testing should proceed using multiple test vessels and a modularised cartridge concept to allow specimens to saturate and mature outside the loading frame apparatus. Given the significant time required for sample saturation and maturation, strict sample preparation and instrument calibration/testing protocols are recommended to ensure successful testing. Instrumentation and monitoring systems required to monitor sample maturation should be designed to accommodate multiple samples in separated test vessels. Protocols and procedures should be developed for instrument replacement in the event of malfunction. Redundancy in instrumentation is recommended to reduce the likelihood of inadequate test measurements.
- Design and fabrication of scaled analogue canisters is envisioned to require significant effort on the part of SKB. This is a critical path activity and should be initiated as soon as practicable. Additional tests can be added to the schedule to accommodate alternate canister and buffer material designs if required by lengthening the testing schedule or fabricating additional instrumented test vessels.
- Analysis of testing results and modification of material models (if deemed appropriate) should adopt methodology and comparison strategies used for previous testing of this type in Sweden. Engagement of Clay Technology AB and possibly other expertise in Sweden as part of the project team is recommended as a means of maintaining consistency in data interpretation and development/refinement of material models.
- Continued interaction with JAEA, JRC and other organisations studying rock shear effects is recommended to benefit from different perspectives and experience with respect to earthquake induced effects and other related technical issues, such as specialised numerical modeling approaches, and laboratory testing techniques and equipment. Participation in international workshops and conferences related to this topic is also recommended to promote technical peer review.

## References

SKB's (Svensk Kärnbränslehantering AB) publications can be found at [www.skb.se/publications](http://www.skb.se/publications).

**Andersson C-G, 2002.** Development of fabrication technology for copper canisters with cast inserts. Status report in August 2001. SKB TR-02-07, Svensk Kärnbränslehantering AB.

**Börgesson L, 1986.** Model shear tests of canisters with smectite clay envelopes in deposition holes. SKB TR 86-26, Svensk Kärnbränslehantering AB.

**Börgesson L, 1988.** Modelling of buffer material behaviour. Some examples of material models and performance calculations. SKB TR 88-29, Svensk Kärnbränslehantering AB.

**Börgesson L, 1990.** Interim report on the laboratory and theoretical work in modeling the drained and undrained behaviour of buffer materials. SKB TR 90-45, Svensk Kärnbränslehantering AB.

**Börgesson L, 1992.** Interaction between rock, bentonite buffer and canister. FEM calculations of some mechanical effects on the canister in different disposal concepts. SKB TR 92-30, Svensk Kärnbränslehantering AB.

**Börgesson L, Hernelind J, 2006.** Earthquake induced rock shear through a deposition hole. Influence of shear plane inclination and location as well as buffer properties on the damage caused to the canister. SKB TR-06-43, Svensk Kärnbränslehantering AB.

**Börgesson L, Hernelind J, 2010.** Earthquake induced rock shear through a deposition hole. Modelling of three model tests scaled 1:10. Verification of the bentonite material model and the calculation technique. SKB TR-10-33, Svensk Kärnbränslehantering AB.

**Börgesson L, Pusch R, 1986.** Basic properties of bentonite-based buffer materials and their function in WP-Cave repositories. SGAB Internal Report 86501, Swedish Geological AB.

**Börgesson L, Hökmark H, Karnland O, 1988.** Rheological properties of sodium smectite clay. SKB TR 88-30, Svensk Kärnbränslehantering AB.

**Börgesson L, Fredrikson A, Johannesson L-E, 1994.** Heat conductivity of buffer materials. SKB TR 94-29, Svensk Kärnbränslehantering AB.

**Börgesson L, Johannesson L-E, Sandén T, Hernelind J, 1995.** Modelling of the physical behaviour of water saturated clay barriers. Laboratory tests, material models and finite element application. SKB TR 95-20, Svensk Kärnbränslehantering AB.

**Börgesson L, Johannesson L-E, Hernelind J, 2003.** Earthquake induced rock shear through a deposition hole. Effect on the canister and the buffer. SKB TR-04-02, Svensk Kärnbränslehantering AB.

**Börgesson L, Sandén T, Johannesson L-E, Knutsson H, 2004.** ROSE, ROck Shear Experiment. A feasibility study. SKB IPR-06-13, Svensk Kärnbränslehantering AB.

**Börgesson L, Dueck A, Johannesson L-E, 2010.** Material model for shear of the buffer – evaluation of laboratory test results. SKB TR-10-31, Svensk Kärnbränslehantering AB.

**Dueck A, Börgesson L, Johannesson L-E, 2010.** Stress-strain relation of bentonite at undrained shear. Laboratory tests to investigate the influence of material composition and test technique. Swedish Nuclear Fuel and Waste Management Company Technical Report TR-10-32, Svensk Kärnbränslehantering AB.

**Harrington J F, Birchall D J, 2007.** Sensitivity of total stress to changes in externally applied water pressure in KBS-3 buffer bentonite. SKB TR-06-38, Svensk Kärnbränslehantering AB.

**Hedin A, 2005.** An analytic method for estimating the probability of canister/fracture intersections in a KBS-3 repository. SKB R-05-29, Svensk Kärnbränslehantering AB.

**Hernelind J, 2010.** Modelling and analysis of canister and buffer for earthquake induced rock shear and glacial load. SKB TR-10-34, Svensk Kärnbränslehantering AB.

- Hirai T, Tanai K, Kikuchi H, Suzuki H, Takaji K, Ohnuma S, 2003.** Assessment on mechanical effect of engineering barrier system to fault movement. JNC TN8400 2003-009, March 2003, Japan Nuclear Cycle Development Institute. (In Japanese.)
- Hirai T, Tanai K, Kikuchi H, Takaji K, 2004.** Assessment on bearing capacity of buffer material to overpack. JNC TN8400 2003-031, February 2004, Japan Nuclear Cycle Development Institute. (In Japanese.)
- Karnland O, Birgersson M, 2006.** Montmorillonite stability. With special respect to KBS-3 conditions. SKB TR-06-11, Svensk Kärnbränslehantering AB.
- La Pointe P, Wallmann P, Thomas A, Follin S, 1997.** A methodology to estimate earthquake effects on fractures intersecting canister holes. SKB TR 97-07, Svensk Kärnbränslehantering AB.
- Munier R, Hökmark H, 2004.** Respect distances. Rationale and means of computation. SKB R-04-17, Svensk Kärnbränslehantering AB.
- Pusch R, 1978.** Highly compacted Na bentonite as buffer substance. KBS TR 74, Svensk Kärnbränsleförsörjning AB.
- Pusch R, 1980a.** Swelling pressure of highly compacted bentonite. SKBF/KBS TR 80-13, Svensk Kärnbränsleförsörjning AB.
- Pusch R, 1980b.** Permeability of highly compacted bentonite. SKBF/KBS TR 80-16, Svensk Kärnbränsleförsörjning AB.
- Pusch R, 1983a.** Use of clays as buffers in radioactive repositories. SKBF/KBS TR 83-46, Svensk Kärnbränsleförsörjning AB.
- Pusch R, 1983b.** Stress/strain/time properties of highly compacted bentonite. SKBF/KBS TR 83-47, Svensk Kärnbränsleförsörjning AB.
- Read R S, 2004.** 20 years of excavation response studies at AECL's Underground Research Laboratory. International Journal of Rock Mechanics and Mining Sciences, 41, pp 1251–1275.
- SKB, 2006.** Long-term safety for KBS-3 repositories at Forsmark and Laxemar – a first evaluation. Main report of the SR-Can project. SKB TR-06-09, Svensk Kärnbränslehantering AB.
- Takaji K, Suzuki H, 1999.** Static mechanical properties of buffer material. JNC TN8400 99-041, November 1999, Japan Nuclear Cycle Development Institute. (In Japanese.)
- Takaji K, Shigeno Y, Shimogouchi T, Shiratake T, Tamura, H, 2004.** Examination of constitutive model for evaluating long-term mechanical behavior of buffer (III). JNC TN8400 2003-007, February 2004, Japan Nuclear Cycle Development Institute. (In Japanese.)

## Background on the Rock Shear Experiment (ROSE)

### The Rock Shear Experiment (ROSE)

The ROSE full-scale test is planned to be conducted at the site of the Äspö Pillar Stability Experiment. As part of that rock mechanics test, two full-scale 1.75-m-diameter deposition holes separated by a 1 m thick rock pillar were drilled vertically into the invert of an access tunnel. The proposed arrangement for ROSE (Figure A-1) involves removing the top part of the pillar separating the two boreholes to accommodate a loading apparatus in the right-hand borehole, and buffer and a canister in the left-hand borehole. Part of the left-hand borehole is removed by sawing away about 200 mm of rock to allow for shear displacement.

The horizontal fracture is simulated by a heavy steel flange anchored to the rock at the top of the left-hand deposition borehole following excavation of the upper 2 m of rock. The flange is located at the upper quarter point on the canister, and is flat with low friction. To compensate for the removed upper 2 m of the left-hand borehole, a steel shear cylinder attached to the steel structure, and mobile in the shearing direction, is used. This shear cylinder has a flange that opposes the flange at the top of the borehole to form the shearing plane. The two flanges are initially fastened during maturation of the buffer, but are unfastened prior to shearing. The loading apparatus includes guides bolted to the rock wall near the left-hand borehole to ensure horizontal displacement during the test. Shear displacement is generated by a system of six pressure cylinders driven by highly-pressurised nitrogen. The buffer and canister are placed within the left-hand borehole and steel cylinder, a steel lid is bolted on the top of the steel tube, then a steel plug anchored to the rock by rock anchors is used to cover the steel tube and borehole. The plane between the steel plug and the lid of the steel cylinder is hydraulically-pressurised to reduce friction.

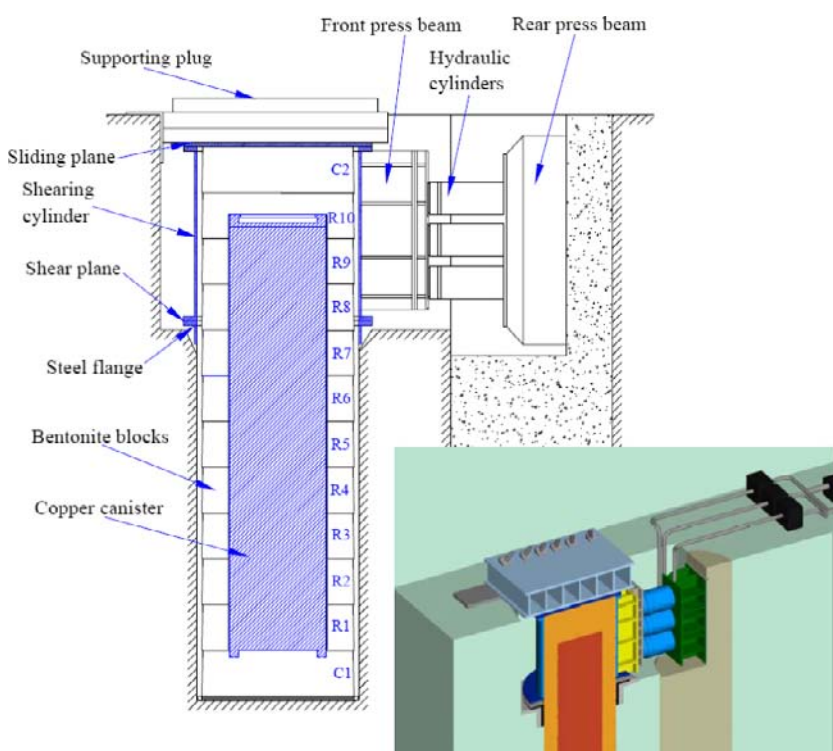


**Figure A-1.** Arrangement of ROSE at the site of the Äspö Pillar Stability Experiment (from /Börjesson et al. 2004/).

The buffer material is to be highly compacted blocks of sodium bentonite MX-80. The buffer will be built with nine rings, two cylinder blocks and one cylinder block that is drilled to form half a ring and half a cylinder. The inner and outer diameters of the buffer are 1.05 and 1.65 m, respectively. The 5 cm annular gap between the buffer and the wall of the borehole is filled with pellets compacted at a water ratio of 17%. Based on performance in other tests, the bulk density of the pellets is anticipated to be 1,200 to 1,300 kg/m<sup>3</sup>. Once installation is complete, the annular gap with pellets will be filled with water, yielding an initial degree of saturation of 90–95%.

The BWR-type copper canister will be obtained from the Encapsulation Project conducted by SKB. The canister will not contain heaters. The top lid of the canister is planned to be welded in place in order to realistically simulate the canister design. The bottom of the test canister will be bolted in place to accommodate cables and tubes running from inside the canister to the data acquisition system. Instrumentation of the canister requires special machining of the canister (mainly for total pressure sensors and strain gauges).

The press apparatus is hydraulic with a press force of 23,750 kN. The main parts of the press are the front and rear beams, 6 hydraulic cylinders in a 3x2 pattern, and guides. For horizontal movement, the beams are vertical, and the surrounding rock is used as the press frame. Owing to the asymmetry of the load caused by the difference in stiffness of the canister and the buffer, the press force centre is located about 125 mm lower than the centre of the shear cylinder (front beam centre). The press is powered by a set of high pressure nitrogen bottles, which generate a hydraulic pressurised flow via two or three media converters. The maximum hydraulic stroke of the cylinders is 200 mm (100 mm for the shear stroke and 50 mm for acceleration and deceleration). The forward stroke speed is 100 mm/s and the return stroke is 1 mm/s. Accounting for elasticity in the loading system oil and mechanics, pressure drops, and other effects, the accuracy of the loading system is expected to be within 1 to 2 mm measured over the front beam.

Prior to shearing, the buffer must be completely water-saturated and matured. This is accomplished using bentonite blocks with a high degree of water saturation, and incorporating filter mats on the rock walls and pumps to apply a water pressure to the blocks to speed the saturation process. Even with this arrangement and using bentonite blocks that are 95 to 98% saturated, the saturation process is expected to take up to two years. In contrast, shearing requires a very large force (2,000 tons) applied over a very short timeframe. The planned shear rate is 0.1 m/s, requiring a regulation system to control movement.

An alternate arrangement for the experiment involves the fracture plane at the same level of the invert of the tunnel. In this scenario, the upper part of the borehole is simulated using a steel cylinder. The loading apparatus is above-ground and uses the sidewall of the tunnel as a reaction surface, hence shearing the emplaced buffer and canister perpendicular to the tunnel axis. Another major difference between this alternative and the original arrangement is that the lid of the shearing cylinder is supported by a pillar against the roof rather than rock anchors.

Because of the very different time scales associated with saturation of the buffer material, and shearing along the simulated fracture, two separate instrumentation systems are envisioned for the experiment to capture the hydromechanical response. The two experiment phases to be monitored are as follows:

- Saturation/maturation phase. This phase will last for about two years, and the monitored processes are very slow. The data collection interval will likely be set to 1 hour or longer during the test period. Monitored parameters (and expected range of measurement) include total pressure (0–10 MPa), pore water pressure (0–2 MPa), relative humidity (95–100%), and anchor loads (0–2,000 kN).
- Shear phase. This phase will last for about two seconds. Several thousands of measurements will be taken during this time, which means that the demands on the data collection system and the sensors are very high. Monitored parameters (and expected range of measurement) include total pressure (0–40 MPa), strain on canister (0–30%), load (0–10 kN), and displacement (0–30 cm).

Many of the sensor types used in the other tests at Äspö (e.g. vibrating wire instruments) are not suitable for the rapid and frequent measurements during the shearing phase.

Planned instrumentation for the saturation/maturation phase is shown in Figure A-2. Instruments are positioned in a vertical plane perpendicular to the shear direction. Total pressure will be measured at six points on the canister, two points on the rock wall in deposition borehole, five points on the sliding shear cylinder, and one point in the upper part of the buffer above the canister. Because maturation of the buffer is expected to be slowest near the canister, pore pressure will be monitored at the same six points on the canister, and at the one location in the buffer. A total of twenty-eight Wescor psychrometers will be positioned in the buffer at various heights to measure relative humidity. In addition, the load in each of the twelve rock anchors holding the steel plug in place will be monitored as the total load needs to be carefully controlled just prior to the shearing phase. Exact locations of the sensors have not been finalised.

Figure A-2 shows the general layout of instruments to monitor the shear phase of the experiment. Instruments are positioned in a vertical plane parallel to the shear direction. At present, all measurements are planned to be made on the surface of the canister and the rock (or shear cylinder). There are ten total pressure sensors on the canister, six on the shearing cylinder, and four on the rock of the deposition borehole wall. Strain gauges are attached to the canister at ten points coinciding with total pressure sensor locations. Load and displacement are measured at three points on the shear cylinder. Additional instruments may be installed inside the canister, but these have yet to be determined. Changes regarding the type, number and position of sensors are likely during the detailed planning of the experiment.

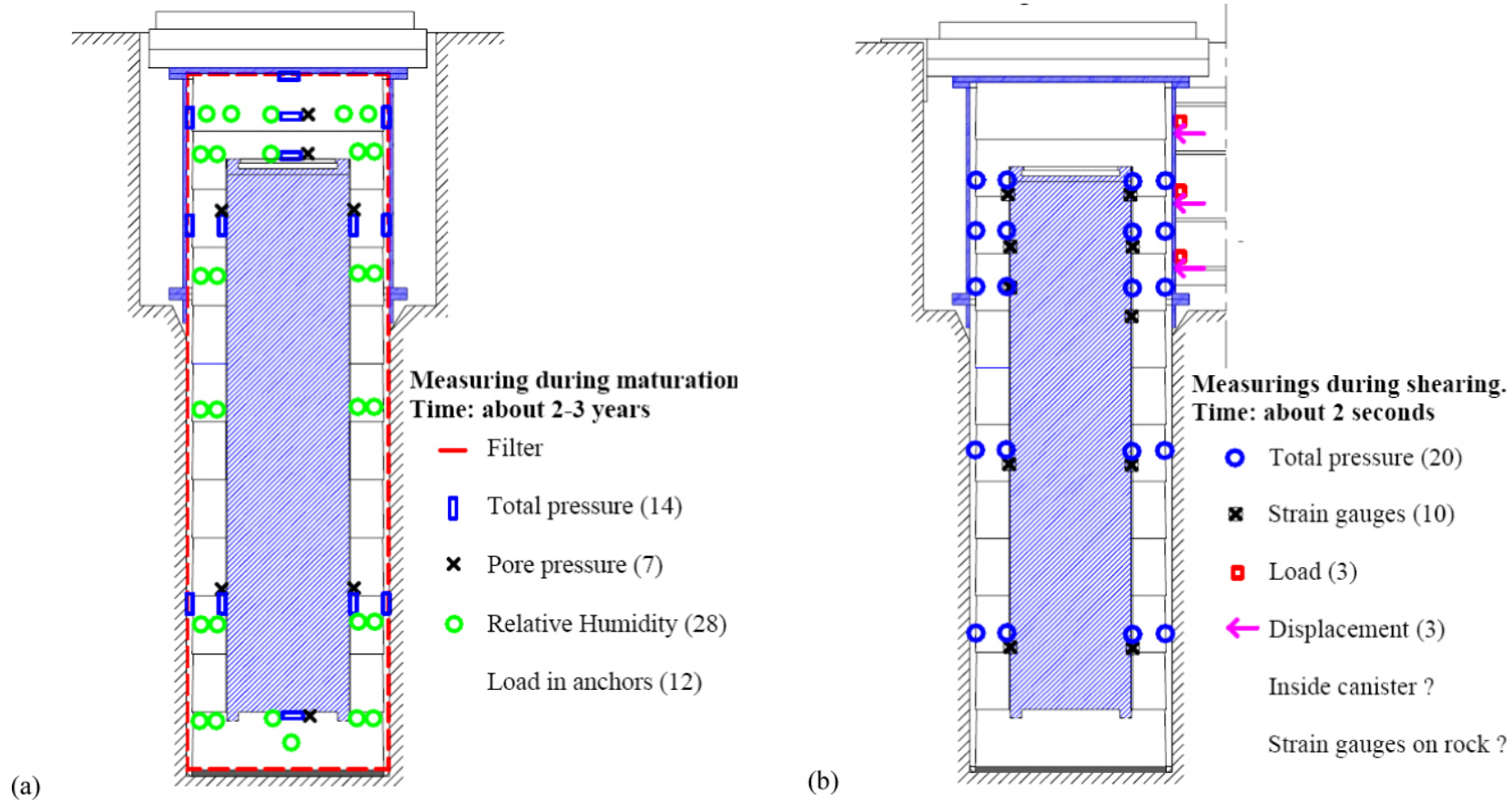


**Figure A-2.** Instrumentation planned to monitor ROSE. (a) saturation/maturation phase instruments are located in a vertical plane perpendicular to the shearing direction, and (b) shearing phase instruments are located in a vertical plane parallel to the shear direction (from /Börgesson et al. 2004/).

## Background on JAEA BORE-SHEAR tests

### JAEA testing facilities and equipment

The Tokai Research Centre at Tokai, Japan is one of JAEA's facilities for research into nuclear waste disposal in Japan. The effects associated with rock shear are being examined using specialised testing apparatus at the Tokai Research Centre. Laboratory shear tests on 1:20 scale composite engineered barrier system specimens are being conducted by JAEA as part of the BORE-SHEAR testing program. The objective of the testing program is to develop, validate and calibrate a numerical model based on the results of scaled laboratory tests for use in predicting effects of earthquake-induced shearing of the rock mass at full-scale under various conditions. The testing uses specially-designed equipment developed by Takenaka Civil Engineering & Construction Co., Ltd., Tokyo (Figure B-1). The main components of the testing apparatus include:

- A stainless steel cylindrical test vessel with a vertical central shear plane and an O-ring between the two halves of the vessel to provide a seal during testing. The test vessel has an internal metal filter system so that distilled water can be supplied at a constant pressure to the buffer material during the saturation phase. The test vessel is mounted on a rail system equipped with hydraulics to allow the vessel to be raised and moved horizontally as required.
- A loading frame and servo-controlled hydraulic loading system equipped with a force and a strain transducer to measure the force applied to the test vessel during shearing, and the relative shear displacement of the two halves of the vessel.
- An internal instrumentation system to measure total pressure and pore pressure at strategic points along the interfaces between the specimen and the test vessel, and along the internal interface between the buffer and overpack. Total pressure and pore pressure transducer locations on the inside surface of the vessel were selected assuming symmetry of the tests; total pressure transducers are located in one half of the vessel and pore water pressure transducers are located in the other half (Figure B-2).
- A control system for supplying distilled water at constant pressure to the test cylinder to saturate the bentonite.
- A data acquisition system and computer to monitor the instruments during both the saturation and shearing phases of the test.

The composite specimens used in these tests are 150 mm in diameter and 350 mm in length. Each specimen contains a central overpack 50 mm in diameter and 100 mm in length. The maximum shear load and shear stroke capacity of the apparatus are 50 tons and 100 mm, respectively. Controlled shear rates between 1 and 100 mm/s are achievable.

The buffer material was prepared by mixing 70 wt% bentonite (Kunigel V1®, made by Kunimine Industry Co., Ltd, in Japan) and 30 wt% silica sand. Initial water content of the bentonite was around 7%. For the silica sand, a mixture of silica sand No.3 (produced in Seto City, Aichi Prefecture in Japan) and silica sand No.5 (produced in West Australia) mixed at a weight ratio of 1:1 was used. The mixture was compacted into either disk- or ring-shaped blocks using a compression molding machine (Figure B-3) to a dry density of 1,600 kg/m<sup>3</sup>.

In total, nine buffer blocks are required to construct a single specimen, with the overpack inserted into the cavity of the three central ring-shaped blocks to form the composite EBS specimen. Two types of overpack models were tested early in the BORE-SHEAR program; one made of solid carbon steel without pressure transducers (Overpack-1) and the other a hollow cylinder of carbon steel with three total pressure transducers (Overpack-2). Based on initial tests, neither overpack model experienced damage during testing, so the Overpack2 design was selected for subsequent testing.



*Figure B-1. Photograph of the Japanese BORE-SHEAR apparatus for shear testing of composite EBS specimens.*

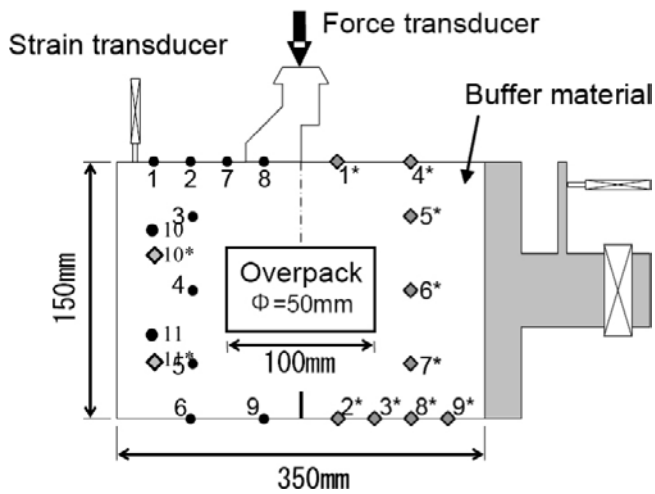


*Figure B-2. Schematic diagram of a typical composite specimen showing the location of total pressure (black circles) and pore pressure (grey diamonds) transducers on the inner surface of the test vessel.*



*Figure B-3. Compression molding machine used to create buffer blocks for the BORE-SHEAR test specimens.*

For a given test, the composite specimen is inserted into the cylindrical test vessel. Distilled water is injected at a pressure of 0.2 MPa to saturate the buffer material in the test vessel, and promote maturation of the buffer (i.e. development of swelling pressure). The saturation/maturation phase of the test can take up to about 6 months using the current procedures for buffer saturation. Once the swelling pressure stabilises, the EBS specimen is sheared along the central shear plane of the test vessel. The total pressure and pore water pressure, as well as the applied load and displacement, are measured during shearing. The shearing phase takes between 1 and 10 seconds to complete depending on the shear rate and desired shear displacement.

At the completion of a test, the specimen is recovered and the angle of rotation of the overpack is measured. Figure B-4 shows a typical specimen immediately following shearing, and a partially dissected specimen and rotated overpack model. Samples of buffer from the specimen are used to characterise the moisture distribution and material properties in different locations relative to the overpack. X-ray CT scanning has been used to assess the void ratio and density distribution in the buffer, but the current setup requires the removal of the metal overpack before scanning. Other industrial CT scanning technology may overcome this issue, thus allowing the immediate post-testing specimen to be assessed in a non-destructive manner before being dissected.

The measured instrument responses from each shear test are compared to predicted results from a numerical model of the test using the three-dimensional finite element code Abaqus. This process is the basis for model validation and calibration, and for identifying key inputs required to reduce any discrepancies between the measured and modeled responses. The post-test characterisation data obtained from each specimen are not used directly in the comparison.

A total of 1,000 solid elements were used in the element mesh, and properties were selected to account for the buffer material, the shear zone through the buffer material, the overpack, and the near-field rock. Numerical simulations of shear testing treat the buffer material as an elasto-plastic material using a modified Cam-clay model based on critical state plasticity theory. The overpack and the near-field rock are modeled as elastic materials.

The model allows for drainage at the contact between the buffer material and the near-field rock. The shear zone generated in the buffer during shearing is modeled as a central narrow zone dividing the specimen. Drainage is allowed along the outer boundary of the shear zone into the annular slot representing the shear plane. The overpack is modeled as a solid elastic metal mass because of its high rigidity and strength. The width of the shear zone and the permeability of the near-field rock were set as variables in these simulations to assess model sensitivity to these parameters. The interfaces between the rock and buffer, and between the buffer and overpack, were not modeled directly. This is a topic currently under investigation by JAEA as a possible means of improving the fit between measured and modeled results.



(a)



(b)

**Figure B-4.** Composite EBS specimen from Test 4 of the JAEA testing program following (a) shearing and (b) partial dissection.

As of July 2007, four shear tests had been completed by JAEA. The shearing conditions for each test are shown in Table B-1. A swelling pressure of about 0.7 MPa was observed in each case, and was used in the numerical simulations as the initial effective stress condition in the buffer.

The numerical modeling results showed similar trends in responses in some cases, but the fit between measured and modeled results generally requires improvement before the model can be considered validated. It was also noted that long power outages occurred during two of the saturation periods, and some transducers produced erratic or erroneous data. Sensors are hardwired into the test vessel and overpack, and are therefore difficult to replace.

Observation of the shearing phase of one of the BORE-SHEAR tests provided insight into the quality control procedures in place for the testing program. Steps in the procedure involved lifting the supporting plate beneath the test vessel, removing twelve bolts holding the two halves of the test vessel together, lifting the loading piston on the loading frame and pressurizing it with the hydraulic system, sliding the test vessel into position on a hydraulic roller system then wedging the vessel in place after releasing the hydraulic pressure on the rollers, positioning a displacement transducer on the half of the test vessel to be displaced, setting up the data acquisition computer program, completing a final check of the test setup, initiating shearing, and collecting data.

### Other related testing equipment

Other testing equipment operated by JAEA includes the DEFORM experimental setup, developed to assess the relation between bearing capacity of the buffer and deformation under representative geometry and boundary conditions. Three different test vessels were developed including the axisymmetric 1/20 model, the 1/10 model and the plane strain model. The difference between the axisymmetric 1/20 and the 1/10 models is the diameter of piston. The equipment is shown in Figures B-5 and B-6.

**Table B-1. Summary of BORE-SHEAR test conditions.**

Test Case	Shear Displacement (mm)	Shear rate (mm/s)
Case-1	40	100
Case-2	40	100
Case-3	70	10
Case-4	70	10



Figure B-5. DEFORM testing apparatus.



**Test vessel**



**The piston set into the buffer**

Figure B-6. Axisymmetric test vessel used in DEFORM testing.

### Translated JAEA abstracts

#### JNC TN8400 99-041

November, 1999

#### Static Mechanical Properties of Buffer Material

Kazuhiko TAKAJI and Hideaki SUZUKI

#### Abstract

The buffer material is expected to maintain its low water permeability, self-sealing properties, radionuclides adsorption and retardation properties, thermal conductivity, chemical buffering properties, overpack supporting properties, stress buffering properties, etc over a long period of time. Natural clay is mentioned as a material that can relatively satisfy above. Among the kinds of natural clay, bentonite when compacted is superior because (i) it has exceptionally low water permeability and properties to control the movement of water in buffer, (ii) it fills void spaces in the buffer and fractures in the host rock as it swells upon water uptake, (iii) it has the ability to exchange cations and to adsorb cationic radioelements. In order to confirm these functions for the purpose of safety assessment, it is necessary to evaluate buffer properties through laboratory tests and engineering-scale tests, and to make assessments based on the ranges in the data obtained.

This report describes the procedures, test conditions, results and examinations on the buffer material of unconfined compression tests, one-dimensional consolidation tests, consolidated-undrained triaxial compression tests and consolidated-undrained triaxial creep tests that aim at getting hold of static mechanical properties. We can get hold of the relationship between the dry density and tensile stress etc by Brazillian tests, between the dry density and unconfined compressive strength etc by unconfined compression tests, between the consolidation stress and void ratio etc by one-dimensional consolidation tests, the stress path of each effective confining pressure etc by consolidated-undrained triaxial compression tests and the axial strain rate with time of each axial stress etc by consolidated-undrained triaxial creep tests.

**Examination of Constitutive Model for Evaluating Long-term Mechanical Behavior of Buffer (III)**

Kazuhiko TAKAJI, Yoshimasa SHIGENO, Takafumi SHIMOGOUCHI,  
Toshikazu SHIRATAKE and Hirokuni TAMURA

**Abstract**

On the R&D of the high-level radioactive waste repository, it is essential that Engineered Barrier System (EBS) is stable mechanically over a long period of time for maintaining each ability required to EBS. After closing the repository, the various external forces will be affected to buffer intricately for a long period of time. So, to make clear the mechanical deformation behavior of buffer against the external force is important, because of carrying out safety assessment of EBS accurately.

In this report, several sets of parameters are chosen for the previously selected two constitutive models, Sekiguchi-Ohta model and Adachi-Oka model, and the element tests and mock-up tests are simulated using these parameters. Through the simulation, applicability of the constitutive models and parameters is examined. Moreover, simulation analyses of EBS using these parameters were carried out, and mechanical behavior is evaluated over a long period of time. Analysis estimated the amount of settlement of the over pack, the stress state of buffer material, the reaction force to a base rock, etc., and the result that EBS is mechanically stable over a long period of time was obtained.

Next, in order to prove analyses results a side, literature survey was conducted about geological age, the dynamics history of a Smectite layer. The outline plan was drawn up about the natural analogue verification method and preliminary examination was performed about the applicability of "Freezing Sampling".

## **JNC TN8400 2003-009**

March, 2003

### **Assessment on Mechanical Effect of Engineering Barrier System to Fault Movement**

Takashi HIRAI, Kenji TANAI, Hirohito KIKUCHI, Hideaki SUZUKI,  
Kazuhiko TAKAJI, and Satoshi OHNUMA

#### **Abstract**

The objective of this report is to clarify mechanical effect of engineered barrier system to the unavoidable fault movement. From the basic policy of the second progress report by JNC, natural phenomenon which affect strongly to the geological disposal system should be avoided. However, small faults as sliprate "C" far from principal fault zone, are difficult to be found out completely. Therefore, it is important to evaluate the influence of these fault movements and to clarify stability and safety of the engineered barrier system.

Accordingly, the effect of a rock displacement across a deposition hole was considered and the medium scale test was carried out. Then medium scale test was simulated by Finite Element Method in which the constitutive model of Tresca was adopted to analyze elastoplastic behavior of buffer material. From the result of the medium scale test and the analysis, it was realised that the buffer material diminish shear stress acting on the overpack.

Further analytical study was conducted to evaluate the real scale engineered barrier system designed in the second progress report by JNC. From the study, it was appeared that stress in buffer corresponded to the stress calculated for the medium scale test model. Consequently, it was obvious that rock displacement, 80% of buffer thickness, didn't affect overpack if velocity of fault movement was under 10 cm/sec.

## **JNC TN8400 2003-031**

February, 2004

### **Assessment on Bearing Capacity of Buffer Material to Overpack**

Takashi HIRAI, Kenji TANAI, Hirohito KIKUCHI, Kazuhiko TAKAJI, Satoshi OHNUMA

#### **Abstract**

The objective of this report is to clarify the characteristics of the bearing capacity of the buffer material against the deformation of the overpack in the engineered barrier system. In the second progress report by JNC, it was reported that the well designed engineered barrier system is stable and safety on mechanical support of the overpack to ensure stability and stress which acts on the overpack by some analysis. However, the degree of the capacity to the ultimate state and the background datas of the design are not necessary clarified in the report. Therefore it is considered to be important to assess the ultimate state and make the relationship clear between deformation and bearing capacity of the overpack in the engineered barrier system. So the scale test and the simulation analysis were carried out for the longitudinal deformation of the overpack in the saturated buffer material constrained by the host rock. From the result of the scale test and the analysis it appears that the bearing capacity is increasing with the deformation of the overpack even if the bearing capacity is over the yielding force and the relationship between deformation and bearing capacity can be approximately expressed by the simple function.